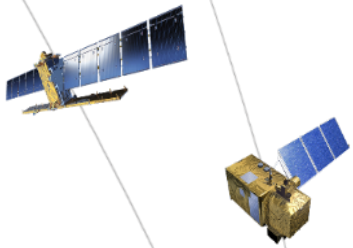

Earth Observation for
Sustainable Development

urban development
eo4sd

Urban Development Project

EO4SD-Urban Project: Saint Louis City Report

ESA Ref:	**AO/1-8346/15/I-NB**
Doc. No.:	**City Operations Report**
Issue/Rev.:	**1.2**
Date:	**19.11.2019**

GAFAG SIRS gisat egis DLR NEO JOANNEUM RESEARCH DIGITAL GISBOX esa

Consortium Partners

No.	Name	Short Name	Country
1	GAF AG	GAF	Germany
2	Système d'Information à Référence Spatiale SAS	SIRS	France
3	GISAT S.R.O.	GISAT	Czech Republic
4	Egis SA	EGIS	France
5	Deutsche Luft- und Raumfahrt e. V	DLR	Germany
6	Netherlands Geomatics & Earth Observation B.V.	NEO	The Netherlands
7	JOANNEUM Research Forschungsgesellschaft mbH	JR	Austria
8	GISBOX SRL	GISBOX	Romania

Summary

This document contains information related to the provision of geo-spatial products from the European Space Agency (ESA) supported project "Earth Observation for Sustainable Development" Urban Applications (EO4SD-Urban) to the benefit of Global Platform for Sustainable Cities (GPSC) programme implemented for the City of Saint Louis and Senegalese authorities.

	Affiliation/Function	Name	Date
Prepared	SIRS NEO JR	S. Delbour, D. Fretin, V. Gastal F. Fang M. Hirschmugl, H. Proske	02/08/2019
Reviewed	SIRS	C. Sannier	05/08/2019
Approved	GAF AG, Project Coordinator	T. Haeusler	05/08/2019

The document is accepted under the assumption that all verification activities were carried out correctly and any discrepancies are documented properly.

Distribution

Affiliation	Name	Copies
ESA	Z. Bartalis	electronic copy
Government agencies	M. Ndaw F. Cheikh M. Diara	electronic copy
UNIDO	M. Draeck K. Barunica	electronic copy

Document Status Sheet

Issue	Date	Details
1.0	05/08/2019	First Document Issue
1.1	28/08/2019	Minor corrections mainly related to the formal structure
1.2	19/11/2019	Addition of section 4.3 Sustainable Development Goal 11 Indicators

Document Change Record

#	Date	Request	Location	Details
1	05/08/2019			Initial version
2	28/08/2019		Full document	Corrected page layout and title numbering errors
3	28/08/2019		Section 4.2	More detailed analysis for LULC
4	28/08/2019		Section 4.2.2	Latest version of the map - Figure 11

This page is intentionally left blank.

Executive Summary

The European Space Agency (ESA) has been working closely together with the International Finance Institutes (IFIs) and their client countries to demonstrate the benefits of Earth Observation (EO) in the IFI development programmes. Earth Observation for Sustainable Development (EO4SD) is a new ESA initiative, which aims to achieve an increase in the uptake of satellite-based information in the regional and global IFI programmes. The overall aim of the EO4SD Urban project is to integrate the application of satellite data for urban development programmes being implemented by the IFIs or Multi-Lateral Development Banks (MDBs) with the developing countries. The overall goal will be achieved via implementation of the following main objectives:

- To provide a service portfolio of Baseline and Derived urban-related geo-spatial products
- To provide the geo-spatial products and services on a geographical regional basis
- To ensure that the products and services are user-driven

This Report describes the generation and the provision of EO-based information products to the GEF supported programme "Global Platform for Sustainable Cities**"** for Senegal and the counterpart City authorities in Saint-Louis. The Report provides a Service Description by referring to the user-driven service requirements and the associated product list with the detailed product specifications. The following products were requested:

- Urban and Peri-Urban Land Use/ Land Cover and Changes
- Settlement Extent and Imperviousness and Changes
- Flood Hazard and Risk Assessment

The current Version of this Report contains the description of the generation and delivery of each requested product, especially the Land Use/Land Cover (LU/LC) and the LU/LC Changes between 2003/2006 and 2018. The Flood Hazard and Risk Assessment study conducted, and the resulting products are also described in details in this Report.

This City Operations Report for Saint Louis systematically reviews the main production steps involved and importantly highlights the Quality Control (QC) mechanisms involved; the steps of QC and the assessment of quality is provided in related QC forms in the Annexe of this Report. Standard analytical work undertaken with the products can be further included as inputs into further urban development assessments, modelling and reports.

This page is intentionally left blank.

Table of Contents

Annexes

Annex 1: AOI calculation based on the DG Regio approach

Annex 2: Processing methods for EO4SD-Urban products

Annex 3: Filled Quality Control Sheets

List of Figures

List of Tables

List of Abbreviations

AOI	Area of Interest
CGIAR	Global Research Partnership for a Food-Secure Future
CDS	City Development Strategy
CS	Client States
DEM	Digital Elevation Model
DLR	German Space Agency
EDF	European Development Fund
EEA	European Environmental Agency
EGIS	Consulting Company for Environmental Impact Assessment and Urban Planning, France
EIA	Environmental Impact Assessment
EIB	European Investment Bank
EO	Earth Observation
ESA	European Space Agency
EU	European Union
GAF	GAF AG, Geospatial Service Provider, Germany
GCC	General Clauses and Conditions for ESA Contracts
GCT	General Conditons of Tender
GEO	Group on Earth Observations
Geo-SDI	Geo Sustainable Development Indicators
GIS	Geographic Information System
GISAT	Geospatial Service Provider, Czech Republic
GISBOX	Romanian company with activities of Photogrammetry and GIS
GPSC	Global Platform for Sustainable Cities
GUF	Global Urban Footprint
HR	High Resolution
HRL	High Resolution Layer
IFI	International Financing Institute
INSPIRE	Infrastructure for Spatial Information in the European Community
ISO/TC 211	Standardization of Digital Geographic Information
JR	JOANNEUM Research, Austria
LC / LU	Land Cover / Land Use
LULCC	Land Use and Land Cover Change
MMU	Minimum Mapping Unit
NDVI	Normalized Difference Vegetation Index
NEO	Geospatial Service Provider, The Netherlands
QA	Quality Assurance
QC	Quality Control
QM	Quality Management
R&D	Research and Development
SAR	Synthetic Aperture Radar
SC	Service Cluster

SME	Small and Medium-sized Enterprise
SO	Service Operations
SP	Service Provider
ToC	Table of Contents
UN	United Nations
UNDP	United Nations Development Programme
UN-ESCAP	United Nations Economic and Social Commission for Asia and the Pacific
UNFCCC	United Nations Framework Convention on Climate Change
UNITAR	United Nations Institute for Training and Research
US	United States of America
UUA	User Utility Assessment
VHR	Very High Resolution
WB	World Bank
WBG	World Bank Group
WP	Work Package

This page is intentionally left blank.

1 General Background of EO4SD-Urban

Since 2008 the European Space Agency (ESA) has worked closely together with the International Finance Institutes (IFIs) and their client countries to harness the benefits of Earth Observation (EO) in their operations and resources management. Earth Observation for Sustainable Development (EO4SD) is a new ESA initiative, which aims to achieve an increase in the uptake of satellite-based information in the regional and global IFI programmes. The EO4SD-Urban project initiated in May 2016 (with a duration of 3 years) has the overall aim to integrate the application of satellite data for urban development programmes being implemented by the IFIs with the developing countries. The overall goal will be achieved via implementation of the following main objectives:

- To provide the services on a regional basis (i.e. large geographical areas); in the context of the current proposal with a focus on S. Asia, SE Asia and Africa, for at least 35-40 cities.
- To ensure that the products and services are user-driven; i.e. priority products and services to be agreed on with the MDBs in relation to their regional programs and furthermore to implement the project with a strong stakeholder engagement especially in context with the validation of the products/services on their utility.
- To provide a service portfolio of Baseline and Derived urban-related geo-spatial products that have clear technical specifications and are produced on an operational manner that are stringently quality controlled and validated by the user community.
- To provide a technology transfer component in the project via capacity building exercises in the different regions in close co-operation with the MDB programmes.

This Report supports the fulfilment of the third objective, which requires the provision of geo-spatial Baseline and Derived geo-spatial products to various stakeholders in the IFIs and counterpart City authorities. The Report provides a Service Description, and then in Chapter 3 systematically reviews the main production steps involved and importantly highlights whenever there are Quality Control (QC) mechanisms involved with the related QC forms in the Annexe of this Report. The description of the processes is kept intentionally at a top leave and avoiding technical details as the Report is considered mainly for non-technical IFI staff and experts and City authorities. Finally, Chapter 4 presents the standard analytical work undertaken with the products which can be inputs into further urban development assessments, modelling and reports.

2 Service Description

The following Section summarises the service as it has been realised for the city of Saint Louis, Senegal, within the EO4SD-Urban Project and as it was delivered to the UNIDO (United Nations Industrial Development Organisation), the GPSC Implementing Agency for the Senegalese city of Saint Louis, and the Senegalese Governmental agencies.

2.1 Stakeholders and Requirements

The EO4SD-Urban products described in this Report were provided for the benefit of the Global Platform for Sustainable Cities (GPSC) programme. GPSC is funded by the Global Environment Facility (GEF) and currently includes 28 cities in 11 countries. The GPSC initiative is supported by different Multi-Lateral Development Banks (MDBs) and UN organisations. The two Senegalese cities of St. Louis and Dakar are part of the GPSC programme and were identified for collaboration with the EO4SD-Urban project via interactions with UNIDO, the Implementing Agency.

The GPSC has an overarching aim to provide a knowledge platform for partner cities, as well as relevant networks and institutions to support the cities via:

- "Knowledge transfer activities that support urban investments and sustainability initiatives,
- A global network for collaborative engagement, tapping into and complementing existing efforts,
- Long-term, systematic engagement with cities, financial institutions, and organizations for transformational impact" (GPSC Programme Booklet, 2016).

Saint Louis is a GPSC Partner City and one the main cities of Senegal. Located along the north coast of the country, its unique geographical position, at the mouth of the Senegal river, exposes the city to major environmental hazards (flood, coastal erosion, rise of the sea level).
In the context of the GPSC programme the city has the objective to "integrate climate risks in urban planning and management and will focus on urban planning and management, capacity building through the development of integrated climate resilience solutions and strengthening the urban national policy framework to promote cities' sustainability at the national level" (GPSC website, 2018). The project also aims at developing a sustainable cities master plan.

The main local stakeholder for the city of Saint Louis is the Directorate of Urbanism and Architecture of the Senegalese Ministry of Urban Renewal, Habitat and Living Environment. Other stakeholders include mostly other Senegalese governmental agencies.
The Directorate of Urbanism and architecture, that works in close collaboration with the Ministry of Territorial Planning, will use the EO4SD products to develop more accurate policy mechanisms. Furthermore, the project will provide a regional view of the environmental dynamics, that will be used by the Directorate of Urbanism and Architecture's team.

2.2 Service Area Specification

So far, no internationally accepted definition for the term "Urban Area" and the related Core and Peri-Urban areas exists. Different initiatives are currently trying to address a standardised approach for defining the terms "Urban Area". During discussions with the GPSC Co-ordinator it was considered important to use a uniform definition for the GPSC cities in order for the cities to exchange information and share products/experiences and conduct potential comparative studies.

In this context, it was decided to use an international approach for the demarcation of the Area of Interest (AOI) for mapping the GPSC cities in terms of Core Urban area and Peri-Urban area. Thus, the approach is based on the European Union's Directorate-General for Regional and Urban Policy (DG REGIO) method and the definitions are described in the Regional Working Paper 2014 from the European Commission on "A harmonised definition of cities and rural areas: the new degree of urbanisation" (European Commission, 2014). Following the naming of the DG Regio approach, the Urban Core is named as "High Density Core" and the Peri-Urban area is termed as "Urban Cluster". Within the DG REGIO approach, the High Density Core area is defined as contiguous grid cells of 1 km^2 with a density of at least 1 500 inhabitants per km^2 and a minimum population of 50 000. The Urban Cluster is defined as clusters of contiguous grid cells of 1 km^2 with a density of at least 300 inhabitants per km^2 and a minimum population of 5 000.

The DG REGIO methodology used in the EO4SD-Urban project was slightly adjusted to Non-European countries. For the first three GPSC cities (namely Bhopal, Vijayawada and Saint-Louis) produced within the project the Global Human Settlement Population (GHSP) grid with a spatial resolution of 1 km were used for the classification into "High Density Core" and "Urban Cluster". The raster dataset is available for the years 1975, 1990, 2000, 2015. This dataset depicts the distribution and density of population, expressed as the number of people per cell. The data can be downloaded under following link http://data.jrc.ec.europa.eu/dataset/jrc-ghsl-ghs_pop_gpw4_globe_r2015a.

In 2019, a higher resolution population layer (spatial resolution of 10 m) produced by the German Aerospace Centre (DLR) became available. The AOIs for the remaining GPSC cities (namely Melaka, Abidjan, Dakar and Campeche) were produced based on the DLR population layer.

The High Density Core AOI for a city is created by merging the contiguous grid cells of 1 km^2 with a density of at least 1500 inhabitants per km^2 and a minimum population of 50 000. In the definition of the High Density Core the contiguity is only allowed via a vertical or horizontal connection. In a next step, gaps are filled. Due to the coarse resolution of the population grid cells additional grid cells were in a last step added for under estimated settlement areas. The same was done for over estimations, here grid cells were removed. The GHSP layer can be directly used for the calculation, while the DLR population has to be aggregated to a resolution of 1 km^2 before being used for the AOI definition. In this aggregation step, each output cell contains the sum of the input cells that are encompassed by the extent of that new cell.

The Urban Cluster is created very similar to the High Density Core. Continuous grid cells of 1 km^2 with a density of at least 300 inhabitants per km^2 and a minimum population of 5 000 are merged together to form the Urban Cluster. The contiguity within the Urban Cluster can also be diagonal. After gaps are filled, areas, which were over or under estimated by the population grid were removed or added to the AOI. The GHSP layer was directly used, the DLR population layer had to undergo an aggregation step in order to reduce the spatial resolution to 1 km^2.

For Bhopal and Vijayawada a buffer of 1 km was calculated around the High Density Core AOI and the Urban Cluster AOI to smoothen the border of the AOIs.

In all remaining GPSC cities, the border was not smoothed, but when the population grid was under or over estimating the real settlement extent, grid cells were added or removed.

In some cases, the city counterparts requested that the AOIs for the High Density Core and the Urban Cluster follow the municipal or administrative boundary of the city. In this case, the municipal/administrative boundary was used, but enlarged in areas where the AOI created according to the adjusted DG Regio approach was bigger. This adjustment of the DG Regio AOI was done for Melaka, Abidjan, Dakar and Campeche. These further adjusted DG Regio AOIs are in the following report named as Core City Area (see Figure 1a) and Larger Urban Area (see Figure 1b).

A more detailed description on how the AOIs are calculated is provided in Annex 1.

The AOIs were presented in a power point and sent to the Users for verification. Figure 1 shows the resulting AOIs after combining the DG Regio AOIs with the municipal/administrative boundaries of the cities.

Figure 1: Illustration of Core City and Larger Urban Areas of Saint Louis.

The Core City has an area of 89 km^2 and the Larger Urban has an area of 299 km^2.

2.3 Product List and Product Specifications

During the discussions related to the AOIs the potential geo-spatial products that could be provided for the Cities were also reviewed with the WB Team and Users. It was noted that the Baseline Land Use/Land Cover (LU/LC) products (for the Core and Peri-Urban areas) were a standard product that would be provided for all Cities as it is required for the derived products. In the case of Saint Louis, the full list of products for both the Core and Peri-Urban areas is as follows:

- Settlement Extent & Change (producer: DLR)
- Percentage Impervious Surface & Change (producer: DLR)
- Urban and Peri-Urban Land Use / Land Cover (LU/LC) & Change (producer: NEO)
- Flood Hazard & Risk Assessment (producer: JR)

The first two products have been generated by the German Aerospace Agency (DLR) over the full metropolitan area for four reference years: 2000 - 2005 - 2010 - 2015.

Two time slots were used to provide historic and recent information regarding LU/LC for Saint Louis, 2003 and 2018 over the Core City Area, 2006 and 2018 over the Larger Urban Area. The last section of the Report is fully dedicated to the Flood Hazard & Risk Assessment study.

2.4 Land Use/Land Cover Nomenclature

A pre-cursor to starting production was the establishment with the stakeholders on the relevant Land Use/Land Cover (LU/LC) nomenclature as well as class definitions. The approach taken was to use a standard remote sensing based LU/LC nomenclature i.e. the European Urban Atlas Nomenclature (European Union, 2011) and adapt it to the User's LU requirements. Thus, the remote-sensing based LU/LC classes in the urban context can be grouped into five Level 1 classes, which are Artificial Surfaces, Natural/ Semi Natural Areas, Agricultural Areas, Wetlands, and Water. These classes can then be sub-divided into several different more detailed classes such that the dis-aggregation can be down to Level 2-4. This hierarchical classification system is often used in operational Urban mapping programmes and is the basis for example of the European Commission's Urban Atlas programme which provides pan-European comparable LU/LC data with regular updates. A depiction of the way the levels and classes in the Urban Atlas programme are structured is presented as follows:

Level I Artificial surfaces

- Level II: Urban Fabric

Level III

- *Continuous Urban Fabric (Sealing Layer-S.L. > 80%)*
- *Discontinuous Urban Fabric (S.L. 10% - 80%)*

Level IV

1) *Discontinuous Dense Urban Fabric (S.L. 50% - 80%)*
2) *Discontinuous Medium Density Urban Fabric (S.L. 30% - 50%)*
3) *Discontinuous Low Density Urban Fabric (S.L. 10% - 30%)*
4) *Discontinuous Very Low Density Urban Fabric (S.L. < 10%)*

- Level II: Industrial, Commercial, Public, Military, Private Units and Transport

Level III

- *Industrial, Commercial, Public, Military and Private Units*
- *Transport Infrastructure*

Level IV

5) *Fast Transit Roads*

6) Other Roads

7) Railway

- *Port and associated land*
- *Airport and associated land*

- Level II: Mine, Dump and Construction Sites

Level III

- *Mineral Extraction and Dump Sites*
- *Construction Sites*
- *Land Without Current Use*

- Level II: Artificial Non-Agricultural Vegetated Areas

Level III

- *Green Urban Areas*
- *Sports and Leisure Facilities*

(Reference: European Union, 2011)

It should be noted that in the current project, the Level 1 classes were used as the basis for classification of the Urban Cluster areas using the High Resolution (HR) data such as Landsat or Sentinel. However, for the High Density Core areas using the Very High Resolution (VHR) data it was possible to go down to Level III and IV.

The different levels, classes and sub-classes from the remote sensing based urban classification, were harmonised within the GPSC cities. The following tables give the nomenclature for the High Density Core and the Urban Cluster region (see Table 1 and Table 2).

Table 1: LU/LC Nomenclature for GPSC Cities (High Density AOI).

Actual and Historic Nomenclature High Density Core			
Level I	**Level II**	**Level III**	**Level IV**
1000 Artificial Surfaces	1100 Residential	1110 Continuous Urban Fabric (80 - 100 % Sealed)	
		1120 Discontinuous Urban Fabric	1121 Discontinuous dense urban fabric (50 - 80 % Sealed)
			1122 Discontinuous medium density urban fabric (30 - 50 % Sealed)
			1123 Discontinuous low density urban fabric (10 - 30 % Sealed)
			1124 Discontinuous very low density urban fabric (0 - 10 % Sealed)
	1200 Industrial, Commercial, Public, Military, Private Units and Transport	1210 Industrial, Commercial, Public, Military and Private Units	
		1220 Transport Infrastructure	1221 Arterial Roads
			1222 Collector Roads
			1223 Railway
		1230 Port Area	
		1240 Airport	
	1300 Mine, Dump and Construction Sites	1310 Mineral Extraction and Dump Sites	
		1330 Construction Sites	
		1340 Land Without Current Use	
	1400 Artificial Non-Agricultural Vegetated Areas	1410 Green Urban Areas	
		1420 Sports and Leisure Facilities	
2000 Agricultural Area			
3000 Natural and Semi-natural Areas	3100 Forest and Shrublands		
	3200 Natural Areas (Grassland)		
	3300 Bare Soil		
4000 Wetlands			
5000 Water	5100 Inland Water		
	5200 Marine Water		

Table 2: LU/LC Nomenclature for GPSC Cities (Urban Cluster Area).

Actual and Historic Nomenclature Urban Cluster Area			
Level I	**Level II**	**Level III**	**Level IV**
1000 Artificial Surfaces			
2000 Agricultural Area			
3000 Natural and Semi-natural Areas	3100 Forest and Shrublands		
	3200 Natural Areas (Grassland)		
	3300 Bare Soil		
4000 Wetlands			
5000 Water	5100 Inland Water		
	5200 Marine Water		

It is important to note that the possibility to classify at Level IV is highly dependent on the availability of reliable reference datasets from the City or sources such as Google Earth. This aspect is further discussed in Chapter 3.

Especially regarding the road hierarchy used in the classification at Level IV, the international road classification standards have been followed; this is for example defined by the European Commission (https://ec.europa.eu/transport/road_safety/specialist/-knowledge/road/designing_for_road_function/road_classification_en).

Roads are divided into three groups: arterial or through traffic flow routes (in our case **Arterial Roads**), distributor roads (in our case **Collector Roads**), and access roads (or **Local Roads**). The three road types are defined as follows:

Arterial Roads:

Roads with a flow function allow efficient throughput of (long distance) motorized traffic. All motorways and express roads as well as some urban ring roads have a flow function. The number of access and exit points is limited. (https://ec.europa.eu/transport/road_safety/specialist/knowledge/-road/designing_for_road_function/road_classification_en)

Collector Roads:

Roads with an area distributor function allow entering and leaving residential areas, recreational areas, industrial zones, and rural settlements with scattered destinations. Junctions are for traffic exchange (allowing changes in direction etc.); road sections between junctions should facilitate traffic in flowing.
(https://ec.europa.eu/transport/road_safety/specialist/knowledge/road/designing_for_road_function/road_classification_en)

Local Roads:

Roads with an access function allow actual access to properties alongside a road or street. Both junctions and the road sections between them are for traffic exchange. (https://ec.europa.eu/transport/-road_safety/specialist/knowledge/road/designing_for_road_function/road_classification_en).

2.5 World Settlement Extent

Reliably outlining settlements is of high importance since an accurate characterization of their extent is fundamental for accurately estimating, among others, the population distribution, the use of resources (e.g. soil, energy, water, and materials), infrastructure and transport needs, socioeconomic development, human health and food security. Moreover, monitoring the change in the extent of settlements over time is of great support for properly modelling the temporal evolution of urbanization and thus, better estimating future trends and implementing suitable planning strategies.

At present, no standard exists for defining settlements and worldwide almost each country applies its own definition either based on population, administrative or geometrical criteria. The German Space Agency (DLR) was responsible for the provision of the "Settlement Extent" product; when generating the settlement extent maps from HR imagery, pixels are labelled as **settlement** if they *intersect any building, lot or – just within urbanized areas – roads and paved surface* where we define:

- **building** as any structure having a roof supported by columns or walls and intended for the shelter, housing, or enclosure of any individual, animal, process, equipment, goods, or materials of any kind;
- **lot** as the area contained within an enclosure (wall, fence, hedge) surrounding a building or a group of buildings. In cases where there are many concentric enclosures around a building, the lot is considered to stop at the inner most enclosure;
- **road** as any long, narrow stretch with a smoothed or paved surface, made for traveling by motor vehicle, carriage, etc., between two or more points;
- **paved surface** as any level horizontal surface covered with paving material (i.e., asphalt, concrete, concrete pavers, or bricks but excluding gravel, crushed rock, and similar materials).

Instead, pixels not satisfying this condition are marked as **non-settlement**.

The settlement extent product is a binary mask outlining - in the given Area of Interest (AOI) – settlements in contrast to all other land-cover classes merged together into a single information class. The settlement class and the non-settlement class are associated with values "255" and "0", respectively.

2.6 Percentage Impervious Surface

Settlement growth is associated not only to the construction of new buildings, but – more in general – to a consistent increase of all the impervious surfaces (hence also including roads, parking lots, squares, pavement, etc.), which do not allow water to penetrate, forcing it to run off. To effectively map the percentage impervious surface (PIS) is then of high importance being it related to the risk of urban floods, the urban heat island phenomenon as well as the reduction of ecological productivity. Moreover, monitoring the change in the PIS over time is of great support for understanding, together with information about the spatiotemporal settlement extent evolution, also more details about the type of urbanization occurred (e.g. if areas with sparse buildings have been replaced by highly impervious densely built-up areas or vice-versa).

In the framework of the EO4SD-Urban project, one pixel in the generated PIS maps is associated with the estimated percentage of the corresponding surface at the ground covered by buildings or paved surfaces, are defined as:

- **building** as any structure having a roof supported by columns or walls and intended for the shelter, housing, or enclosure of any individual, animal, process, equipment, goods, or materials of any kind;
- **paved surface** as any level horizontal surface covered with paving material (i.e. asphalt, concrete, concrete pavers, or bricks but excluding gravel, crushed rock, and similar materials).

The product provides for each pixel in the considered AOI the estimated PIS. Specifically, values are integer and range from 0 (no impervious surface in the given pixel) to 100 (completely impervious surface in the given pixel) with step 5.

2.7 Terms of Access

The Dissemination of the digital data and the Report was undertaken via FTP.

3 Service Operations

The following Sections present all steps of the service operations including the necessary input data, the processing methods, the accuracy assessment and the Quality Control procedures. Methods are presented in a top-level and standardised manner for all the EO4SD-Urban City Reports.

3.1 Source Data

This Section presents a summary of the remote sensing and ancillary datasets that were used. Different types of data from several data providers have been acquired. A complete list of source data as well as a quality assessment is provided in Annex 3.

High Resolution Optical EO Data

The major data sources for the current and historic mapping of LULC for Larger Urban Area, Settlement Extent and PIS products were Landsat and Sentinel-2 data which were accessible and downloadable free of charge.

- **Landsat 5:** As a source of historical data one scene of Landsat TM 5 from the 1st of December 2006 has been acquired which covers the whole area of interest.
- **Sentinel-2:** The most recent data coverage comprises one Sentinel-2 data set from the 9th of December 2018. The data was downloaded and processed at Level 1C.

Very High Resolution Optical EO Data

The VHR data for the core urban area mapping had to be acquired and purchased through commercial EO Data Providers such as Airbus Defence and European Space Imaging.

It has to be noted that under the current collaboration project the VHR EO data had to be purchased under **mono-license agreemen**ts between GAF AG and the EO Data Providers. If EO data would have to be distributed to other stakeholders then further licences for multiple users would have to be purchased.

The following VHR sensor data have been acquired to cover the entire AOI:

- **Quickbird-2:**
  - 2 scenes from the 13th of March 2003
- **WorldView-2:**
  - 4 scenes from the 29th of November 2018

Detailed lists of the used EO data as well as their quality is documented in the attached Quality Control Sheets in Annex 3.

Ancillary Data

Open Street Map (OSM) data: OSM data is freely available and generated by volunteers across the globe. The so-called crowd sourced data is not always complete but has for the most parts of the world valuable spatial information. Data was downloaded to complement the Transport Network layer and further enhanced. The spatial location of the OSM based streets was used a geospatial reference.

Detailed lists of the used EA and ancillary data as well as their quality is documented in the attached Quality Control Sheets in Annex 3.

3.2 Processing Methods

Data processing starts at an initial stage with quality checks and verification of all incoming data. This assessment is performed in order to guarantee the correctness of data before geometric or radiometric pre-processing is continued. These checks follow defined procedures in order to detect anomalies, artefacts and inconsistencies. Furthermore, all image and statistical data were visualized and interpreted by operators.

The main techniques and standards used for data analysis, processing and modelling for each product are described in Annex 2.

3.3 Accuracy Assessment of Map Products

Data and maps derived from remote sensing contain - like any other map - uncertainties which can be caused by many factors. The components, which might have an influence on the quality of the maps derived from EO include quality and suitability of satellite data, interoperability of different sensors, radiometric and geometric processing, cartographic and thematic standards, and image interpretation procedures, post-processing of the map products and finally the availability and quality of reference data. However, the accuracy of map products has a major impact on secondary products and its utility and therefore an accuracy assessment was considered as a critical component of the entire production and products delivery process. The main goal of the thematic accuracy assessment was to guarantee the quality of the mapping products with reference to the accuracy thresholds set by the user requirements.

The applied accuracy assessments were based on the use of reference data and applying statistical sampling to deduce estimates of error in the classifications. In order to provide an efficient, reliable and robust method to implement an accuracy assessment, there are three major components that had to be defined: the **sampling design**, which determines the spatial location of the reference data, the **response design** that describes how the reference data is obtained and an **analysis design** that defines the accuracy estimates. These steps were undertaken in a harmonized manner for the validation of all the geo-spatial products.

3.3.1 Accuracy Assessment of the LU/LC Products

Sampling Design

The sampling design specifies the sample size, sample allocation and the reference assessment units (i.e. pixels or image blocks). Generally, different sampling schemes can be used in collecting accuracy assessment data including: simple random sampling, systematic sampling, stratified random sampling, cluster sampling, and stratified systematic unaligned sampling. In the current project a **single stage stratified random sampling** based on the method described by Olofson et al (2013[1]) was applied which used the map product as the basis for stratification. This ensured that all classes, even very minor ones were included in the sample.

The sampling design is applied separately for the High Density Core Area and for the Urban Cluster Area classification.

[1] Olofsson, P., Foody, G. M., Stehman, S. V., & Woodcock, C. E. (2013). Making better use of accuracy data in land change studies: Estimating accuracy and area and quantifying uncertainty using stratified estimation. Remote Sensing of Environment, 129, 122–131. doi:10.1016/j.rse.2012.10.031

In the complex LU/LC product with many classes, this usually results in a large number of strata (one stratum per LU/LC classes), of which some classes cover only very small areas (e.g. sport fields, cemeteries) and not being adequately represented in the sampling. In order to achieve a representative sampling for the statistical analyses of the mapping accuracy it was decided to extend the single stage stratified random sampling. Slightly different approaches were used for the High Density and the Urban Cluster classification.
The first step is the same for both classifications: the number of required samples is allocated within each of the Level I strata (1000 Artificial Surfaces, 2000 Agricultural Area, 3000 Natural and Semi-natural Areas, 4000 Wetlands, 5000 Water).
In the second step, all Level III classes that were not covered by the first sampling were grouped into one new stratum for the High Density classification. For the Urban Cluster classification all Level II classes that were not covered by the first sampling were grouped into one new stratum.

Within that stratum the same number of samples was randomly allocated as the Level I strata received. To avoid a clustering of point samples within classes and to minimise the effect of spatial autocorrelation a minimum distance in between the sample points was set to be 150 m. The final sample size for each class can be considered to be as close as possible to the proportion of the area covered by each stratum considering that the target was to determine the overall accuracy of the entire map.

The total sample size per stratum was determined by the expected standard error and the estimated error rate based on the following formula, which assumes a simple random sampling (i.e. the stratification is not considered):

$$n = \frac{P*q}{(\frac{E}{Z})^2}$$

n = number of samples per strata / map class
p = expected accuracy
$q = 1 - p$
E = Level of acceptable (allowable) sample error
Z = z-value (the given level of significance)

Hence, with an expected accuracy of $p = 0.85$, a 95% confidence level and an acceptable sampling error of 5%, the minimum sample size is 196. A 10% oversampling was applied to compensate for stratification inefficiencies and potentially inadequate samples (e.g. in case of cloudy or shady reference data). For each Level I strata 215 samples have been randomly allocated. Afterwards, for all classes of Level III of the High Density classification that did not received samples in the first run, additionally 215 samples were randomly drawn across all these classes. A summary of the number of sample point for each High Density class is given in Table 3.

The same applies for the Urban Cluster classification: All Level II classes that did not receive samples in the first run, additionally 215 samples were randomly drawn across all these classes. A summary of the number of sample point for each High Density class is given in Table 4.

The main difference of the sampling design for the two areas is that the resampling is done at Level III for the High Density areas and at Level II for the Urban Cluster areas.

Table 3: Number of sampling points for the Core City area classes after applied sampling design with information on overall land cover by class.

Class Name	Class ID	No. Of Sampling Points	Km² Coverage
Continuous Urban Fabric	1110	47	6.07
Discontinuous Urban Fabric	1120	44	5.33
Industrial, Commercial, Public, Military and Private Units	1210	40	5.50
Transport Infrastructure	1220	9	0.78
Airport	1240	6	0.67
Construction Sites	1330	23	2.70
Land Without Current Use	1340	18	4.67
Green Urban Areas	1410	3	0.21
Sports and Leisure Facilities	1420	2	0.39
Agricultural Area	2000	26	3.44
Forest and Shrublands	3100	132	17.94
Natural Areas (Grassland)	3200	16	1.47
Bare Soil	3300	75	6.47
Wetlands	4000	83	2.28
Inland Water	5100	148	29.18
Marine Water	5200	11	2.09
Total	**-**	**683**	**89.20**

Table 4: Number of sampling points for the Larger Urban area classes after applied sampling design with information on overall land cover by class.

Class Name	Class ID	No. Of Sampling Points	Km² Coverage
Artificial Surfaces	1000	177	37.81
Agriculture	2000	224	28.05
Forest and Shrublands	3100	95	63.27
Natural Areas	3200	5	2.19
Bare Soil	3300	129	72.81
Wetlands	4000	285	37.39
Inland Water	5100	148	53.60
Marine Water	5200	11	3.69
Total	**-**	**1074**	**232.95**

Response Design

The response design determines the reference information for comparing the map labels to the reference labels. Collecting reference data on the ground by means of intensive fieldwork is both costly and time-consuming, and is in most projects not feasible. The most cost-effective reference data sources are VHR satellite data with 0.5 m to 1 m spatial resolution. Czaplewski (2003)[2] indicated that visual interpretation of EO data is acceptable if the spatial resolution of EO data is sufficiently better compared to the thematic classification system. However, if there are no EO data with better spatial resolution available, the assessment results need to be checked against the imagery used in the production process.

The calculated number of necessary sampling points for each mapping category was randomly distributed among the strata and overlaid onto the two LULC mapping products. The following two Figures (see Figure 2 and Figure 3) are showing the mapping result with the overlaid sample points.

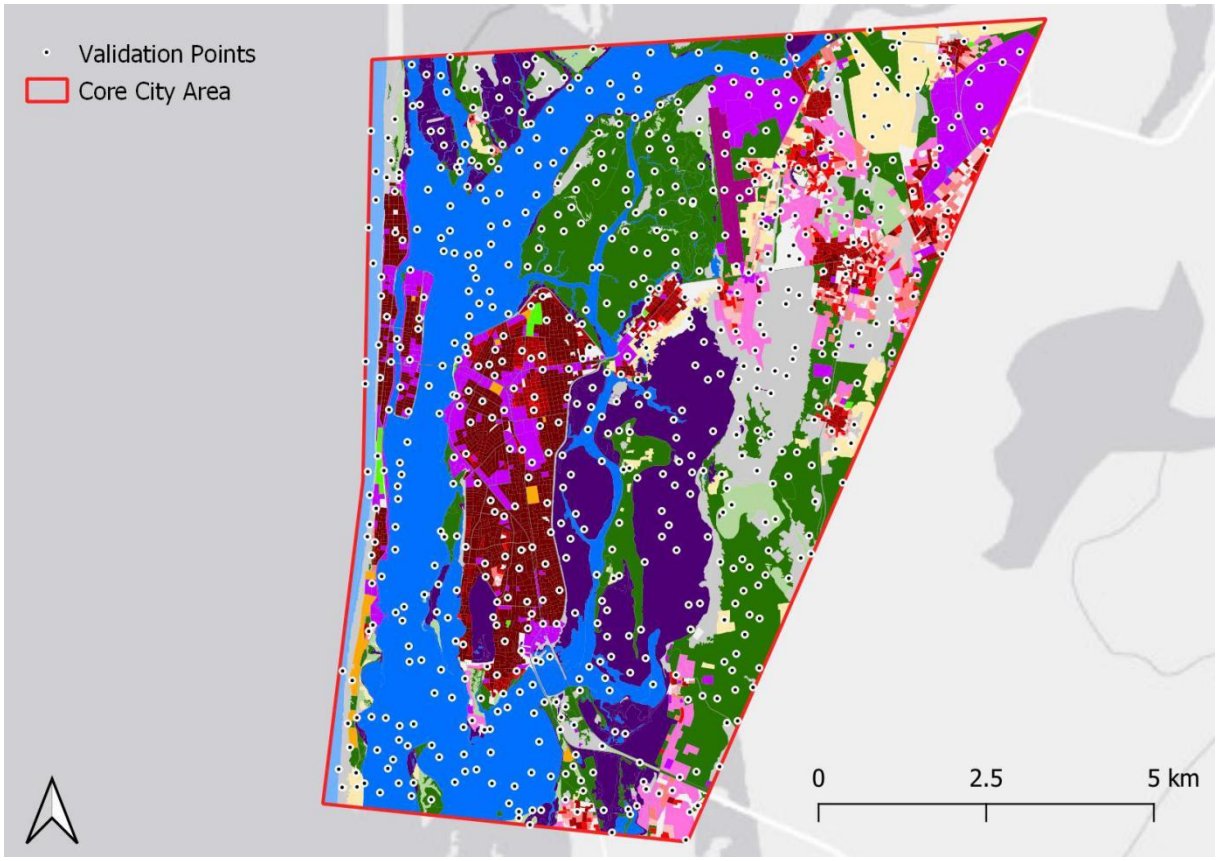

Figure 2: Mapping result of the Core City area of Saint Louis of the year 2018 overlaid with randomly distributed sample points used for accuracy assessment.

[2] Czaplewski, R. L. (2003). Chapter 5: accuracy assessment of maps of forest condition: statistical design and methodological considerations, pp. 115–140. In Michael A.Wulder, & Steven E. Franklin (Eds.), Remote sensing of forest environments: concepts and case studies. Boston: Kluwer Academic Publishers (515 pp.).

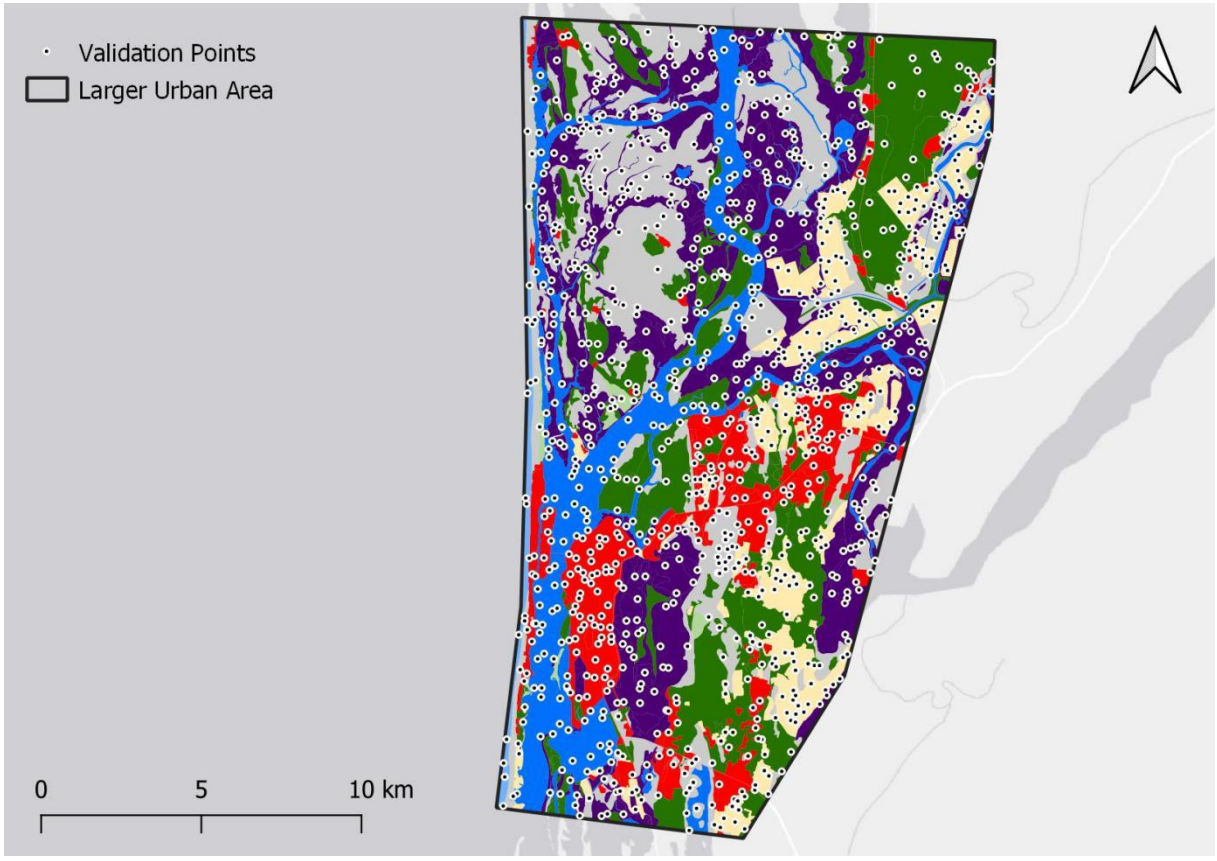

Figure 3: Mapping result of the Larger Urban area of Saint Louis of the year 2018 overlaid with randomly distributed sample points used for accuracy assessment.

In this way a reference information could be extracted for each sample point by visual interpretation of the VHR data for all mapped classes. The size of the area to be observed had to be related to the Minimum Mapping Unit (MMU) of the map product to be assessed. The reference information of each sampling point was compared with the mapping results and the numbers of correctly and not-correctly classified observations were recorded for each class. From this information the specific error matrices and statistics were computed (see next Section).

Analysis

Each class usually has errors of both omission and commission, and in most situations, these errors for a class are not equal. In order to calculate these errors as well as the uncertainties (confidence intervals) for the area of each class a statistically sound accuracy assessment was implemented.

The confusion matrix is a common and effective way to represent quantitative errors in a categorical map, especially for maps derived from remote sensing data. The matrices for each assessment epoch were generated by comparing the "reference" information of the samples with their corresponding classes on the map. The *Reference* represented the "truth", while the *Map* provided the data obtained from the map result. Thematic accuracy for each class and overall accuracy is then presented in error matrices. Unequal sampling intensity resulting from the random sampling approach was accounted for by applying a weight factor (*p*) to each sample unit based on the ratio between the number of samples and the size of the stratum considered[3]:

[3] Selkowitz, D. J., & Stehman, S. V. (2011). Thematic accuracy of the National Land Cover Database (NLCD) 2001 land cover for Alaska. Remote Sensing of Environment, 115(6), 1401–1407. doi:10.1016/j.rse.2011.01.020.

$$\hat{p}_{ij} = \left(\frac{1}{M}\right) \sum_{x \in (i,j)} \frac{1}{\pi^*_{uh}}$$

Where *i* and *j* are the columns and rows in the matrix, M is the total number of possible units (population) and π is the sampling intensity for a given sample unit *u* in stratum *h*.

Overall accuracy and User and producer accuracy were computed for all thematic classes and 95% confidence intervals were calculated for each accuracy metric.

The standard error of the error rate was calculated as follows: $\sigma_h = \sqrt{\frac{p_h(1-p_h)}{n_h}}$ where n_h is the sample size for stratum h and p_h is the expected error rate. The standard error was calculated for each stratum and an overall standard error was calculated based on the following formula:

$$\sigma = \sqrt{\sum w_h^2 . \sigma_h^2}$$

In which w_h is the proportion of the total area covered by each stratum. The 95% Confidence Interval (CI) is +/- 1.96*σ.

Results

The confusion matrices are provided within the Annex 3 and show the mapping error for each relevant class. For each class the number of samples which are correctly and not correctly classified are listed, this allows the calculation of the user and producer accuracies for each class as well as the confidence interval at 95% confidence levels based on the formulae above.

The Land Use/Land Cover product for Saint Louis in 2018 in Core City Area has an overall mapping accuracy of 90.67% with a CI ranging from 88.47% to 92.87% at a 95% CI. For the Larger Urban Area, the overall accuracy is 91.94% with a CI ranging from 90.32% to 93.57% at a 95% CI. The specific class accuracies are given in Annex 3.

3.3.2 Accuracy Assessment of the World Settlement Extent Product

In the following, the strategy designed for validating the World Settlement Extent (WSE) or World Settlement Footprint (WSF) 2015, i.e. a global settlement extent layer obtained as a mosaic of ~18.000 tiles of 1x1 degree size where the same technique employed in the EO4SD-Urban project is presented. In particular, specific details are given for all protocols adopted for each of the accuracy assessment components, namely response design, sampling design, and analysis; final results are discussed afterwards. In the light of the quality and amount of validation points considered, it can be reasonably assumed that the corresponding quality assessment figures are also representative for any settlement extent map generated in the framework of EO4SD-Urban.

Response Design

The response design encompasses all steps of the protocol that lead to a decision regarding agreement of the reference and map classifications. The four major features of the response design are the source of information used to determine the source of reference data, the spatial unit, the labelling protocol for the reference classification, and a definition of agreement.

- **Source of Reference Data:** Google Earth (GE) satellite/aerial VHR imagery has been used given its free access and the availability for all the project test sites in the period 2014-2015. In particular, GE automatically displays the latest available data, but it allows to browse in time over all past historical images. The spatial resolution varies depending on the specific data source; in the case of SPOT imagery it is ~1.5m, for Digital Globe's WorldView-1/2 series, GeoEye-1, and Airbus' Pleiades it is in the order of ~0.5m resolution, whereas for airborne data (mostly available for North America, Europe and Japan) it is about 0.15m.
- **Spatial Assessment Unit:** A 3x3 block spatial assessment unit composed of 9 cells of 10x10m size has been used. Specifically, this choice is justified one the one hand by the fact that input data with different spatial resolutions have been used to generate the WSF2015 (i.e. 30m Landsat-8 and 10m S1). On the other hand, GE imagery exhibited in some cases a mis-registration error of the order of 10-15m, hence using a 3x3 block allows defining an agreement e.g. based on statistics computed over 9 pixels, thus reducing the impact of such shift.
- **Reference Labelling Protocol:** For each spatial assessment block any cell is finally labelled as **settlement** if *it intersects any building, lot or – just within settlements – roads and paved surface*. Instead, pixels not satisfying this condition are marked as **non-settlement**.
- **Definition of Agreement:** Given the classification and the reference labels derived as described above, three different agreement criteria have been defined:
    8) for each pixel, positive agreement occurs only for matching labels between the classification and the reference;
    9) for each block, a majority rule is applied over the corresponding 9 pixels of both the classification and the reference; if the final labels match, then the agreement is positive;
    10) for the classification a majority rule is applied over each assessment block, while for the reference each block is labelled as “settlement” only in the case it contains at least one pixel marked as “settlement”; if the final labels match, then the agreement is positive.

Crowd-sourcing was performed internally at Google. In particular, by means of an ad-hoc tool, operators have been iteratively prompted a given cell on top of the available Google Earth reference VHR scene closest in time to the year 2015 and given the possibility of assigning to each cell a label among: “building”, “lot”, “road/paved surface” and “other”. For training the operators, a representative set of 100 reference grids was prepared in collaboration between Google and DLR.

Sampling Design

The stratified random sampling design has been applied since it satisfies the basic accuracy assessment objectives and most of the desirable design criteria. In particular, stratified random sampling is a probability sampling design and it is one of the easier to implement; indeed, it involves first the division of the population into strata within which random sampling is performed afterwards. To include a representative population of settlement patterns, 50 out of the ~18.000 tiles of 1x1 degree size considered in the generation of the WSF2015 have been selected based on the ratio between the number of estimated settlements (i.e. disjoint clusters of pixels categorized as settlement in the WSF2015) and their area. In particular, the *i*-th selected tile has been chosen randomly among those whose ratio belongs to the interval $]P_{2(i-1)}; P_{2i}], i \in [1; 50] \subset \mathbb{N}$ (where P_x denotes the *x*-th percentile of the ratio).

Table 5: Accuracies exhibited by the WSF2015 according to the three considered agreement criteria for different definitions of settlement.

Settlement =	Accuracy Measure	Agreement Criterion					
		1		2		3	
buildings	*OA%*	86.96		87.86		91.15	
	AA%	88.57		90.35		88.91	
	Kappa	0.6071		0.6369		0.7658	
	UA_{NS}% - UA_S%	98.11	54.69	98.73	56.76	94.84	80.58
	PA_{NS}% - PA_S%	86.24	90.90	86.72	93.98	93.32	84.51
buildings + lots	*OA*	88.08		88.94		91.26	
	AA%	88.64		90.19		88.71	
	Kappa	0.6510		0.6784		**0.7716**	
	UA_{NS}% - UA_S%	97.54	60.71	98.13	62.66	94.29	82.62
	PA_{NS}% - PA_S%	87.79	89.49	88.26	92.12	93.95	83.48
buildings + lots + roads / paved surface	*OA*	88.77		90.09		88.51	
	AA%	86.34		88.28		84.27	
	Kappa	**0.6938**		**0.7317**		0.7219	
	UA_{NS}% - UA_S%	94.49	72.20	95.35	75.06	88.13	89.60
	PA_{NS}% - PA_S%	90.78	81.91	91.62	84.94	96.04	72.51

As the settlement class covers a sensibly small proportion of area compared to the merger of all other non-settlement classes (~1% of Earth's emerged surface), an equal allocation reduces the standard error of its class-specific accuracy. Moreover, such an approach allows to best address user's accuracy estimation, which corresponds to the map "reliability" and is indicative of the probability that a pixel classified on the map actually represents the corresponding category on the ground. Accordingly, in this framework for each of the 50 selected tiles we randomly extracted 1000 settlement and 1000 non-settlement samples from the WSF2015 and used these as centre cells of the 3x3 reference block assessment units to label by photointerpretation. Such a strategy resulted in an overall amount of $(1000 + 1000) \times 9 \times 50 = 900.000$ cells labelled by the crowd.

Analysis

As measures for assessing the accuracy of the settlement extent maps, we considered:

- the percentage overall accuracy *OA%*;
- the Kappa coefficient;
- the percentage producer's (PA_S%, PA_{NS}%) and user's (UA_S%, UA_{NS}%) accuracies for both the settlement and non-settlement class;
- the percentage average accuracy *AA%* (i.e., the average between PA_S% and PA_{NS}%).

Results

Table 5 reports the accuracies exhibited by the WSF2015 according to the three considered agreement criteria for different definitions of settlement; specifically, we considered as "settlement" all areas covered by: i) buildings; ii) buildings or building lots; or iii) buildings, building lots or roads / paved surfaces. As one can notice, accuracies are always particularly high, thus confirming the effectiveness of the employed approach and the reliability of the final settlement extent maps. The best performances in terms of kappa are obtained when considering settlements as composed by buildings, building lots and roads / paved surfaces for criteria 1 and 2 (i.e., 0.6938 and 0.7317, respectively) and by buildings and building lots for criteria 3 (0.7716); the OA% follows a similar trend. This is in line with the adopted settlement definition. Moreover, agreement criteria 3 results in accuracies particularly high with respect to criteria 1 and 2 when considering as settlement just buildings or the combination of buildings and lots. This can be explained by the fact that when the detection is mainly driven by Landsat data then the whole 3x3 assessment unit tends to be labelled as settlement if a building or a lot intersect the corresponding 30m resolution pixel.

3.3.3 Accuracy Assessment of the Percentage Impervious Surface Product

In the following section, the strategy designed for validating the PIS product is presented; specifically, details are given for all protocols adopted for each of the accuracy assessment components, namely response design, sampling design, and analysis. Results are discussed afterwards.

Response Design

The response design encompasses all steps of the protocol that lead to a decision regarding agreement of the reference and map classifications. The four major features of the response design are the source of information used to determine the source of reference data, the spatial unit, the labelling protocol for the reference classification, and a definition of agreement.

- **Source of Reference Data:** Cloud-free VHR multi-spectral imagery (Visible + Near Infrared) acquired at 2m spatial resolution (or higher) covering a portion of the AOI for which the Landsat-based PIS product has been generated;
- **Spatial Assessment Unit:** A 30x30m size unit has been chosen according to the spatial resolution of the Landsat imagery employed to generate the PIS product;
- **Reference Labelling Protocol:** As a first step, the NDVI is computed for each VHR scene followed by a manual identification of the most suitable threshold that allows to exclude all the vegetated areas (i.e. non-impervious). Then, the resulting mask is refined by extensive photointerpretation.
- **Definition of Agreement:** The above-mentioned masks are aggregated at 30m spatial resolution and compared per-pixel with the resulting VHR-based reference PIS to the corresponding portion of the Landsat-based PIS product.

Sampling Design

The entirety of pixels covered by the available VHR imagery over the given AOI is employed for assessing the quality of the Landsat-based PIS product.

Analysis

As measures for assessing the accuracy of the PIS maps, following indices are computed:

- the *Pearson's Correlation coefficient*: it measures the strength of the linear relationship between two variables and it is defined as the covariance of the two variables divided by the product of their standard deviations; in particular, it is largely employed in the literature for validating the output of regression models;
- The *Mean Error (ME)*: it is calculated as the difference between the estimated value (i.e., the Landsat-based PIS) and the reference value (i.e., the VHR-based reference PIS) averaged over all the pixels of the image;
- The *Mean Absolute Error (MAE)*: it is calculated as the absolute difference between the estimated value (i.e., the Landsat-based PIS) and the reference value (i.e., the VHR-based reference) averaged over all the pixels of the image.

Results

To assess the effectiveness of the method developed to generate the PIS maps, its performances over 5 test sites is analysed (i.e. Antwerp, Helsinki, London, Madrid and Milan) by means of WorldView-2 (WV2) scenes acquired in 2013-2014 at 2m spatial resolution. In particular, given the spatial detail offered by WV2 imagery, it was possible to delineate with a very high degree of confidence all the buildings and other impervious surfaces included in the different investigated areas. Details about acquisition date and size are reported in Table 6, along with the overall number of final 30x30m validation samples derived for the validation exercise. Such a task demanded a lot of manual interactions and transferring it to other AOIs would require extensive efforts; however, it can be reasonably assumed that the final quality assessment figures (computed on the basis of more than 1.9 million validation samples) shall be considered representative also for PIS maps generated in the framework of EO4SD-Urban. Table 6 reports the quantitative results of the comparison between the PIS maps generated using Landsat-7/8 data acquired in 2013-2014 and the WV2-based reference PIS maps. In particular, the considered approach allowed to obtain a mean correlation of 0.8271 and average ME and MAE equal to -0.09 and 13.33, respectively, hence assessing the great effectiveness of the Landsat-based PIS products. However, it is worth also pointing out that due to the different acquisition geometries, WV2 and LS8 images generally exhibit a very small shift. Nevertheless, despite limited, such displacement often results in a one-pixel shift between the Landsat-based PIS and the WV2-based reference PIS aggregated at 30m resolution. This somehow affects the computation of the MAE and of the correlation coefficient (which however yet resulted in highly satisfactory values). Instead, the bias does not alter the ME, which always exhibited values close to 0, thus confirming the capabilities of the technique and the reliability of the final products.

Table 6: Acquisition dates and size of the WV2 images available for the 5 test sites analysed in the validation exercise along with the number of corresponding 30x30m validation samples.

	Acquisition Date [DD.MM.YYYY]	Original Size [2x2m pixel]	Validation Samples [30x30m unit]
Antwerp	31.07.2014	5404 x 7844	188.280
Helsinki	21.04.2014	12468 x 9323	516.882
London	28.08.2013	7992 x 8832	313.937
Madrid	20.12.2013	10094 x 13105	588.202
Milan	14.05.2014	8418 x 7957	297.330

3.3.4 Accuracy Assessment of the Flood Extent Product

The Accuracy Assessment of the Flood Extent product was performed only for the flood events for which Google Earth VHR images are available for performing the extraction of the reference dataset by independent visual interpretation. Sampling points are selected for each event to ensure a representative sampling for evaluating the product accuracy. Flood event periods are:

- August 2009
- October 2011
- August 2012
- October 2013
- November 2016
- October 2017
- November 2018

Single-stage stratified random sampling approach was implemented. For each event, 15 sampling points were randomly selected within the flood extent extracted by the producer (stratum 1), and additional 10 points within a buffer area of 200 meters (stratum 2). The samples selected for each event and combined in a single layer are illustrated in Figure 4.

In this way, the reference information was extracted for each sample point by visual interpretation of the VHR data made available to image analysis expert. Then, the results were compiled through confusion matrices allowing to calculate the overall thematic accuracy for each event. The results of the accuracy assessment for the whole series of flood events are presented in Table 7.Table 7: Results of the accuracy assessment of flood extents in Saint Louis - Overall Accuracy 90.86 %.

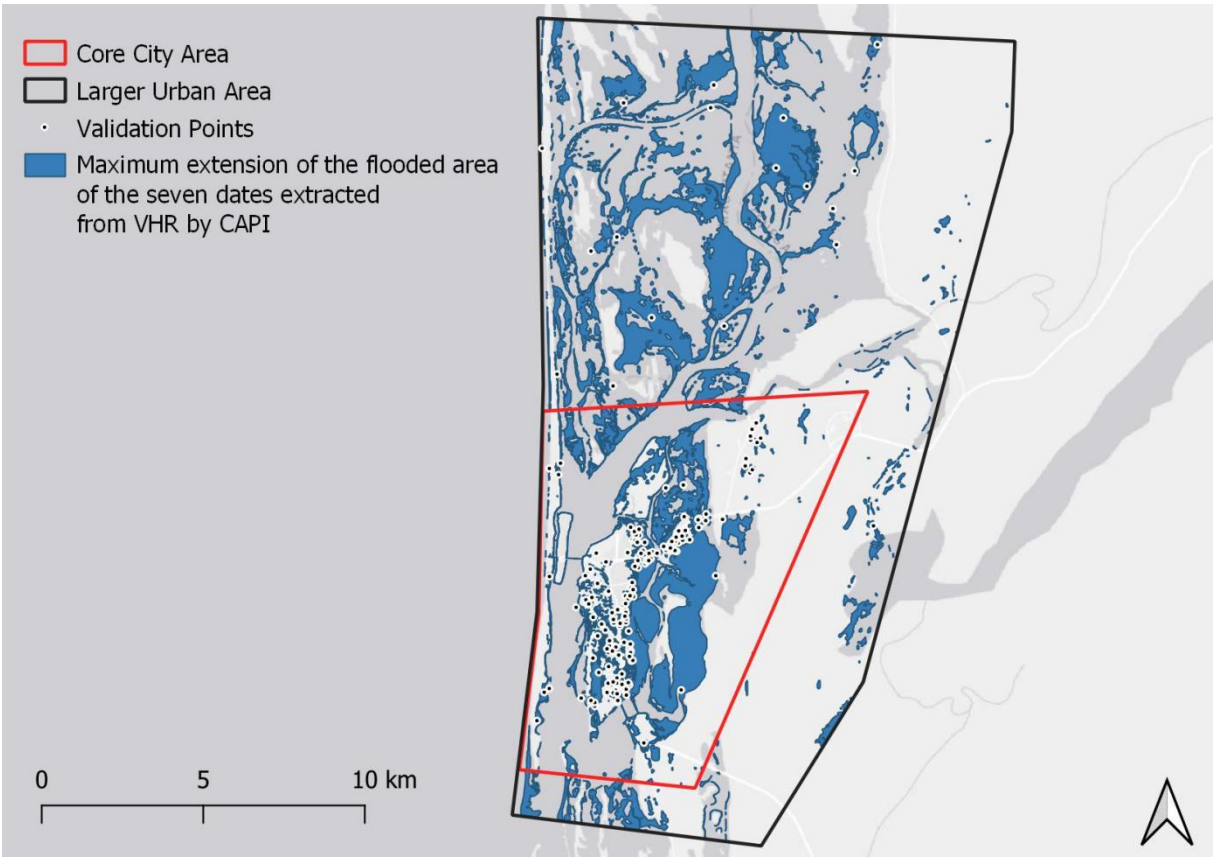

Figure 4: Result of the Flood extent mapping in Saint Louis with sampling points used for product validation.

Table 7: Results of the accuracy assessment of flood extents in Saint Louis - Overall Accuracy 90.86 %.

Flood Extent Dates extracted by CAPI	Reference Data		Totals
	Non flooded area	Flooded area	
Non flooded area	62	8	**70**
Flooded area	8	97	**105**
Totals	**70**	**105**	**175**

The number of samples which were correctly and not correctly classified is made clearly visible, allowing the calculation of the overall accuracy, the user and producer accuracies for each class, as well as the confidence interval at 95% confidence level. The matrices and analysis results for the whole series of events and for each of them are made available in Annex 3.

3.4 Quality Control/Assurance

A detailed Quality Control and Quality Assurance (QC/QA) system has been developed which records and documents all quality relevant processes ranging from the agreed product requirements, the different types of input data and their quality as well as the subsequent processing and accuracy assessment steps. The main goal of the QC/QA procedures was the verification of the completeness, logical consistency, geometric and thematic accuracy and that metadata are following ISO standards on geographic data quality and INSPIRE data specifications. These assessments were recorded in Data Quality Sheets which are provided in Annex 3. The QC/QA procedures were based on an assessment of a series of relevant data elements and processing steps which are part of the categories listed below:

- Product requirements;
- Specifications of input data: EO data, in-situ data, ancillary data;
- Data quality checks: EO data quality, in-situ data quality, ancillary data quality;
- Geometric correction, geometric accuracy, data fusion (if applicable), data processing;
- Thematic processing: classification, plausibility checks;
- Accuracy: thematic accuracy, error matrices
- Delivery checks: completeness, compliancy with requirements

After each intermediate processing step a QC/QA was performed to evaluate products appropriateness for the subsequent processing (see Figure 5).

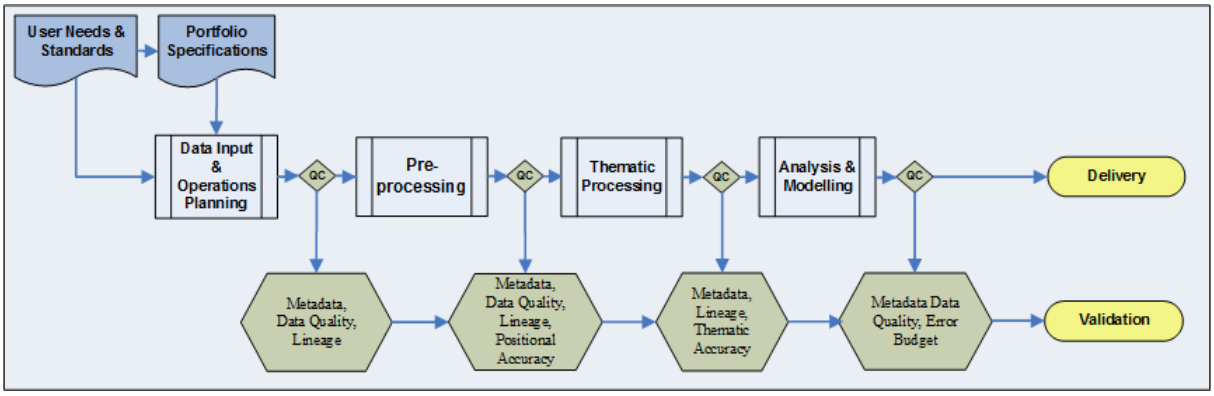

Figure 5: Quality Control process for EO4SD-Urban product generation. At each intermediate processing step output properties are compared against pre-defined requirements.

After the initial definition of the product specifications (output) necessary input data were defined and acquired. Input data include all satellite data and reference data e.g. in-situ data, reference maps, topographic data, relevant studies, existing standards and specifications, statistics. These input data were the baseline for the subsequent processing and therefore all input data had to be checked for **completeness**, **accuracy** and **consistency**. The evaluation of the quality of input data provides confidence of their suitability for further use (e.g. comparison with actual data) in the subsequent processing line. Data processing towards the end-product required multiple intermediate processing steps. To guarantee a traceable and quality assured map production the QC/QA assessment was performed and documented by personnel responsible for the Quality Control/Assurance. The results of all relevant steps provided information of the acceptance status of a dataset/product.

The documentation is furthermore important to provide a comprehensive and transparent summary of each production step and the changes made to the input data. With this information the user will be able to evaluate the provided services and products. Especially the accuracy assessment of map products and the related error matrices are highly important to rate the quality and compare map products from different service providers.

The finalised QC/QA forms are attached in Annex 3.

3.5 Metadata

Metadata provides additional information about the delivered products to enable it to be better understood. In the current project a harmonised approach to provide metadata in a standardised format applicable to all products and end-users was adopted. Metadata are provided as XML files, compliant to the ISO standard 19115 "Metadata" and ISO 19139 "XML Scheme Implementation". The metadata files have been created and validated by the GIS/IP-operator for each map product with the Infrastructure for Spatial Information in Europe (INSPIRE) Metadata Editor available at: http://inspire-geoportal.ec.europa.eu/editor/.

The European Community enacted a Directive in 2007 for the creation of a common geo-data infrastructure to provide a consistent metadata scheme for geospatial services and products that could be used not only in Europe but globally. The geospatial infrastructure called INSPIRE was built in a close relation to existing International Organization for Standardization (ISO) standards. These are ISO 191115, ISO 19119 and ISO 15836. The primary incentive of INSPIRE is to facilitate the use and sharing of spatial information by providing key elements and guidelines for the creation of metadata for geospatial products and services.

The INSPIRE Metadata provides a core set of metadata elements which are part of all the delivered geo-spatial products to the users. Furthermore, the metadata elements provide elements that are necessary to perform queries, store and relocate data in an efficient manner. The minimum required information is specified in the Commission Regulation (EC) No 1205/2008 of 3 December 2008 and contains 10 elements:

- Information on overall Product in terms of: Point of contact for product generation, date of creation
- Identification of Product: Resource title, Abstract (a short description of product) and Locator
- Classification of Spatial Data
- Keywords (that define the product)
- Geographic information: Area Coverage of the Product
- Temporal Reference: Temporal extent; date of publication; date of last revision; date of creation
- Quality and Validity: Lineage, spatial resolution
- Conformity: degree of conformance to specifications
- Data access constraints or Limitations
- Responsible party: contact details and role of contact group/person

These elements (not exhaustive) constitute the core information that has to be provided to meet the minimum requirements for Metadata compliancy. Each element and its sub-categories or elements have specific definitions; for example, in the element “Quality” there is a component called “Lineage” which has a specific definition as follows: “a statement on process history and/or overall quality of the spatial data set. Where appropriate it may include a statement whether the data set has been validated or quality assured, whether it is the official version (if multiple versions exist), and whether it has legal validity. The value domain of this element is free text,” (INSPIRE Metadata Technical Guidelines, 2013). The detailed information on the Metadata elements and their definitions can be found in the “INSPIRE Metadata Implementing Rules: Technical Guidelines,” (2013). Each of the EO4SD-Urban products will be accompanied by such a descriptive metadata file. It should be noted that the internal use of metadata in these institutions might not be established at an operational level, but the file format (*.xml) and the web accessibility of data viewers enable for the full utility of the metadata.

4 Analysis of Mapping Results

This Chapter presents and assesses all results that have been produced within the framework of the current project. Especially, it provides the results of some standard analytics undertaken with these products including the following:

- Settlement Extent – Developments from 2000, 2005, 2010 to 2015
- Land Use / Land Cover - Status and Trends between 2003/2006 and 2018

It is envisaged that these analytics provide information on general trends and developments in the Core and Peri-Urban areas, which can then be further interpreted and used by Urban planners and the City Authorities for city planning.

It should be noted that all digital data sets for these products are provided in concurrence with this City Report with all the related metadata and Quality Control documentation.

4.1 Settlement Extent – Developments 2000, 2005, 2010 and 2015

The Urban or World Settlement Extent (WSE) product in the EO4SD-Urban project is provided by the German Aerospace Centre (DLR) and is provided for 4 points in time; this product and its accuracy was described in Section 2.5 and 3.3.2. In the current project, the Urban Extent product for Saint Louis was first used to assess historical developments from 2000-2015 (see Figure 6 and Figure 7). Further analysis by overlaying administrative boundaries can be performed to assess urbanisation extent patterns based on administrative units.

Figure 6: Settlement Extent developments in the epochs 2000 to 2005, 2005 to 2010 and 2010 to 2015 in Saint Louis and surrounding region.

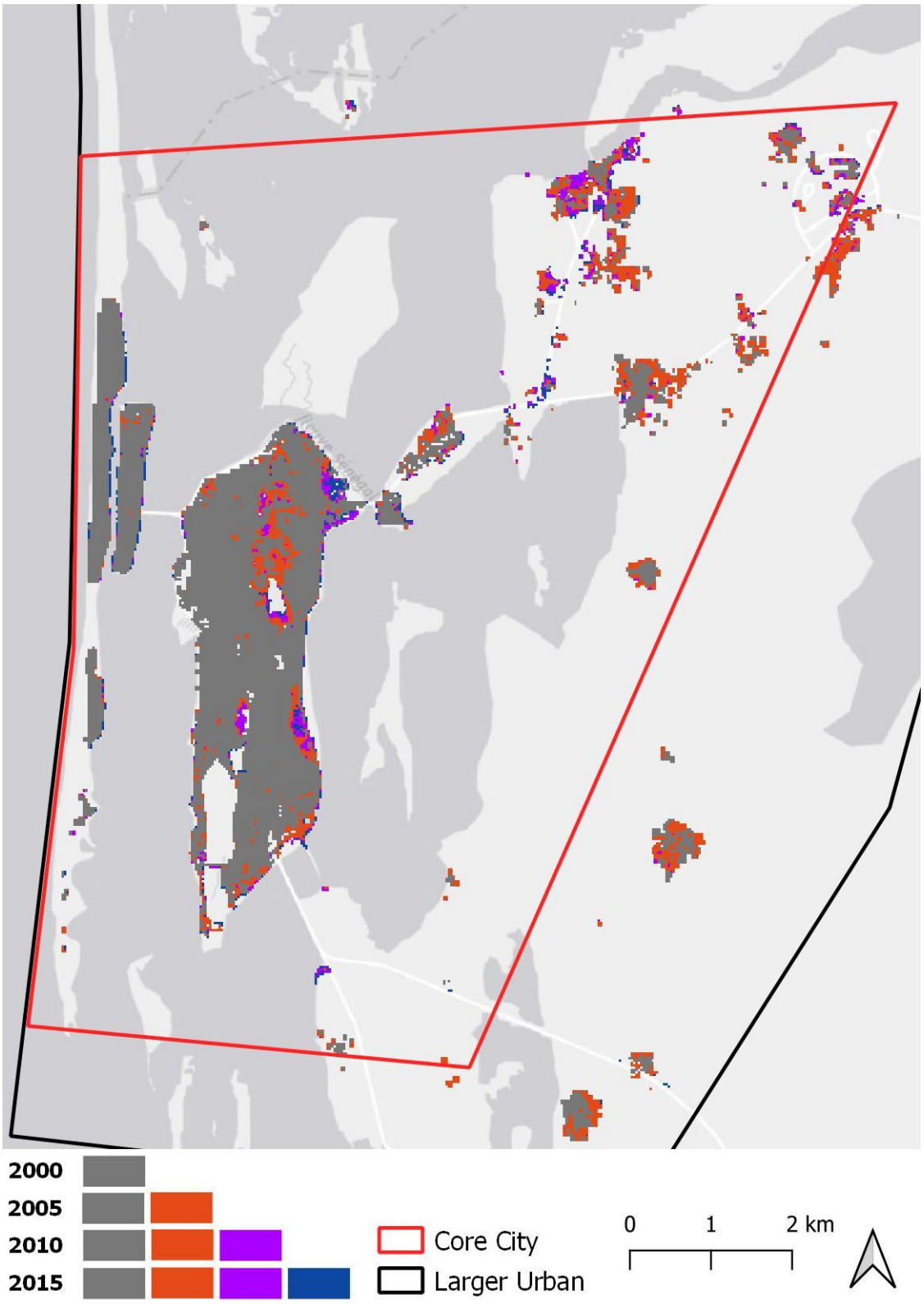

Figure 7: Settlement Extent developments in the epochs 2000 to 2005, 2005 to 2010 and 2010 to 2015 in Saint Louis within the High Density Area.

4.2 Land Use / Land Cover 2003/2006 and 2018

This Section presents the results of the LU/LC mapping for the Historic and Current status as well the statistical information on the changes between these two epochs, first for the Core City Area, and then for the Larger Urban Area.

4.2.1 LU/LC Mapping for Core City Area

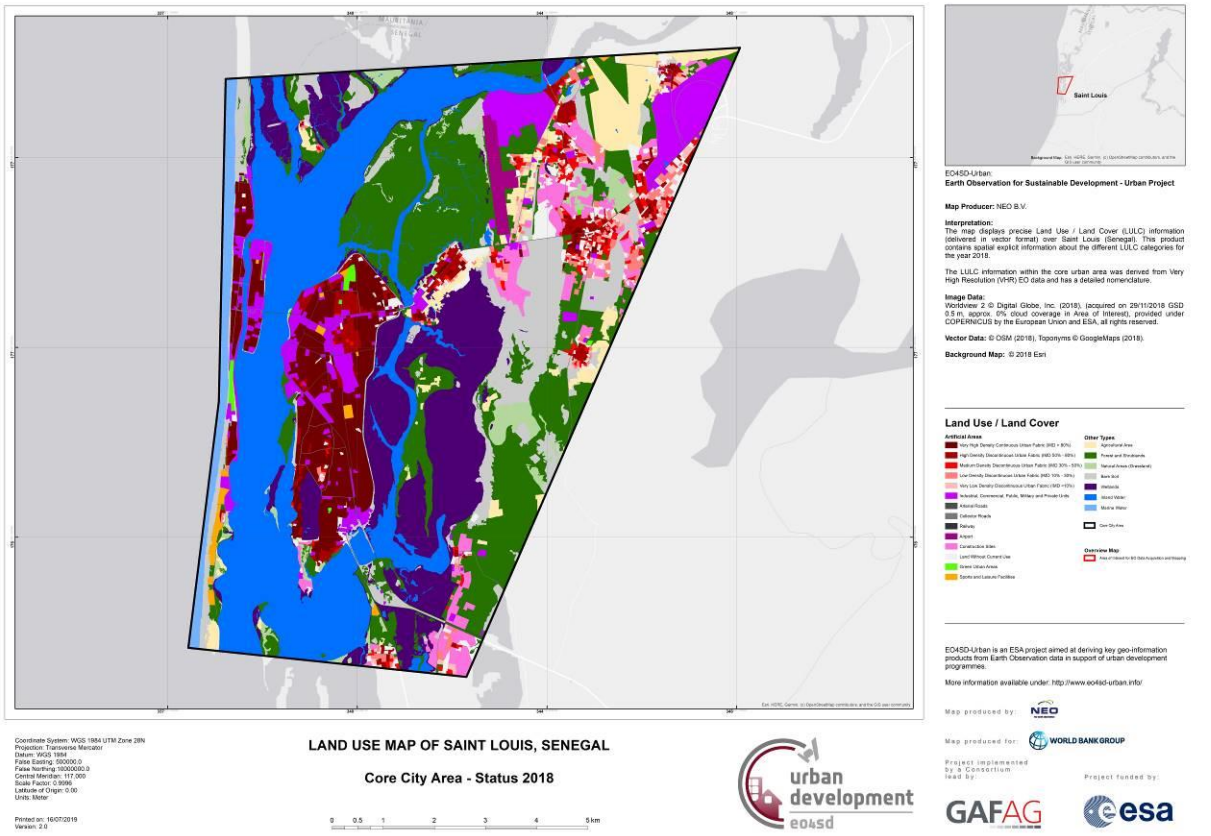

Figure 8: Core City Area - Detailed LU/LC 2018 in Saint Louis.

The LU/LC map generated for 2018 reference year is depicted in Figure 8 for the Core City area. A cartographic version of the map layout is provided as a pdf file in addition to the geo-spatial product.

The Core City Area regroups the more densified parts of Saint-Louis (Sor, Khor), going from the coast on the west (Langue de barbarie), also highly densified, to the east to the Banga and Ngallèl areas, less densified.

The major land cover is from no artificial surfaces, with approximatively 75% of the area. The water surfaces represent above 25% of the total, with also a significant presence of wetlands at 14% (tidal marshes inside the Backwater of Khor). Inside the artificial areas, green urban areas are rare, mainly corresponding to cemeteries (less than 1% of the Core City Area). Activities, public and private units represents around 6% of surfaces instead of up of 12% of the residential blocks. Remarkable units are the Saint-Louis Airport on the north alongside the Momar Gary Military Camp, and the Gaston Berger University on the east of the area.

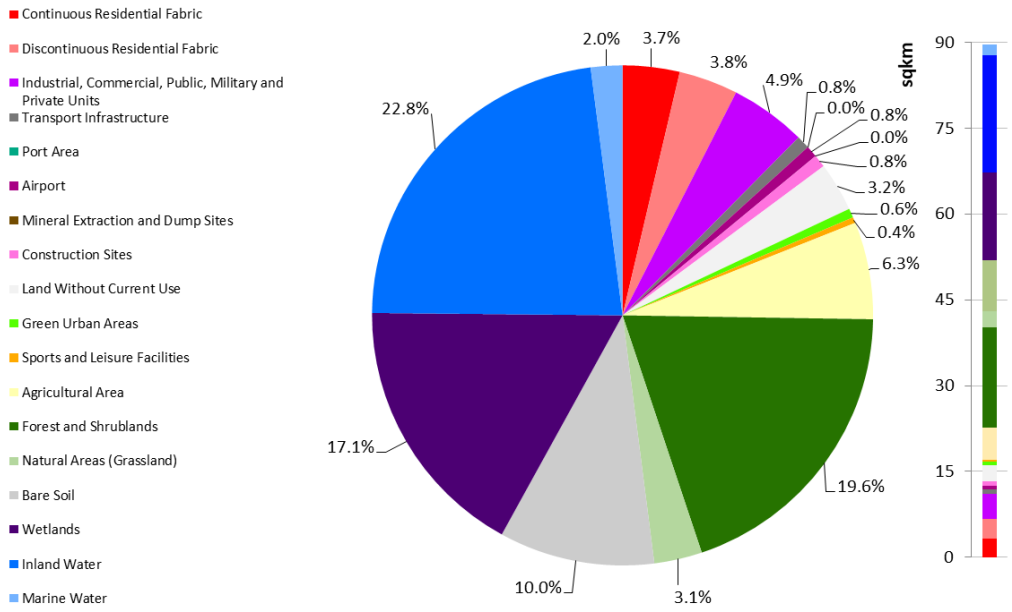

Figure 9: Core City Area - Detailed LU/LC 2003 structure, in % (left) and km² (right).

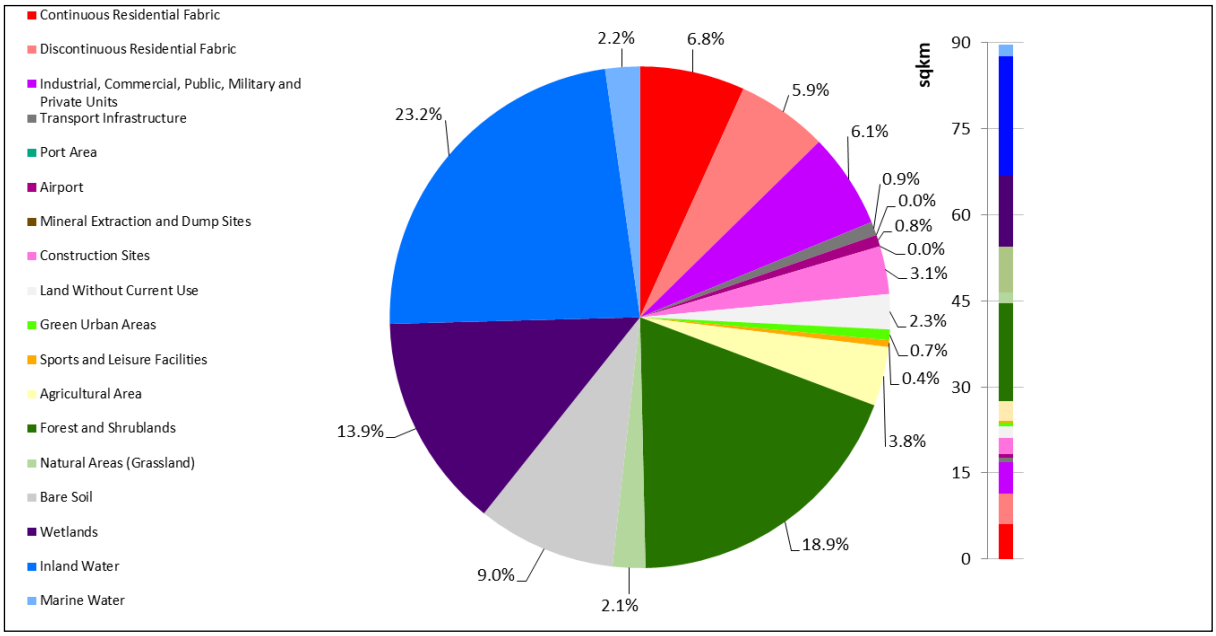

Figure 10: Core City Area - Detailed LU/LC 2018 structure, in % (left) and km² (right).

Figure 9 and Figure 10 provide more detailed information on the class disaggregation and area coverage for the epochs 2003 and 2018.

Description of LULC Changes:

In addition to the overall LU/LC classification for the two epochs it is interesting to assess the different trends between classes over the 15 year time period. The quantitative figures for each class are first provided in Table 8 for the Core City area to get an overview. The next Section will highlight the LU/LC change information between the two epochs in more detail.

Table 8: Detailed information on area and percentage of total area for each class for 2003 and 2018 as well as the changes for the Core City area

LU/LC Classes	2018		2003		Change		Change per Year	
	sqkm	% of total	sqkm	% of total	sqkm	%	sqkm	%
1110 - Continuous Urban Fabric (80 - 100 % Sealed)	6.07	6.81%	3.29	3.68%	2.79	84.8%	0.23	7.1%
1121 - Discontinuous dense urban fabric (50 - 80 % Sealed)	2.34	2.62%	1.86	2.09%	0.48	25.7%	0.04	2.1%
1122 - Discontinuous medium density urban fabric (30 - 50 % Sealed)	0.93	1.04%	0.75	0.84%	0.19	25.0%	0.02	2.1%
1123 - Discontinuous low density urban fabric (10 - 30 % Sealed)	1.35	1.52%	0.55	0.62%	0.80	144.1%	0.07	12.0%
1124 - Discontinuous very low density urban fabric (0 - 10 % Sealed)	0.66	0.74%	0.25	0.29%	0.40	158.6%	0.03	13.2%
1210 - Industrial, Commercial, Public, Military and Private Units	5.49	6.15%	4.40	4.93%	1.09	24.7%	0.09	2.1%
1221 - Arterial Roads	0.31	0.35%	0.31	0.35%	0.00	0.0%	0.00	0.0%
1222 - Collector Roads	0.45	0.51%	0.43	0.48%	0.03	6.0%	0.00	0.5%
1223 - Railway	0.02	0.02%	0.02	0.02%	0.00	0.0%	0.00	0.0%
1240 - Airport	0.67	0.76%	0.67	0.76%	0.00	0.0%	0.00	0.0%
1330 - Construction Sites	2.77	3.10%	0.74	0.83%	2.03	275.6%	0.17	23.0%
1340 - Land Without Current Use	2.03	2.27%	2.84	3.19%	-0.82	-28.7%	-0.07	-2.4%
1410 - Green Urban Areas	0.22	0.24%	0.19	0.22%	0.02	12.8%	0.00	1.1%
1420 - Sports and Leisure Facilities	0.39	0.44%	0.34	0.38%	0.06	17.1%	0.00	1.4%
2000 - Agricultural Area	3.41	3.83%	5.63	6.31%	-2.21	-39.3%	-0.18	-3.3%
3100 - Forest and Shrublands	16.97	19.02%	17.57	19.70%	-0.60	-3.4%	-0.05	-0.3%
3200 - Natural Areas (Grassland)	1.89	2.12%	2.77	3.11%	-0.88	-31.6%	-0.07	-2.6%
3300 - Bare Soil	8.02	8.99%	8.99	10.07%	-0.97	-10.8%	-0.08	-0.9%
4000 - Wetlands	12.42	13.92%	15.35	17.21%	-2.93	-19.1%	-0.24	-1.6%
5100 - Inland Water	20.77	23.29%	20.42	22.89%	0.35	1.7%	0.03	0.1%
5200 - Marine Water	2.00	2.25%	1.82	2.05%	0.18	9.8%	0.01	0.8%
Total	**89.20**	**100%**	**89.20**	**100%**	-	-	-	-

The main change between the two epochs comes from agriculture whose area was reduced by near 40% in comparison with the situation in 2003, mainly in favour of the urban expansion on the east part (Banga and Ngallèl areas). Inside the main urban area of Saint-Louis, two main changes occurred over time: residential densification and constructions on land without use in 2003. As a result, this area is almost completely covered by artificial surfaces. Finally, in the south-east of the Core City Area, very low density urban fabric units were settled, which explains the decrease of shrublands.

4.2.2 Spatial Distribution of Main LU/LC Change Categories for Core City Area

In order to better analyze the growth trends and the spatial distribution of changes, meaningful aggregations of the Core city area LU/LC classes in both epochs were used. The following categories were developed for the City Core Area:

- Urban Densification: Changes from lower Residential Density Class into a higher Residential Density class;
- Urban Residential Expansion: all changes from Non-Urban Residential classes to a Residential class;
- Other Urban Land Use Expansion: all changes from Non-Residential Urban classes to Other Urban and Non-Urban classes.
- Changes within Natural and Semi-Natural Areas: all changes in between the natural and semi-natural classes (e.g. Forest into Agriculture).

The overlay analysis of these aggregated categories of the epochs 2003 and 2018 is depicted in Figure 11 and Figure 12 for the Core City area.

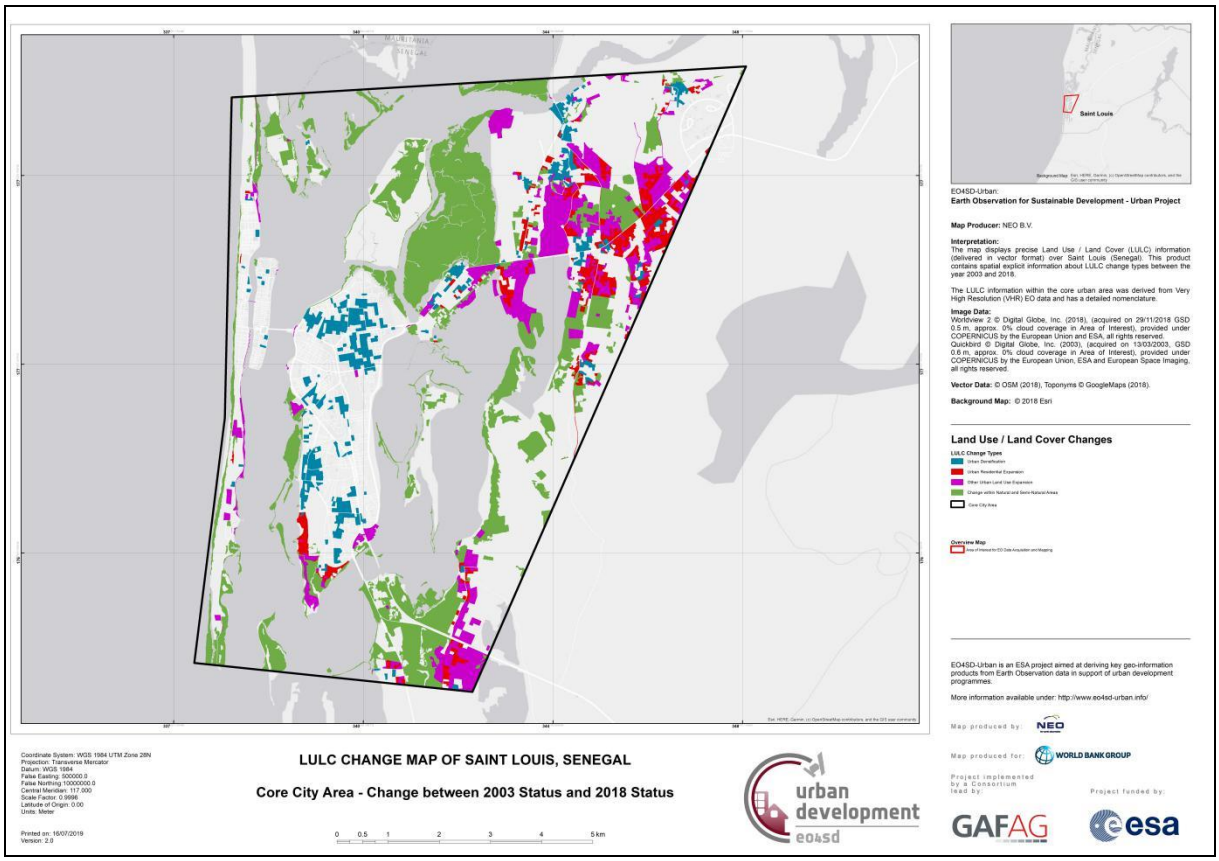

Figure 11: Core City Area – LU/LC change types and spatial distribution

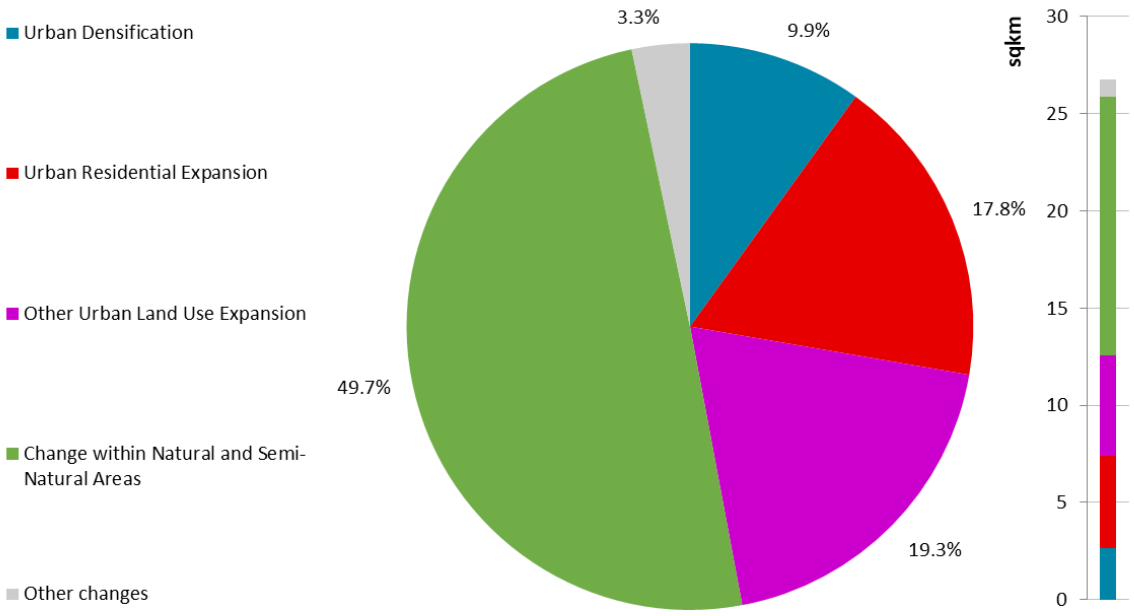

Figure 12: Core City Area – LU/LC Change types between 2003 and 2018 presented in % (left) and km² (right) in Saint Louis.

For the Core City Area, half of the changes occurred within Natural and Semi-Natural areas surrounding the city. The Urban Densification was significant mostly within the main city area of Saint-Louis (Sor) representing nearly 10% of the total, while the residential areas expanded mainly in the eastern and southern part of the area of interest representing 17.8%. Table 9 summarizes these analysis results.

Table 9: Overall Main LU/LC Changes Statistics for the Core City Area.

Change Classes	Change Core city area	
	sqkm	**%**
Urban Densification	2.66	9.9%
Urban Residential Expansion	4.75	17.8%
Other Urban Land Use Expansion	5.17	19.3%
Change within Natural and Semi-Natural Areas	13.27	49.7%
Other changes	0.88	3.3%
Total	**26.7**	**100%**

4.2.3 LU/LC Mapping for Larger Urban Area

The LU/LC for 2018 is depicted in Figure 13 for the Larger Urban area. A cartographic version of the map layout is provided as a PDF file in addition to the geo-spatial product.

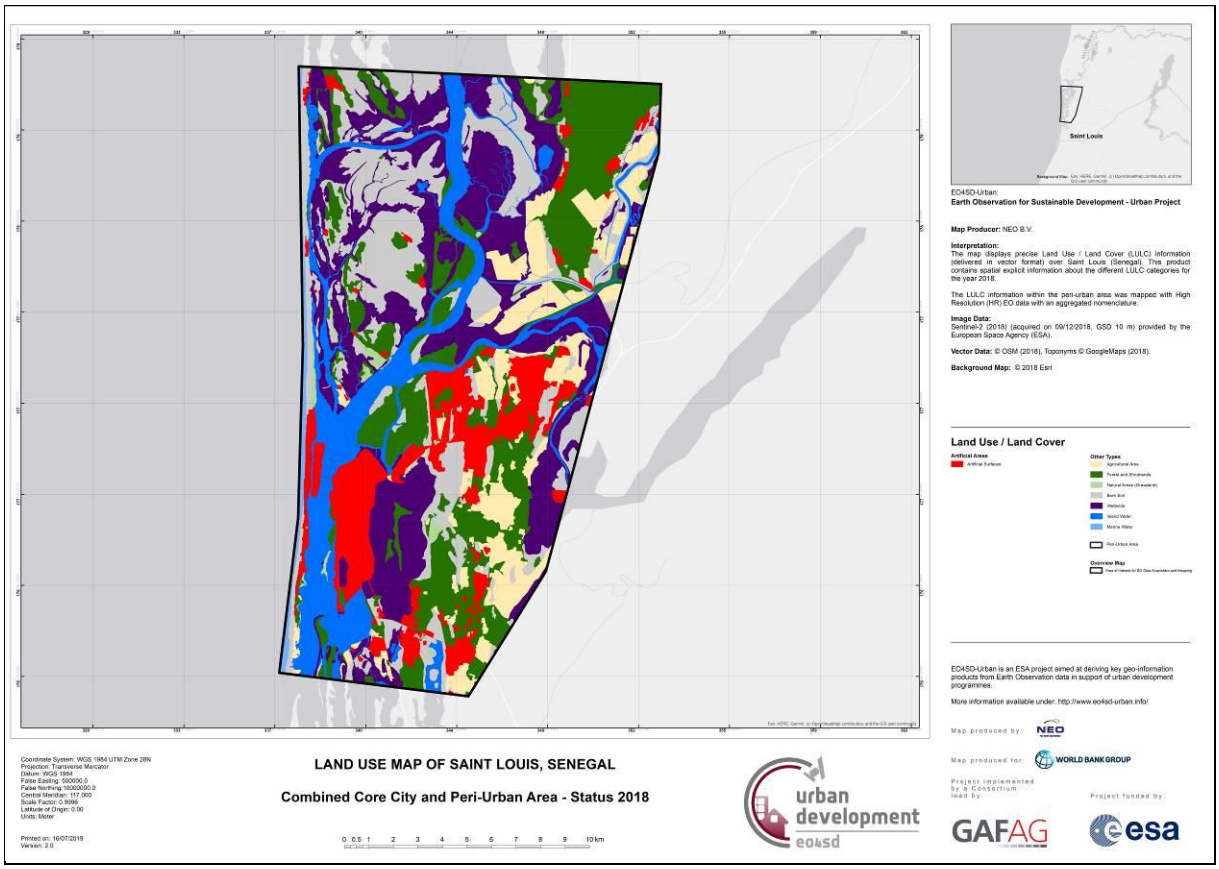

Figure 13: Larger Urban area – LU/LC 2018 in Saint Louis.

Regarding the larger urban area of Saint-Louis, the LU/LC is mainly composed by wetlands (24%) alongside the Senegal and N'Galam Rivers and tidal marshes of Backwater of Khor, followed by bare soil surfaces (20%) and forests and shrublands representing 20% of the total area too. Agricultural areas (with rice fields in the north east) represent around 10%, as well as the artificial surfaces. Outside the Core City Area, only isolated settlements are present in the north of the larger urban area.

Figure 14 and Figure 15 provide more detailed information on the class disaggregation and area coverage for the epochs 2003 and 2018.

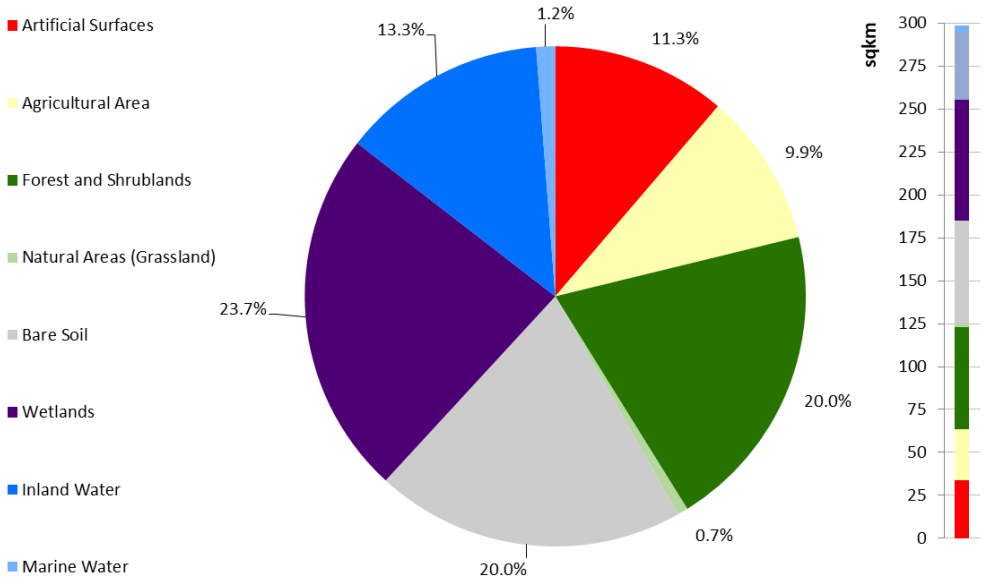

Figure 14: Larger Urban Area - Detailed LU/LC 2018 structure presented in % (left) and km² (right).

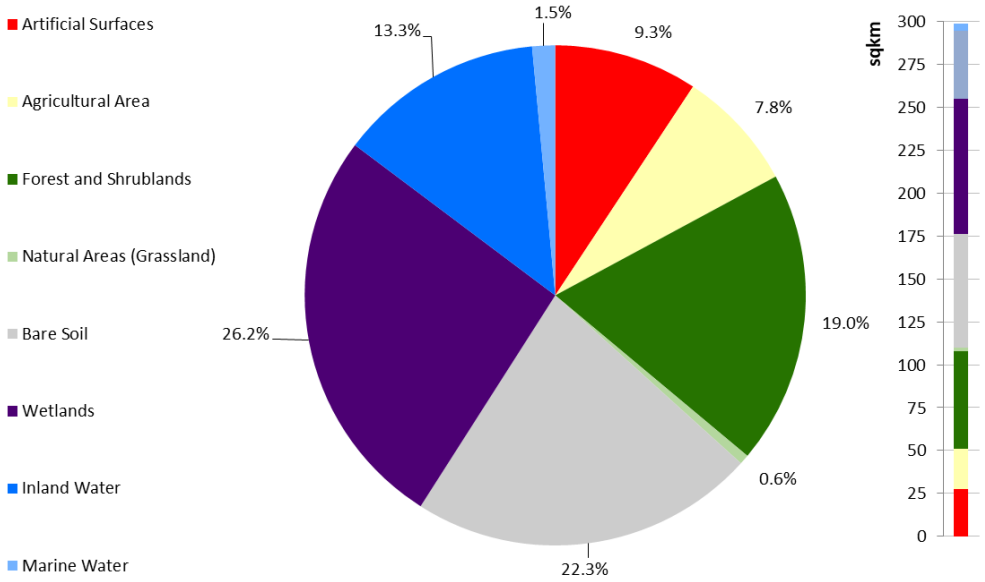

Figure 15: Larger Urban Area - Detailed LU/LC 2006 structure presented in % (left) and km² (right).

Description of LULC Changes:

In addition to the overall LU/LC classification for the two epochs it is interesting to assess the different trends between classes over the 15 year time period. The quantitative figures for each class are first provided in Table 10 for the Larger Urban area to get an overview.

Major evolutions are the Agricultural Areas increasing in the north east part of Larger Urban Area (+26.5%), as well as the artificial surfaces (+21.3%). Inversely, the area covered by bare soil and wetlands has been reduced by 10% more or less between 2006 and 2018.

Table 10: Larger Urban Area - Detailed information on area and percentage of total area for each class for 2006 and 2018 as well as the changes.

LU/LC Classes	2018		2006		Change		Change per Year	
	sqkm	% of total	sqkm	% of total	sqkm	%	sqkm	%
Artificial Surfaces	33.62	11.3%	27.71	9.3%	5.91	21.3%	0.49	1.8%
Agricultural Area	29.67	9.9%	23.45	7.8%	6.22	26.5%	0.52	2.2%
Forest and Shrublands	59.71	20.0%	56.68	19.0%	3.03	5.3%	0.25	0.4%
Natural Areas (Grassland)	2.04	0.7%	1.87	0.6%	0.17	9.0%	0.01	0.7%
Bare Soil	59.72	20.0%	66.68	22.3%	-6.96	-10.4%	-0.58	-0.9%
Wetlands	70.70	23.7%	78.37	26.2%	-7.68	-9.8%	-0.64	-0.8%
Inland Water	39.70	13.3%	39.63	13.3%	0.07	0.2%	0.01	0.0%
Marine Water	3.65	1.2%	4.42	1.5%	-0.77	-17.4%	-0.06	-1.5%
Total	298.81	100.0%	298.81	100.0%	-	-	-	-

4.2.4 Spatial Distribution of Main LU/LC Change Categories for Larger Urban Area

In order to better analyze the trends and the spatial distribution of changes, meaningful aggregations of the Larger Urban Area LU/LC classes in both epochs were used. The following categories were developed:

- Artificial Surface Expansion: all changes from non-artificial surfaces to artificial surface class
- Changes within Natural and Semi-Natural Areas: all changes in between the natural and semi-natural classes (e.g. Forest to Agriculture).

The overlay analysis of these aggregated categories of the epochs 2006 and 2018 is depicted in Figure 16 and Figure 17 for the Larger Urban Area. Table 11 summarizes the analysis results.

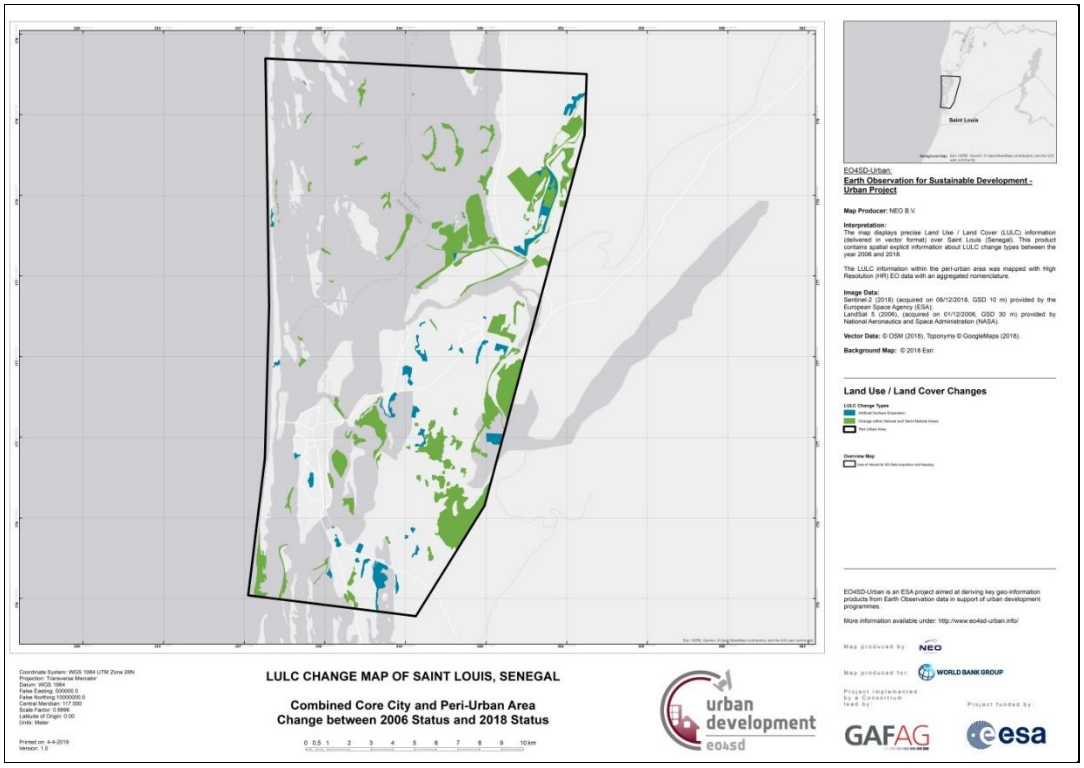

Figure 16: Larger Urban Area – LU/LC Change types and spatial distribution.

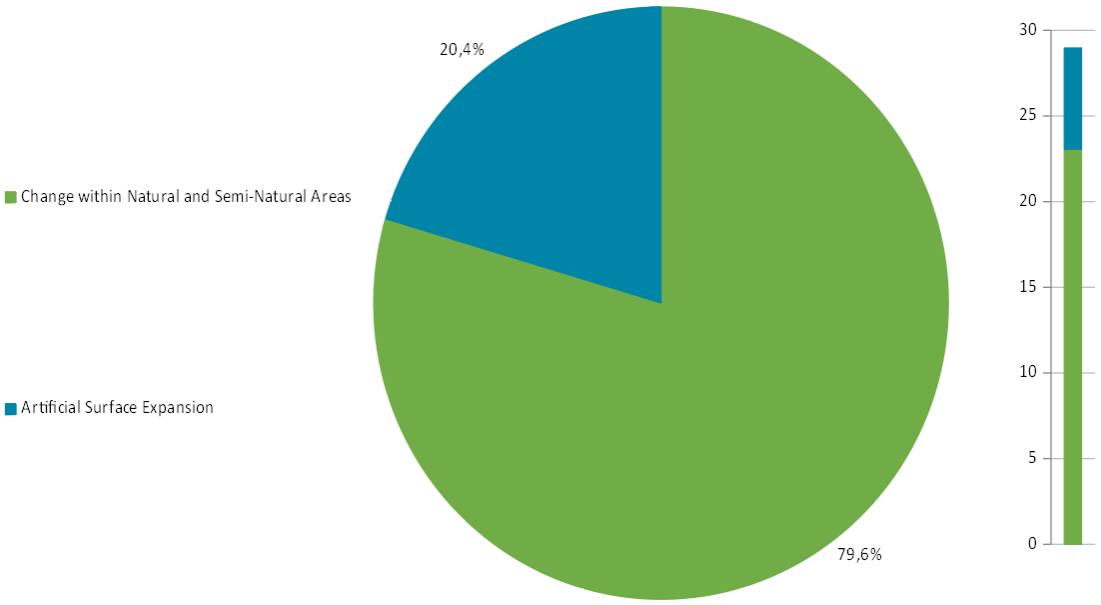

Figure 17: Larger Urban Area – LU/LC Change types 2006 -2018 area in % (left) and km² (right)

The artificial expansion especially concerns the main part of Saint Louis as well as the south of Larger Urban Area, like described in section 4.2.2 concerning the changes inside the Core City Area. For the changes inside Natural and Semi-Natural Areas, it concerns mainly a transition from wetlands to shrublands, and shrublands to agricultural areas.

Table 11: Overall LU/LC statistics of the Larger Urban area.

Change Classes	Change Larger urban area	
	sqkm	**%**
Artificial Surface Expansion	5.91	20..4%
Change within Natural and Semi-Natural Areas	23.06	79.6%
Total	**21.97**	**100%**

4.2.5 **Changes of Agricultural Areas**

Even if agriculture land globally increased in the Larger Urban Area over the period, mainly in the north-eastern part, it has been reduced in the Core City Area due to urban expansion as noted previously. In order to analyze this relatively large loss of agricultural areas, further change analysis was performed and the following categories were developed for this purpose:

- Agriculture to Artificial Surface (Class 2000 to 1000)
- Agriculture to Natural Area (Class 2000 to 3200)
- Agriculture to Forest and Shrublands (Class 2000 to 3100)

The spatial distribution of these changes is displayed in Figure 18.

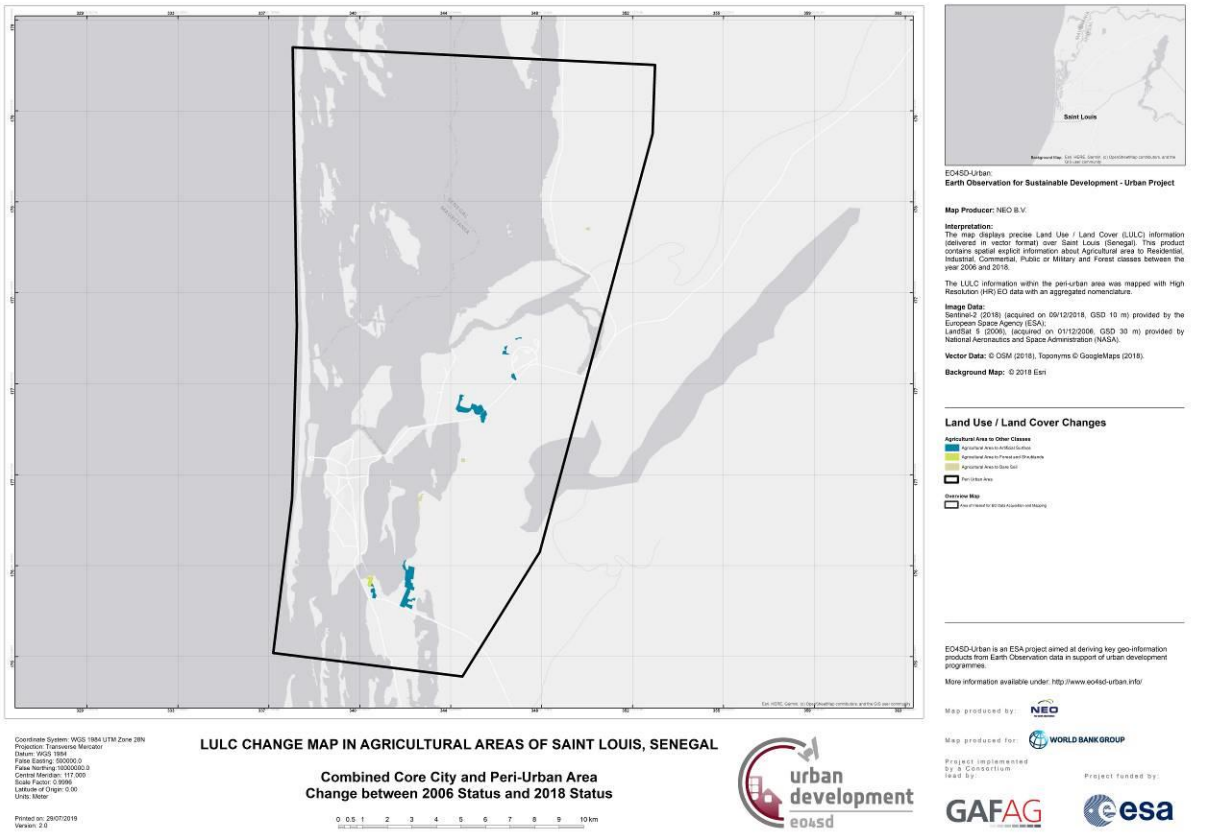

Figure 18: Larger Urban Area - Spatial distribution of changes from agricultural areas to other LU/LC classes between 2006 and 2018.

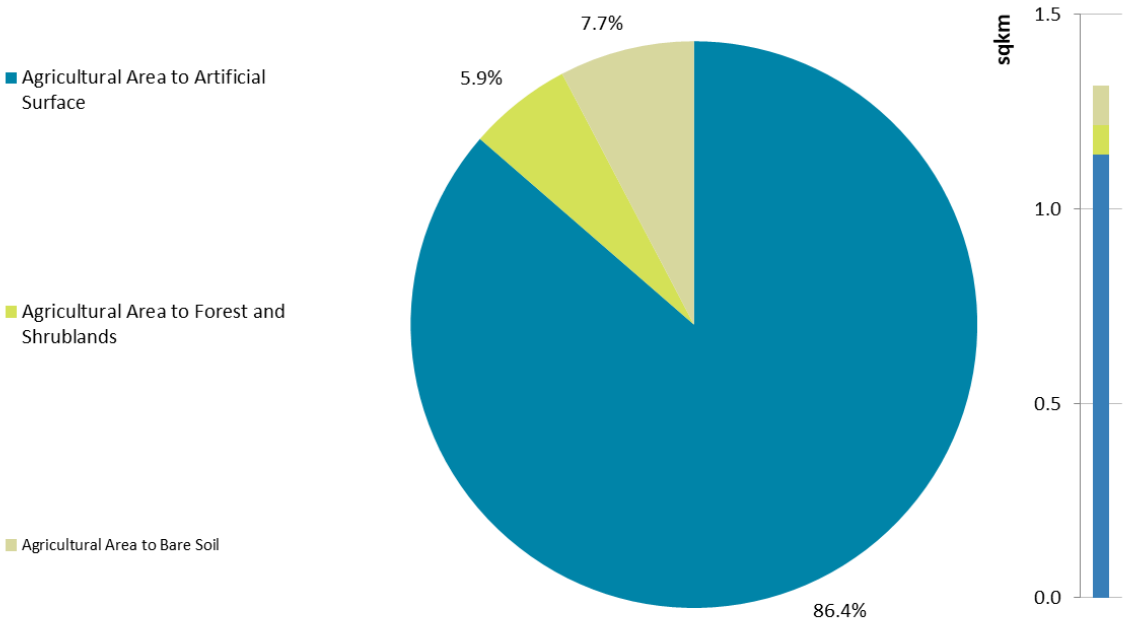

Figure 19: Larger Urban Area - Changes of agricultural areas into other LU/LC classes between 2006 and 2018 presented in % (left) and km2 (right).

Figure 18 shows that agricultural areas that have been changed into another LU/LC class are mostly located on the outskirts of the Saint Louis urban area. Figure 19 and Table 12 quantify the changes that occurred, and precise their types. Most of the changes between the two epochs concern agricultural areas that were converted into artificial surfaces (86.4%), new forests and shrublands and new bare soils only represent respectively 5.9% and 7.7% of the total change area.

Table 12: Statistics of changes of agricultural areas.

Change Classes	Change Urban Cluster	
	sqkm	**%**
Agricultural Area to Artificial Surface (1000)	1.14	86.4%
Agricultural Area to Forest and Shrublands (3100)	0.08	5.9%
Agricultural Area to Bare Soil	0.10	7.7%
Total	**1.32**	**100%**

4.3 Sustainable Development Goal 11 Indicators

A main objective of the EO4SD-Urban Product Portfolio is to support the reporting requirements of Urban Development Policies and Strategies. One of the most important policy frameworks that countries are trying to implement are the UN Sustainable Development Goals (SDGs). Seventeen SDGs were developed with a focus on "ending extreme poverty; fighting inequality & injustice; and addressing climate change," by 2030. To achieve the 17 goals there are 169 targets and for each target, indicators will be used to assess the level of achievement of the countries.

The SDG Goal 11 "Make cities and human settlements inclusive, safe, resilient and sustainable" is specifically dedicated to Sustainable Urban Development. A list of Urban Sustainability Indicators specific to the SDG Goal 11, have been defined in March 2016 by the UN and are described in the UN-Habitat "SDG Goal 11 Monitoring Framework Report (UN, 2016a)".

The EO4SD-Urban project supports seven GPSC cities, namely Bhopal and Vijayawada in India, Campeche in Mexico, Saint-Louis and Dakar in Senegal, Abidjan in Ivory Coast and Lima in Peru. For these seven cities, the indicators for which the needed input data is available were calculated and are described in the following subsections. The EO4SD-Urban products can be fully or partly used for the calculation of four SDG 11 indicators (see Table 13).

Table 13: SDG 11 indicators measurable with the support of EO4SD-Urban products.

TARGETS	INDICATORS
Target 11.1: By 2030, ensure access for all to adequate, safe and affordable housing and basic services and upgrade slums	11.1.1: Proportion of urban population living in slums, informal settlements or inadequate housing
Target 11.2: By 2030, provide access to safe, affordable, accessible and sustainable transport systems for all, improving road safety, notably by expanding public transport, with special attention to the needs of those in vulnerable situations, women, children, persons with disabilities and older persons	11.2.1: Proportion of the population that has convenient access to public transport by sex, age and persons with disabilities
Target 11.3: By 2030, enhance inclusive and sustainable urbanization and capacity for participatory, integrated and sustainable human settlement planning and management in all countries	11.3.1: Ratio of land consumption rate to population growth rate
Target 11.7: By 2030, provide universal access to safe, inclusive and accessible, green and public spaces, in particular for women and children, older persons and persons with disabilities	11.7.1: Average share of the built-up area of cities that is open space for public use for all, by sex, age and persons with disabilities

A short description of the calculation as well as the needed input data and the achieved outputs are described in the next sections for the indicators 11.2.1, 11.3.1 and 11.7.1. For Saint-Louis, it is not possible to calculate the Indicator 11.1.1, as the needed input data is not available.

More information including the exact calculation steps of each indicator are described in the UN-Habitat Methodological Guidance document to monitor and report on the SDG Goal 11 indicators (UN-Habitat, 2016).

4.3.1 SDG 11 Indicator 11.2.1

The 11.2.1 Indicator calculates the ***Proportion of the population that has convenient access to public transport by sex, age and persons with disabilities*** and describes the Target 11.2: "By 2030, provide access to safe, affordable, accessible and sustainable transport systems for all, improving road safety, notably by expanding public transport, with special attention to the needs of those in vulnerable situations, women, and children, persons with disabilities and older persons."

The indicator aims to monitor the use and access of public transportation system and move towards reaching a convenient access for all. According to UN-Habitat and described in the Methodological Guidance document (UN-Habitat, 2016) the access to public transport is considered convenient when an officially recognised stop is accessible within a distance of 0.5 km from a reference point such as home, school, workplace, market, etc.

The indicator is calculated by using the following formula:

$$\% \text{ with access to public transport} = \frac{100x \text{ (population with convenient access to public transport)}}{\text{city population}}$$

At a diagnosis phase, this indicator helps urban planners in identifying areas that are underserved and to be put as a priority in the Master Plans for the localisation of transport stations and addition of new transport lines (bus, metro, tramway, train).

Calculating this indicator considering parameters such as sex, age and persons with disabilities would require additional census data, as not available through EO data. However, the indicator can be calculated over the Larger Urban Area using the Global Human Settlement Population Layer and the OpenStreetMap (OSM) transportation features (bus and subway stations and stops, railway stations, ferry terminals), both available for the reference year 2015. It provides a first good estimate of the proportion of the population that has convenient access to public transport.

The results are presented in Figure 20 below. For comparative reasons the graphic shows the indicator results for all GPSC cities, but Bhopal and Vijayawada. The proportion of the population that has convenient access to public transport is estimated around 20% of the total population of Campeche and 30% of Abidjan and Saint-Louis, while this indicator is higher for Dakar and Lima with a value close to 50%.

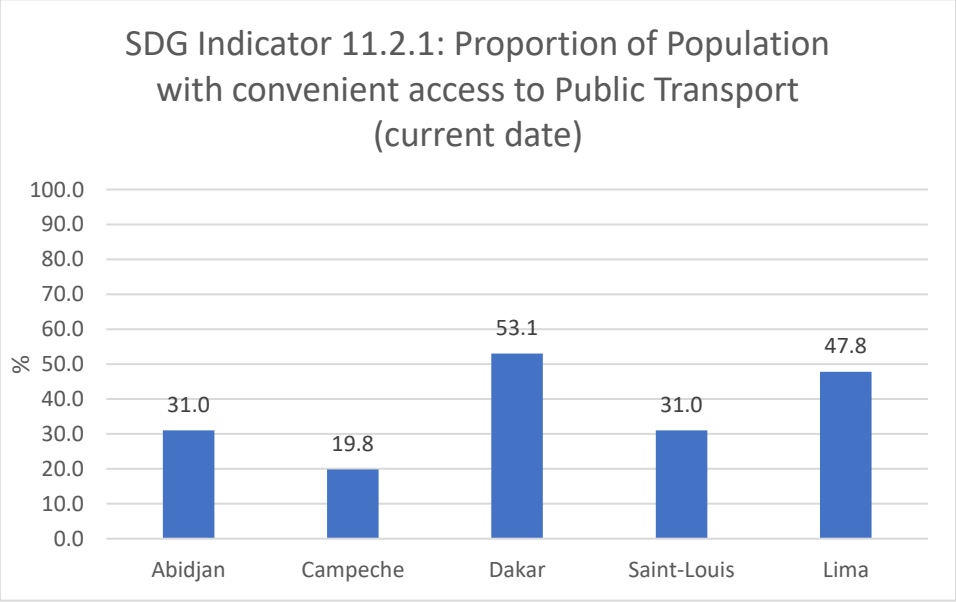

Figure 20: Proportion of population with convenient access to public transport.

4.3.2 SDG 11 Indicator 11.3.1

The 11.3.1 Indicator calculates the ***Ratio of land consumption rate to population growth rate*** and describes the Target 11.3: "By 2030, enhance inclusive and sustainable urbanization and capacity for participatory, integrated and sustainable human settlement planning and management in all countries."

The indicator needs the definition of the two components population growth and land consumption rate. According to the UN-Habitat Methodological Guidance document (UN-Habitat, 2016) the population growth rate (PGR) is the increase of population in a country during a specific period, usually one year. The PGR is expressed as a percentage of the population at the start of that period.

Further, the land consumption rate includes a) the expansion of build-up area that can be directly measured and b) the absolute extent of land that is subject to exploitation by agriculture, forestry or other economic activities and c) the over-intensive exploitation of land that is used for agriculture and forestry.

The indicator is calculated by using following formula:

$$\text{Ratio of land consumption rate to population growth rate (LCRPGR)} = \frac{\text{Land consumption rate}}{\text{Annual population growth rate}}$$

The ratio of land consumption rate to population growth rate is an indicator for measuring land use efficiently and is intended to answer the questions of whether the remaining undeveloped urban land is being developed at a rate that is less than or greater than the prevailing rate of population growth. As the ratio of land consumption rate to population growth rate is dimensionless and not straightforward in its interpretation, several countries report the urban expansion and the population growth rate in terms of percentage change instead of using the ratio values (Nicolau et. al., 2018).

In the following, the ratio (see Figure 21) and the percentage change values (see Figure 22) for all GPSC cities were calculated. For the calculation of the population growth rate the Global Human Settlement Population Layer available for the years 2000 and 2015 were used. For the calculation of the land consumption rate the built-up area extracted from the Larger Urban Area LU/LC classification is taken by dissolving all artificial classes.

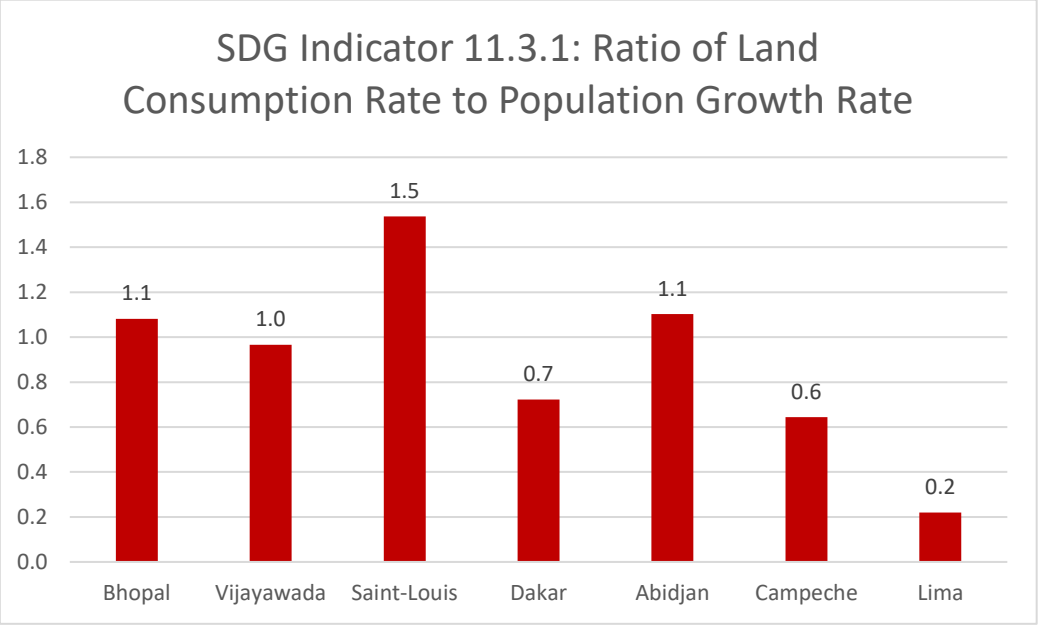

Figure 21: Ratio of land consumption rate to population growth rate between 2005 and 2015.

Figure 21 shows the ratio of land consumption rate to population growth rate for all GPSC cities. All GPSC cities are visualised in the bar chart for comparative reasons. Saint-Louis has a value significantly above one, which means that the population growth rate is lower than the land consumption rate and let assume that the land is not as efficiently used as for example in Dakar.
Indeed, Dakar, as well as Campeche and Lima, has a value significantly below one, which means that the population growth rate is higher than the land consumption rate and let assume that the land is efficiently used. Cities with values close to one have a population growth rate similar to the land consumption rate. This indicates that the land is efficiently used too.
European countries, for comparison very often have values below zero. This means that either the population or the land consumption shows a decrease.

Looking at the percentage change values of population and land consumption between 2000/2006 and 2015/2018 all cities have a growing population and a growing urban extent, which is typical for cities in developing countries. Saint-Louis' population grew by 17% between 2000 and 2015, while its land consumption grew by 21.3% between 2006 and 2018. This means that the built-up area grew faster than the population of the city and indicates also that the city seems to grow in a scattered way.

In the other GPSC cities presented, it is the other way around, i.e. the population grew faster than the land consumption, indicating that these cities had a more compact growth in the last years.

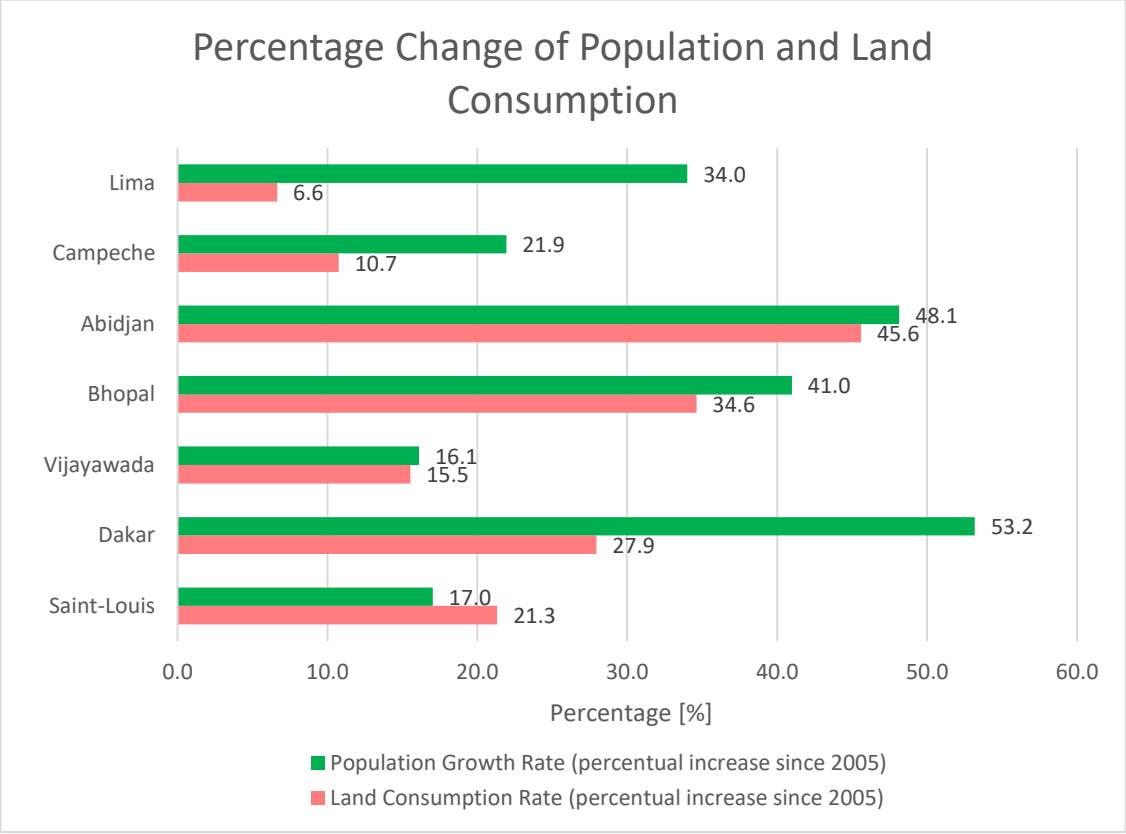

Figure 22: Percentage change of population and land consumption between 2005 and 2015.

A significant limitation of this indicator is that the approach captures only the urban extent change, not the internal city dynamics.

4.3.3 SDG 11 Indicator 11.7.1

The SDG 11 Indicator 11.7.1 ***"Average share of the built-up area of cities that is open space for public use for all, by sex, age and persons with disabilities"*** refers to the Target 11.7.: By 2030, provide universal access to safe, inclusive and accessible, green and public spaces, in particular for women and children, older persons and persons with disabilities.

The indicator aims to monitor the amount of land that is dedicated by cities for public space. According to the UN-Habitat Methodological Guidance document (UN-Habitat, 2016) public space includes open spaces and streets and should be accessible by all.

The indicator is calculated by using following formula:

$$\%\ \text{of land that is dedicated by cities for public space (open spaces and streets)} = \frac{(\text{Total surface of open public space} + \text{Total surface of land allocated to streets})}{\text{Total surface of built up area of the urban agglomeration}}$$

The share of land in public open spaces cannot be obtained directly from the use of high-resolution satellite imagery, because it is not possible to determine the ownership or use of open spaces by remote sensing. Additional metadata that helps to describe the land use patterns in the locale is additionally required to map out land that is for public and non-public use.
As this information is not available, the LU/LC classes *Urban Green Areas* and *Sports and Leisure Facilities*, which are available in the Core City Area LU/LC classification, were taken with the assumption that these places are public places and accessible by all.
To calculate the total surface of land allocated to streets, the road network was used. Different buffers were applied for three different road types (6m for Arterial Roads, 5m for Collector Roads and 3m for Local Roads) to assess the total surface of streets. The total surface of built-up area of the urban agglomeration is extracted from the LU/LC classification by summarising all artificial classes of the Core City Area.

The results are presented in Figure 23 below. For comparative reasons the graphic shows the indicator results for all GPSC cities, but Lima.
The indicator was calculated for two points in time i.e. around 2005 and 2015. In Saint-Louis, the average share of built-up area that is open space for public use decreases from 17.6% in 2006 to 14.9% in 2018. Bhopal, Vijayawada and Campeche also show a decrease, while Abidjan and Dakar show a slight increase in open spaces.

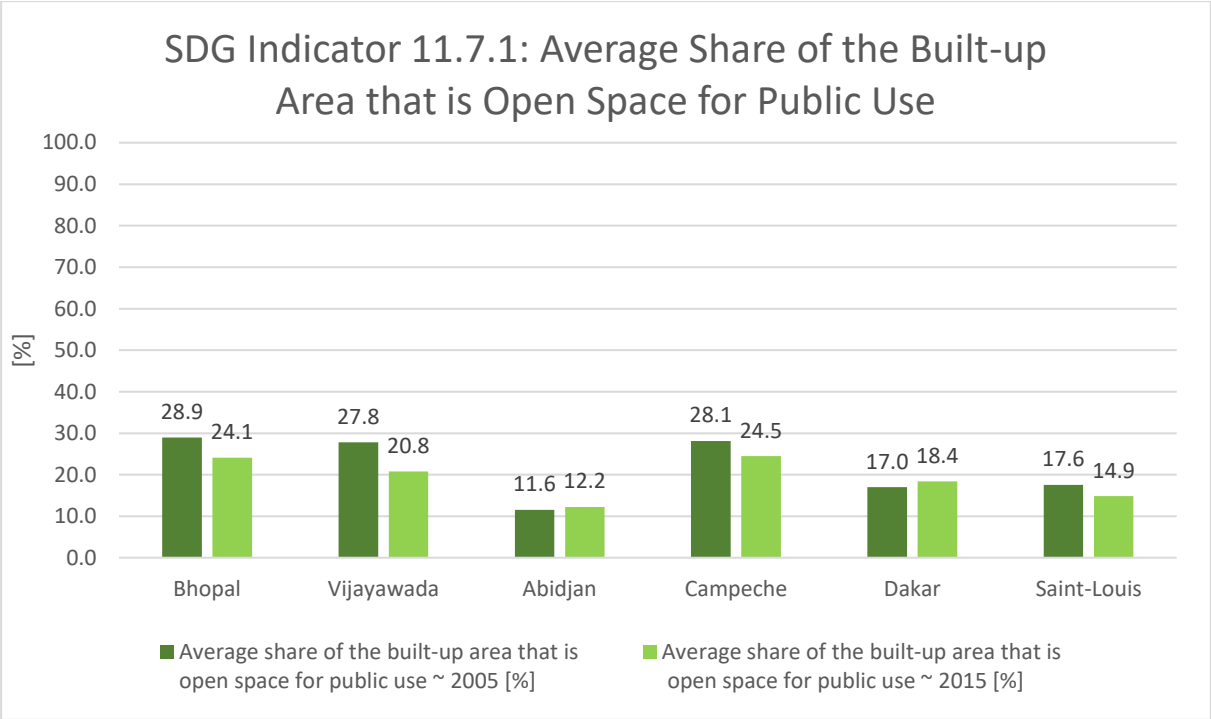

Figure 23: Average share of the built-up area that is open space for public use.

4.4 Concluding Points

This Chapter 4 presented a summary and an overview of what is possible in term of analytics with the geo-spatial datasets provided for Saint Louis in the current project. This Report is a living document and will be complemented with further analysis during the project.

5 Flood Hazard and Risk Assessment

Flood Hazard and Risk Mapping is a vital component for appropriate land use planning in flood-prone areas. First of all, Flood Hazard and Risk Maps are designed to increase awareness of the likelihood of flooding among the public, local authorities and other organisations.

Specific flood regimes and underlying causes for the flooding events in the area of interest have to be analysed carefully, as these can be very varied in different regions.

For the urban and peri-urban area of St. Louis, basically three main flood scenarios have to be considered:

a. Fluvial floods (seasonal floods from the Senegal River) after heavy tropical rains in the upper part of the catchment area

   For the Lower Senegal River Basin, the potential flood season covers the period between August and November (Kane et al. 2014, Steijn 2011).

b. Floods triggered by rainfall stagnation after heavy local cloudbursts

   According to (among others) Diagne (2007), Steijn (2011), GFDRR (2014), Vedeld et al. (2016), these floods are often connected with problems with the drainage system. The ground water table is very shallow and Saint Louis' drainage system is not yet adequate to cope with heavy rain. Furthermore, rubbish is often blocking the drains, and debris and trash clog the outlets (cf. Figure 26).

c. Floods caused by sea-level rise, tidal waves and coastal erosion - also intensified by illegal sand mining

Scenario a.) and b.) may occur at the same time.

Several reports (e.g. Seck 2010) affirm that since 1990, the city has suffered recurrent flooding due to the combination of rainwater and peak flows of the Senegalese river. The rise in the river level can be traced to a combination of factors. These include a rise in the level of the riverbed, uncontrolled urban development that has led to the shrinkage of zones that allow infiltration of rain water and a ground water table that rises to the ground level during the flooding period. This phenomenon has been accentuated after the construction of dikes after the 1994 flood. In fact, especially on the Island of Sor, where ground level (topography) is very low in some parts, with the shallow water table (less than 1m deep at low points) the dike barrier creates a kind of pressure in the ground water due to high river discharge. This results in reducing the capacity of rainwater infiltration. In the old colonial part (Island of Ndar), most of the colonial buildings have underground basements. The upwelling of ground water causes floods in these parts during high river discharges (Seck 2010).

The water levels around the city are also influenced by the ocean tides: once the water on the seaside of the inlet starts to rise, a water level gradient directing towards the inlet starts to develop. At a certain point in time, this leads to an inflow of ocean water into the estuary (towards the city). Water levels will then start to rise. Water levels in the estuary fall again once the water levels outside the river mouth become low enough (Steijn 2011).

Figure 24: Flooded area on Island of Sor (neighbourhood of Citè Niakh) in September 2018: insufficient drainage and missing sewage infrastructure exacerbate the flood risk situation (photo: NDARINFO)

5.1 General Characteristics of the Study Area

Alioune Badiane of the United Nations' UN-Habitat agency designated Saint-Louis as "the city most threatened by rising sea levels in the whole of Africa", citing climate change as the main cause (BBC 2008).

The city of Saint Louis is the former capital of Senegal (until 1958) and a regional economic center in Northern Senegal. It is located on low-lying land near the mouth of the Senegal River on the shore of the Atlantic Ocean (Figure 27 and Figure 31). It is built on an area dominated by deposits of mud and sand and is strongly influenced by the omnipresence of water (Kane et al. 2014).

The Senegal River drains a catchment area of some 300,000 km². One of its main tributaries (Bahfing) originates from mountains in the republic of Guinea. The other main tributary (Bahkoye) originates from the Siguiri basin and incises a plateau in Mali. On its way down, the river receives input from numerous smaller tributaries, which all rise in humid tropical regions. The hydrologic regime of the river is therefore determined by the rainfalls in the upper regions and not by the semi-arid and arid regions through which it flows before reaching the Atlantic Ocean. The highest discharges occur in the months from August to November. Very low discharges can be observed during the months from January to June (Steijn 2011).

Saint Louis can be characterized as a medium-scale African coastal city (population about 250.000 in 2011) which is highly exposed to diverse types of climate and flood risks (Coly et al. 2012).

The particular location of St. Louis in the estuary of the Senegal River complicates urban planning. Many districts of the town are located on pieces of land (islands) which are so low that floods take place during periods of extreme water level. The situation is expected to become worse if sea level rise continues and if urban development continues (Steijn 2011).

The old colonial city which is a UNESCO world heritage and because of its unique French colonial architecture the most popular area for tourists is located on a narrow island (the "Ile Saint Louis" or "Island of Ndar", cf. Figure 25) in the Senegal River. At this point the river is separated from the Atlantic Ocean to the west by a narrow sand spit, the "Langue de Barbarie" (cf. Figure 25), which has also been urbanized (the seaside neighborhoods of Ndar Tout, Guet Ndar and Goxxumbacc, cf. Figure 26). The main part of the city, "Faubourg de Sor" (Island of Sor" (named "Sor" in Figure 25), lies near the eastern mainland and is nearly surrounded by tidal marshes.

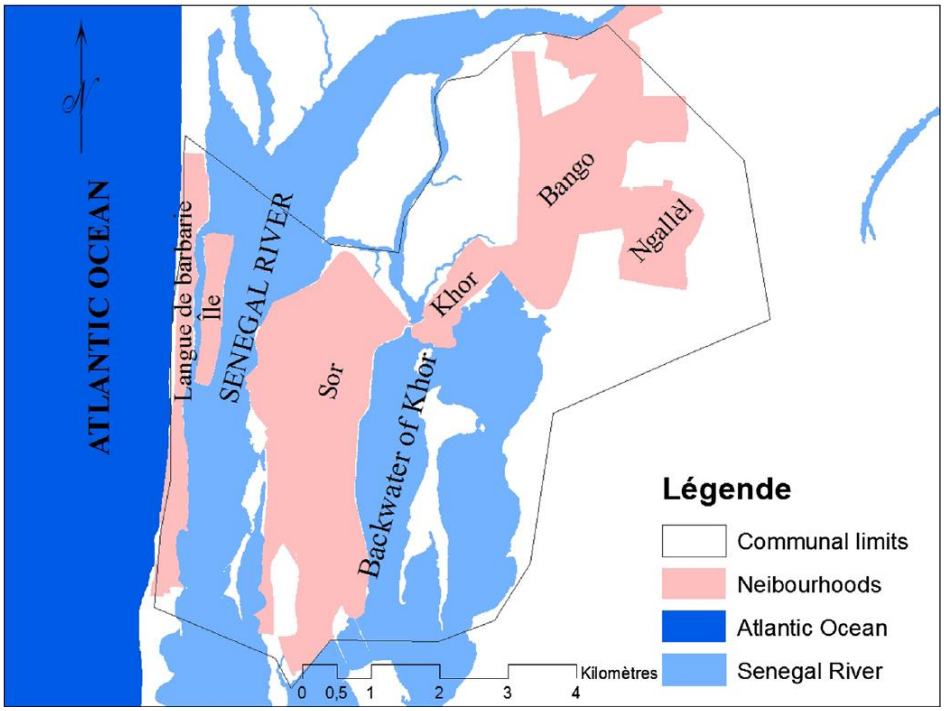

Figure 25: Position of main parts of Saint Louis (taken from Vedeld et al. 2016)

The outskirts towards the inland (north-east, e.g. neighbourhoods of Khor and Bango) are a prime zone for the urban expansion. Although this part offers great possibilities for development from a spatial perspective, it is still a little bit isolated from the rest of the city (Seck 2010).

The peri-urban region is characterized by marshes - flood basins that form during the rainy season when the Senegal river overflows into the countryside, creating ponds and stretches of mangroves.

Saint-Louis has a hot desert climate (Köppen climate classification BWh). It only has two seasons, the rainy season from August to November, characterized by heat, humidity and storms with heavy cloudbursts, and the dry season from November to May, characterized by a cool ocean breeze. The average annual rainfall is about 300 mm (Vedeld et al. 2016).

As in much of the Sahel, Senegal has experienced a history of highly uncertain climatic conditions, varying between cycles of drought to eras of frequent and severe flooding. After several very dry decades between 1968–1997, regional Senegalese climate has shown a 35% increase in average rainfall between 2000 and 2005 (Nicholson 2005). In recent years, the Sahelian zone has recorded a return of heavy rainy seasons.

CLUVA's (CLimate change and Urban Vulnerability in Africa: FP7 Environment, 2010 – 2013) analysis of extreme rainfall events, based on climate projection data until 2050, suggests that intensity and frequency of extreme events will significantly increase and enhance flood risks in the future (Kane 2010; Coly et al. 2011; Coly et al. 2012).

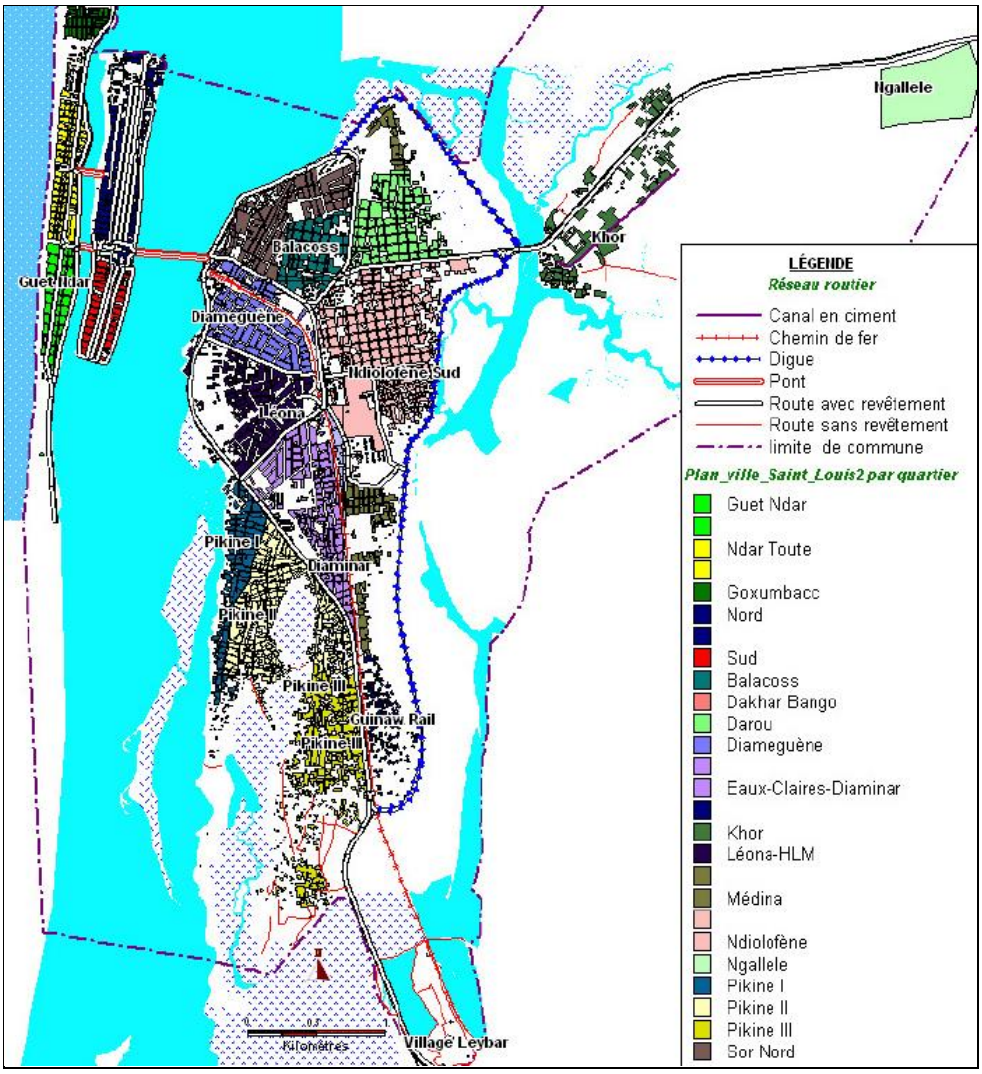

Figure 26: Districts of Saint Louis (taken from Seck 2010, original source: Kane 2003)

Some major technical measures in recent decades have changed the hydrological balance of the lower reach of the Senegal River significantly:

- the Diama Dam about 22 km north of *Saint-Louis was completed in July 1986, and is controlling most of the water influx into the estuary; the dam was built as anti-salt dam to create large irrigation fields along the Senegal valley. Flood regulation was not a criterion during the construction. Diama dam does not play any major role for discharge control but is opened during high river discharge in the wet season to ensure a normal flow of the river. During dry season it is closed to block salt intrusion into the agricultural lands (Seck 2010).*
- *the* Manantali Dam in Mali, a hydro-electric dam, which was completed in 1988 also has some influence on the flow conditions despite being situated more than 1000 km from the mouth of the Senegal River;
- finally, in 2003, a major flood event of the Senegal River urged the Senegalese authorities to take the initiative to open a breach in the coastal sand strip of the "Langue de Barbarie" in order to evacuate the water surplus from the river to the ocean and therefore resolve forever the problem of river flooding. However, the disruption of estuarine dynamics has led to a rapid expansion of this gap: a few meters wide at its excavation, it reached over 2,700 m in August 2009 (Kane et al. 2013). Some months after the widening of the gap, the old river mouth was completely closed. This measure has greatly increased other environmental issues severely such as coastal erosion and salinization of arable land and groundwater with impacts on local housing and settlements. (Vedeld et al 2016). The new river mouth continued to grow

in size and at the same time moved in southward direction. These morphological changes had some serious consequences such as damage on the now exposed inland coast, opposite the new river mouth. The village of Doune Baba Diéye with some 40 houses, south of Saint Louis even completely disappeared in 2011 - cf. Figure 27 and Figure 28.

Figure 27: The village of Doune Baba Diéye south of Saint Louis (slightly south of peri-urban AOI) in VHR imagery as available in Google Earth, acquisition date 26/01/2004 (© DigitalGlobe)

Figure 28: Situation in Senegal estuary south of Saint Louis (slightly south of peri-urban AOI) in VHR imagery as available in Google Earth, acquisition date 13/10/2013 (© CNES / Airbus)

The vulnerability of Saint Louis and its inhabitants is characterized by the significant land use change triggered by extreme drought in the 1970s, 80s, and 90s which forced rural populations into urban areas. Today, almost half of Senegal's population lives in urban areas (GFDRR 2014).

Simulations performed by Durand et al. (2010), based on the potential height of water at the end of the rainy season and carried out for several scenarios for the rise in sea level, show that a 0.5-m sea level rise would be enough to flood part of the town of Saint-Louis at times of annual high waters and that it would be almost completely submerged in the event of a 1- m rise. Saint Louis Island and Langue de Barbarie will be less affected than the area of Island of Sor. Sea levels are predicted to increase by one meter towards the end of the century (Vedeld et al. 2016).

Seck (2010) presented a Digital Terrain Model (DTM) with detailed topographic heights of the city and its surroundings (see Figure 29). It could not be determined which data was used as the basis for this model.

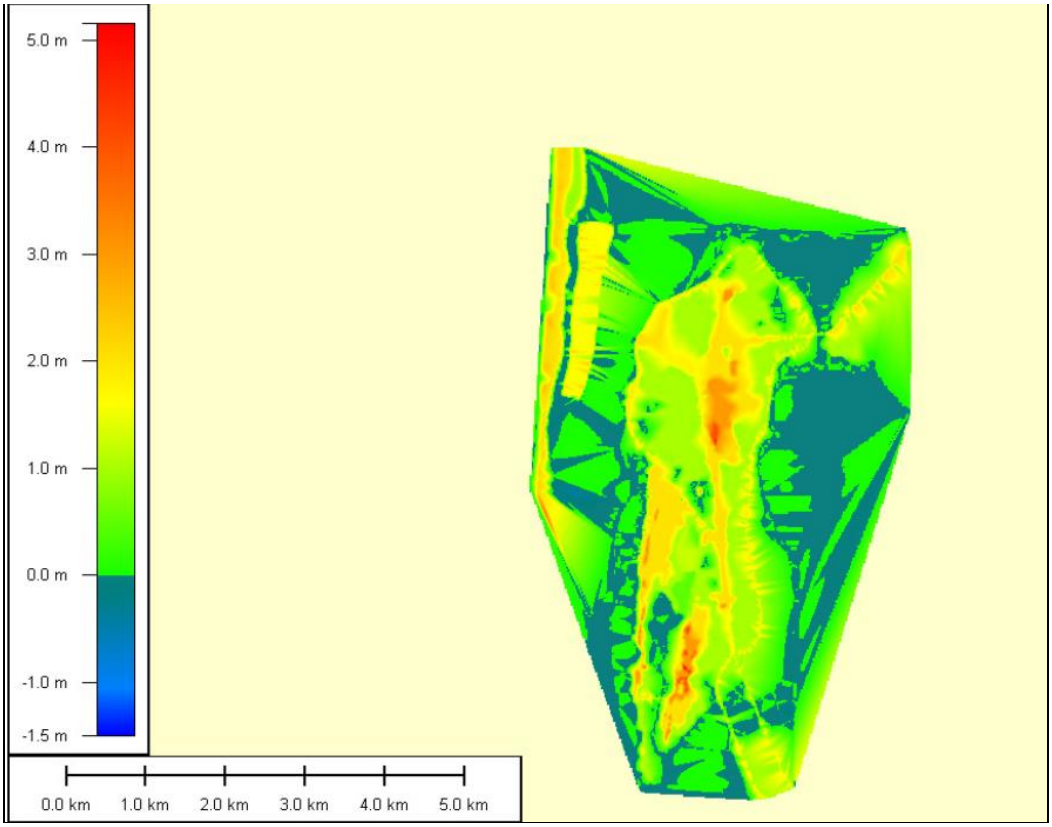

Figure 29: Land heights in Saint Louis core urban area (taken from Seck, 2010)

In order to avoid that certain districts are flooded in case of extreme water levels, different attempts have been made by the authorities to install a flood defence system: an approximately 0.5 m high concrete flood wall was built at different locations along the perimeters of the Island of Ndar and the northernmost parts of the Island of Sor. Along the rest of the perimeter of the Island of Sor, a dike was built in the Nineties, with heights varying from MSL + 1.5 m to MSL +1.8 m. However, the dike is not in a technical state that it can actually avoid any flood. The dike itself does not enclose all districts, so that even if it functioned it would not avoid flooding in all districts of the Island of Sor (Seck 2010, Steijn 2011, Vedeld 2016).

The population of Langue de Barbarie is mainly threatened by the acceleration of coastal erosion (cf. Figure 30). The rapid erosion of the beaches is partly caused by sand mining – the sand for construction projects directly taken from the beaches. The only realistic adaptive option had been perceived to relocate those houses along the seashore which were severely affected or at risk of being destroyed by coastal flooding and storm surges. Some families had been offered to resettle to another location in the city periphery, but few had opted to move (Roca et al 2017).

Figure 30: Remains of houses on Langue de Barbarie that were abandoned because of the approaching sea. Photo: AFP Photo / Seyllou (26/10/2015)

The World Bank meanwhile unveiled a $30 million (24 million euros) program to relocate 900 families, or about 10,000 people living in the most vulnerable areas,

It is on the background of significant climate change risks and experiences of frequent floods, combined with increasing population and settlement of people in flood-exposed areas, that the urban authorities from the mid-1990s started to take climate and flood risks more seriously. However, the city has very limited powers and legal mandates, finances, staff, and technical competence. This undermined the municipal capacity for autonomous self-governing and provisioning of key public services and infrastructure to perform planning and service functions, including the climate risk management (Vedeld et al. 2016).

The 2009 floods (affecting Dakar and surrounding areas primarily) appear to mark a new start for the Senegal Government, with three steps to commit permanently to a sustainable recovery and flood management policy. These three steps were:

1. Assessing damage, losses and post disaster needs (PDNA) for 2009;
2. The storm water management and climate change adaptation project;
3. The ten-year flood management program (2012-2022).

Flood management nowadays is a major part of the Senegalese government's Disaster Risk Reduction framework and building resistance to flooding is a top priority within the country's INDC submission.

Not only scientific studies with regard to flood risk and disaster management have been performed in recent years (e.g. CLUVA - CLimate change and Urban Vulnerability in Africa: FP7 Environment, 2010 – 2013).

Supported by international organizations, also some adaptation and technical mitigation measures have been initiated:

- The Senegal Integrated Urban Flood Management project (2016 – 2021, Green Climate Fund) is aiming at protecting urban areas in Senegal from flood risk, investing in drainage infrastructure and establishing a national disaster risk management policy.
- The development objective of the current (2018 – 2023) Saint-Louis Emergency Recovery and Resilience World Bank Project for Senegal is to reduce the vulnerability of populations to coastal hazards along the Langue de Barbarie and strengthen urban and coastal resilience planning of the city of Saint-Louis (World Bank 2018).
- Several UN agencies provided support to small capacity and training programs and a resettlement program for flood victims to move to a peri-urban area (e.g., UNDP, UNEP, UN-HABITAT, UNESCO).
- The French development agency AFD has unblocked 15 million Euros so that a dyke could be built within a year to protect the inhabitants of the Langue de Barbarie (RFI 2018). The dyke currently is under construction.

The Saint Louis area of interest covers an area of 298,8 km² (core city area and larger urban area of interest) while the core city area covers 89,2 km² (cf. Figure 31).

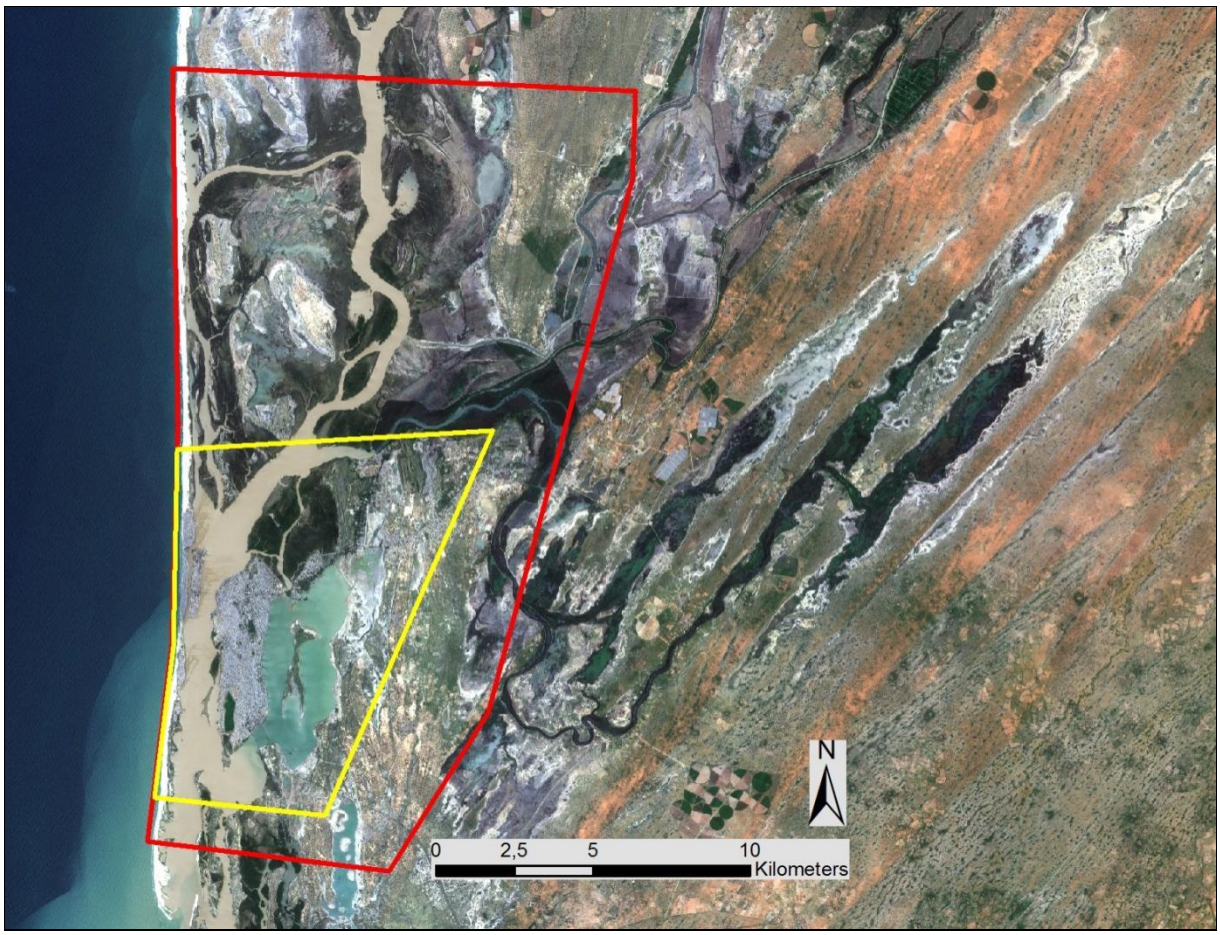

Figure 31: Saint Louis, Senegal – Service Area: yellow: core city area of interest; red: larger urban area of interest (Background Image: Sentinel2 10/09/2017, European Space Agency)

5.2 Flood History

Floods of the Senegal River have marked the history of the city of Saint-Louis since its creation in the 18th century north of the river's mouth (Durand et al. 2010).

Nine major floods causing flooding in the colonial city were recorded in the nineteenth century (1827, 1841, 1843, 1854, 1855, 1858, 1866, 1871, 1890) and nine in the twentieth century (1906, 1922, 1924, 1935, 1950, 1994, 1997, 1998, 1999). No major floods occurred during the 1960s, 1970s and 1980s, which were marked by a drought that affected the whole of West Africa. The construction of the Diama and Manantali dams in 1986 and 1988 did not provide sufficient control of the hydrological regime to avoid flooding in the city when conditions returned to more humid climate in the early 1990s. Thus, the city was partially flooded during the floods of 1994 (maximum level: 1.26 m), 1997 (1.28 m), 1998 (1.43 m), 1999 (1.47 m) and 2003 (1.35 m; Durand et al. 2010).

More recent flood events as taken from local sources and press releases are:

- 2009: a tidal wave impacted the Langue de Barbarie.
- July to October 2010: severe floods due to heavy rainfall, flash floods and inadequate drainage systems: more than 80,000 people or 40 % of the citizens were affected
- August to October 2012: severe floods due to heavy rainfall, flash floods and inadequate drainage systems
- August 2012: heavy rains as rainy season starts
- August 2013: floods due to inadequate drainage
- August 2015: peninsula flooded, incl. important cemetery and tourist spots
- July to August 2016: extreme rainfall causing floods
- September 2018: flooding due to rainfall on Island of Sor (cf. Figure 32)

Based on hydrological calculations and land heights, it is estimated that the lowest parts of the Island of Sor are likely to be flooded each year, and that other areas including the historic center are likely to be flooded with a frequency of less than once a year. Compared to other regions in the world these probabilities are very high (Steijn 2011).

Figure 32: Flooding caused by poor drainage of rainwater in neighbourhood of Cité Niakh (Island of Sor) in September 2018 (photo: NDARINFO)

Furthermore, the consequences of coastal erosion and rising sea levels seem to be on the increase (cf. Figure 30): “Since 2016, two or three times a year, the ocean has swelled and knocked another row of houses off the coast. For two years now, the water has been rising. It doesn’t recede” (Floodlist 2018).

5.3 EO Data Used

In general, there are two types of data available for this purpose: optical and Radar data. Available HR optical data from the sensors Landsat 5, Landsat 8, and Sentinel-2 covering the period from 2009 to 2018 was downloaded and analysed with regard to regional and/or local flooding.

The following datasets were used for flood extent mapping:

- Landsat 5, recorded on 12/10/2011
- Landsat 8, recorded on 05/09/2015
- Landsat 8, recorded on 14/08/2013
- Sentinel 2 recorded on 30/09/2016
- Sentinel 2 recorded on 10/09/2017
- Sentinel 2 recorded on 20/09/2018

VHR Imagery covering the core city area was provided by the Project Coordinators:

- QuickBird-2 recorded on 13/03/2003
- WorldView-4 recorded on 29/11/2018

This data gives a good impression of the rapid development and expansion of Saint Louis but no information about flooding could be obtained as VHR data was acquired in the dry season.

Radar data from the current European Space Agency (ESA) Sentinel-1 data is recorded constantly and it is free of charge. Sentinel-1 Radar GRD Data (39 datasets) covering the period between 17/07/2015 and 22/11/2018 during the rainy season from June to end of November, was downloaded and processed with regard to water extent.

The data tend to give unreliable results in urban environment due to the high number of low backscattering objects.

The flood risk product is a combination of hazard with Land Use / Land Cover (LULC) information. The latter is derived from the Very High Resolution (VHR) satellite data based LULC classification produced by NEO covering the core city area.

The larger urban area LULC classification is based on Landsat 5 (01/12/2006) and Sentinel 2 (09/12/2018) respectively. Thus these datasets are also indirectly used for the flood risk product.

For following events VHR imagery is available in GoogleEarth and was used for visual interpretation of flood extents (cf. Figure 35):

- August 2009 (recorded on 17/08/2009)
- October 2011 (recorded on 11/10/2011)
- August 2012 (recorded on 30/08/2012)
- October 2013 (recorded on 13/10/2013)
- November 2016 (recorded on 22/11/2016)
- October 2017 (recorded on 03/10/2017)
- November 2018 (recorded on 19/11/2018, 22/11/2018, 29/11/2018)

The assessment of coastal floods and erosion hazard in Langue de Barbarie is based on VHR images as available in Google Earth (13/03/2003, 22/02/2019, cf. Figure 35 and Figure 36).

The ALOS Global Digital Surface Model "ALOS World 3D - 30m (AW3D30)", version 2.1 (©JAXA) was used for physiographic analyses.

5.4 Short Description of Methodological Approach

Historic flood extent mapping

Flood extent mapping based on EO data heavily depends on available datasets as well as on types of floods in focus. Whereas there is a good chance to identify large-scale river floods, normally no information regarding short-term local floods (flash-floods) can be obtained from EO data due to short duration and/or cloud cover. In some cases, short-term local floods can be recorded and localized based on reports (e.g. in social media) and press releases but such inventory never will meet the claim of being complete.

The flood extent is derived from historical optical satellite imagery of 30 meter resolution (Landsat 5 and Landsat 8) and 10 meter resolution (Sentinel 2).

The relevant datasets were corrected atmospherically applying the Dark Object Subtraction (DOS) approach. Landsat 8 imagery was pan-sharpened to 15 m resolution.

For defining the water extent, the water cover was classified by applying the Automated Water Extraction Index AWEIsh (Feyisa et al. 2014) which makes use of the reflectance values of Blue, Green, Near Infrared and Shortwave Infrared spectral bands of the Landsat 5, Landsat 8, and Sentinel-2 sensors. The AWEIsh is an index formulated to effectively eliminate non-water pixels, including dark built surfaces in areas with urban background. The equation is intended to effectively eliminate shadow pixels and improve water extraction accuracy in areas with shadow and/or other dark surfaces.

Sentinel-1 Radar Data is processed to Gamma Nought and orthorectified to 10m spatial resolution. A multitemporal filter is applied to improve the signal to noise ratio of individual images. A set of multitemporal statistics is calculated from the stack of Sentinel-1 images, such as: mean, minimum, maximum, coefficient of variation and variance.

Two sets of water and flood masks are produced from the S1 stack. The first is based on simple backscattering thresholds applied to individual VH polarization images. This results in 39 individual water masks, which can be analysed in terms of their frequency of being water.

The second approach uses the multitemporal stack statistics to separate flooded areas from periodically flooded areas and permanent water based on thresholds derived from reference data. Areas with a low mean backscatter and a low coefficient of variation are classified as permanent water. Flooded areas show a higher coefficient of variation and a low minimum backscatter, but periodically flooded areas tend to show a higher mean backscatter than areas with short-period flooding.

The delimitation of permanent water cover (representing a high water-level during the rainy season) is based on the EO4SD LULC classification (performed by NEO).

Finally, mapping of flood extents by visual interpretation of VHR imagery as available in Google Earth was done (cf. Figure 33). For Saint Louis, a large archive of VHR imagery is available.

Figure 33: Flooded areas on Island of Sor (neighbourhood of Diaminar) in October 2011 (image recorded on 11/10/2011, © Digital Globe)

Flood hazard mapping

The flood hazard map was generated based on the occurrence of flood events during the past 10 years. The map aims to give an idea about the flood presence in terms of both frequency and extent in the city, and illustrates which part is in generally flooded more often than other areas (cf. Figure 36).

Water extents representing seasonal floods of the Senegal River as well as rainwater stagnation after heavy rains (6 events) are based on:

- data from Landsat 5 (acquired on 12/10/2011), Landsat 8 (acquired on 14/08/2013, 05/09/2015, both provided by the US Geological Survey), and Sentinel-2 (acquired on 30/09/2016, 10/09/2017, 20/09/2018, provided by the European Space Agency)
- and on visual interpretation of VHR data as available in Google Earth (7 events, see Chapter 4.5.2).

The flood hazard classification was done according to the approach selected by NEO on Cambodia cities during EO4SD Phase 1: a "number of occurrences" was calculated by combining flood extents as derived from HR imagery and from visual interpretation of VHR imagery. This data was classified according to the following specifications for the hazard definition:

- area flooded once between 2009 and 2018: low hazard
- area flooded twice or three times: medium hazard
- area flooded more than three times: high hazard

It has to be underlined that both approaches for the flood extent identification differ significantly and that the analysis of VHR data does not cover the peri-urban area. Furthermore, in some cases, the areas identified as flooded in HR and VHR data respectively refer to the same event.

Therefore the "number of occurrences" may not be used for any further sub-classifications or interpretations.

The estimation of the area threatened by tidal waves and coast erosion in Langue de Barbarie is based on available reports and press releases as well as on the extrapolation of the mapped difference (done by visual interpretation) of the coastline between 2003 and 2019 (cf. Figure 34 and Figure 35).

Figure 34: Coastline of northern part of Langue de Barbarie (neighbourhood of Goxxumbacc) in 2003 (recorded on 13/03/2003, © Digital Globe)

Figure 35: Coastline of northern part of Langue de Barbarie (neighbourhood of Goxxumbacc) in 2019 (recorded on 22/02/2019, © Digital Globe)

Flood risk mapping

Risk is defined as a combination of probability and consequences. A detailed and uniform land-use map is an important prerequisite to perform flood risk calculations, since it determines what is damaged in case of flooding.

Two different datasets regarding the urban land use were made available for this analysis:

- LULC product generated by NEO through EO4SD-Urban based on VHR data covering the core city area (approx. 89,2 km²)
- LULC product generated by NEO through EO4SD-Urban based on HR data covering the larger urban area (approx. 298,8 km²)

As a consequence, because of the difference in terms of resolution and extraction scale, some small discrepancies at the limits of the Core City AOI appear between the two products.

The exposition is classified following an approach developed by NEO (based on: Dasgupta et al. 2015) integrating economic costs, social damage, physical damage and flood duration. Four land use damage levels (A, B, C, D) are defined based on this estimation.

Both land-use classification results were recoded to pre-defined categories (as given in Table 14 and Table 15) and merged after categorization.

The flood risk product is a combination of hazard with Land Use / Land Cover (LULC) information. The latter is derived from the Very High Resolution (VHR) satellite data based LULC classification produced by NEO covering the core city area.

The larger urban area LULC classification is based on Landsat 5 and Sentinel 2. These datasets are thus also indirectly used for the flood risk product.

Table 14: Land use classes and reclassification to pre-defined damage levels in Core City area

Classes	Damage				Total	Level
	Economic Costs 0-2	Social Damage 0-2	Physical Damage 0-2	Flood Duration 0-2		
Agricultural area	1.5	0.5	0	1	3	B
Industrial, commercial, public units	2	0.5	1	0.5	4	B
Construction sites	1	0.5	0	0	1.5	A
Forests ans shrublands	0.5	0	0	0	0.5	A
Residential – continuous urban fabric	1.5	1.5	2	1.5	6.5	D
Residential – discontinuous dense and medium density urban fabric	1.5	1	2	1	5.5	C
Residential – discontinuous low and very low density urban fabric	0.5	1.5	1.5	1	4.5	C
Bare soil	0	0	0	0	0	A
Land without current use	0	0	0	0	0	A
Natural areas (grassland)	0	0	0	0	0	A
Wetlands	0	0	0	0	0	A
Roads and railways	1.5	1	2	1.5	6	C
Airport	2	0.5	1.5	1.5	5.5	C
Sports and leisure facilties	0.5	0.5	0	0.5	1.5	A
Green urban area	0.5	0.5	0.5	1	2.5	B
Inland and marine water	0	0	0	0	0	A

Table 15: Land use classes and reclassification to pre-defined damage levels in Larger Urban area

Classes	Damage				Total	Level
	Economic Costs 0-2	Social Damage 0-2	Physical Damage 0-2	Flood Duration 0-2		
Agricultural area	1.5	0.5	0	1	3	B
Artificial Surfaces	1.5	1.5	2	1.5	6.5	D
Forests ans shrublands	0.5	0	0	0	0.5	A
Bare soil	0	0	0	0	0	A
Natural areas (grassland)	0	0	0	0	0	A
Wetlands	0	0	0	0	0	A
Inland and marine water	0	0	0	0	0	A

The Flood Risk matrix is generated based on above code and flood hazard classified into three hazard levels. The flood risk level is classified in four qualitative classes based on the combination of flood hazard and land use damage as shown in Table 16.

Table 16: Flood Hazard and Risk classification

		Damage cost on land use			
		A	**B**	**C**	**D**
Flood Hazard	**1 (low)**	1A	1B	1C	1D
	2 (medium)	2A	2B	2C	2D
	3 (high)	3A	3B	3C	3D
Flood Risk classification					
Low Risk	1A 1B 2A				
Medium Risk	1C 1D 2B 2C 3A 3B				
High Risk	2D 3C				
Very high Risk	3D				

5.5 Product Description and Accuracy Assessment

There are three final layers in this product: (1) the raw data on past flood extents as derived from EO data and ancillary data (flood history), (2) the Flood Hazard map which summarizes past flood events and thus gives information about the likelihood of future events, and (3) the Flood Risk map combining this data with information on urban and peri-urban land use and its damage potential in case of flooding.

The Flood Hazard map (subset see Figure 36) displays flood hazard information (delivered in vector format). This data is based on the occurrence of floods of the past 10 years. It takes into account both the hazard from seasonal floods and rainwater stagnation in the rainy season as well as from tidal waves and coast erosion. The classification in three qualitative hazard levels is expert-based under consideration of mapped frequencies of floods.

The map aims to give an idea about the flood presence in terms of both frequency and extent in Saint Louis and illustrates which part is in general flooded more often than other areas.

Since no independent reference data are available no accuracy assessment is possible. The plausibility of the results nevertheless was evaluated on basis of local reports and press releases.

The Flood Risk Map (subset see Figure 37) displays flood risk information (delivered in vector format). This data is based on the occurrence of floods of the past 10 years combined with information of the land use map provided by NEO of this project area. It takes into account both the hazard level and potential damages, based on different land uses. The damages are assessed on 4 aspects: economic, social, physical and flood duration.

Since this product is a direct derivation and combination of the Hazard Classification and the Land Use Classification, its plausibility can be rated high when the mentioned input datasets are rated as being plausible and reliable.

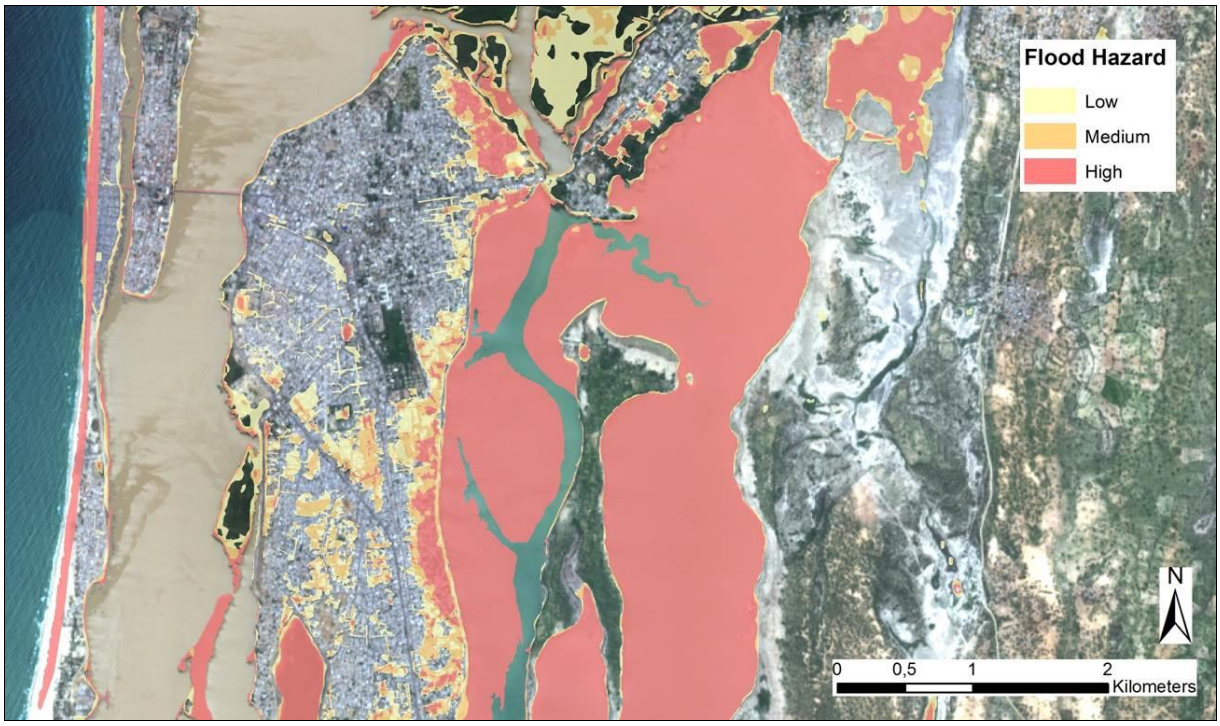

Figure 36: Subset of Flood Hazard Map of Saint Louis (Ile Saint Louis, northern part of Island of Sor, Khor) (Background Image: Sentinel 2, recorded on 10/09/2017)

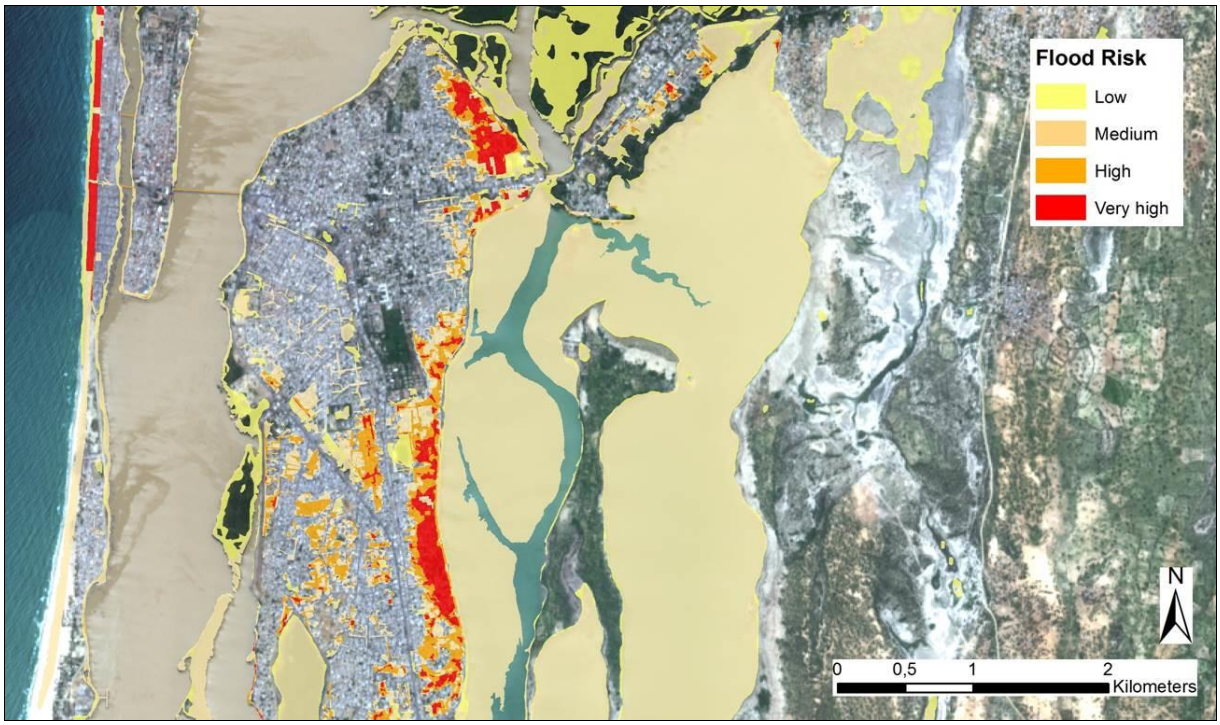

Figure 37: Subset of Flood Risk Map of Saint Louis (Ile Saint Louis, northern part of Island of Sor, Khor) (Background Image: Sentinel 2, recorded on 10/09/2017)

5.6 Analysis of Mapping Results

Flood Hazard

For the Island of Ndar (old colonial city) no major flood events were reported within the last decade except for the shoreline which may be flooded in the rainy season. However, because of the low altitude of the island, flooding cannot be excluded in case of future extreme events. Based on hydrological calculations and land heights, it is estimated that the historic centre is also likely to be flooded (Steijn 2011).

Generally, the same is true for the Langue der Barbarie area. Additionally, for the immediate coastal zone, high hazard with regard to tidal waves and erosion by the sea has to be considered.

In the Core city area, zones representing high hazard can be identified mainly in the new settlements of the Island of Sor. The specific topography of the Island of Sor is a disadvantage, with its depressions in the districts of Leona and Diaminar (cf. Figure 26). It is known that water from the surrounding districts flows into these depressions, increasing the local problems (Steijn 2011).

Finally, the large depression in the southern part of the Island of Sor, classified mainly as bare soil in the EO4SD LULC classification, is marked as high hazard area as it is flooded every year.

For the following calculations the permanent water cover as defined by the EO4SD LULC classification by NEO is not considered. While the share of permanent water cover in the core city area is about 25,8%, this share is only approx. 10,9% in the peri-urban area. For the total area of interest a percentage of 15,4% was calculated.

With regard to the flood hazard zones it can be observed that the expansion of such zones differs significantly in Saint Louis core city area and in the larger urban region: approx. 36,4% in the core city area and 44,8% in the larger urban region are classified as flood prone. Also the distribution of medium and high hazard zones show significant differences (cf. Figure 38 and Figure 39): 28,3% of the core city area are defined as such zones whereas this percentage is 35,0% in the peri-urban region. Low-hazard zones show similar shares.

This is mainly due to the fact that the extensive marshes to the north of Saint Louis are flooded regularly during the rainy season and thus are classified as high- and medium-hazard areas with the selected approach.

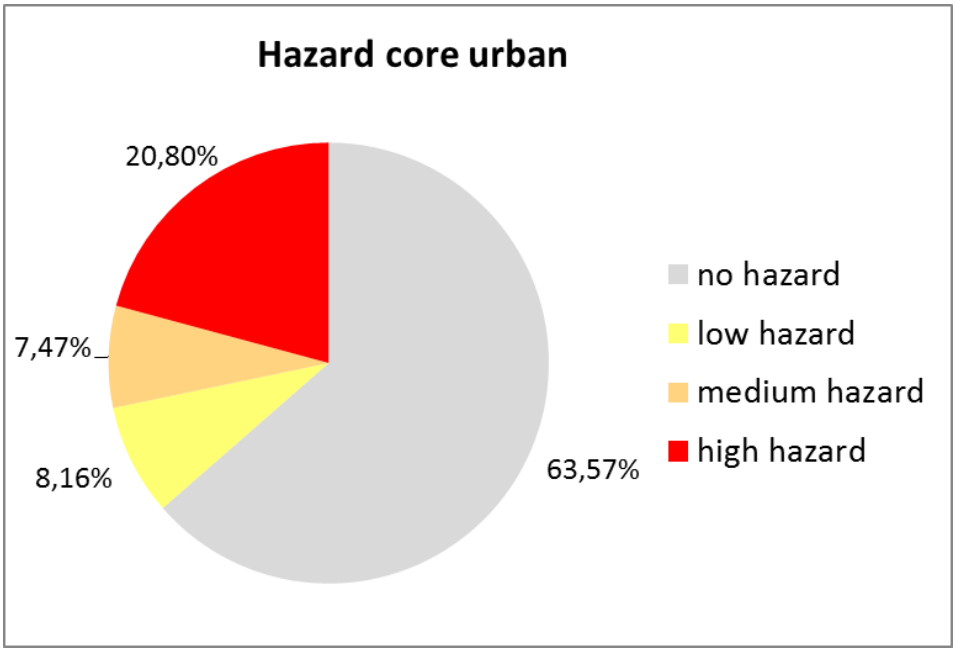

Figure 38: Percentages of flood hazard zones in Saint Louis Core City area

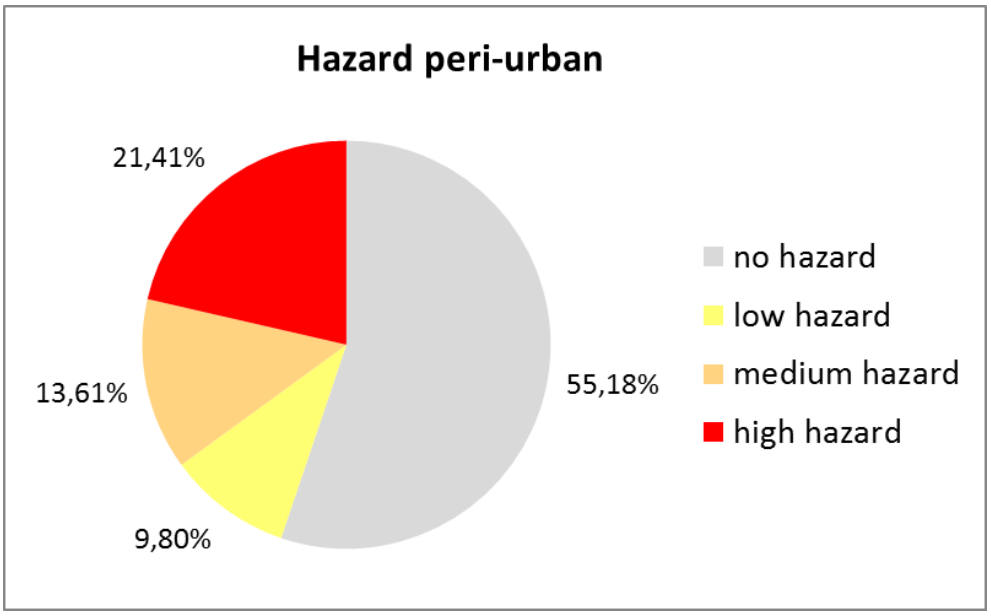

Figure 39: Percentages of flood hazard zones in Saint Louis Peri-Urban region

Residential Urban Fabric with high damage potential (LU classes: Residential – continuous urban fabric, Residential – discontinuous dense urban fabric, Residential – discontinuous medium density urban fabric, Residential – discontinuous low density urban fabric, Residential – discontinuous very low density urban fabric) was analyzed more detailed and combined with the Flood Hazard Map in the core city area of interest.

For the peri-urban area the LU class "Artificial Surfaces" was analyzed in detail and combined with the Flood Hazard Map.

The statistics for Residential Urban Fabric in the core city area is shown in Figure 40; based on these statistics, approx. 11,2% of Saint Louis' Residential Urban Fabric is situated in Medium and High Flood Hazard Zones. Additional 7,13% of these land use classes is situated in Low Flood Hazard Zones.

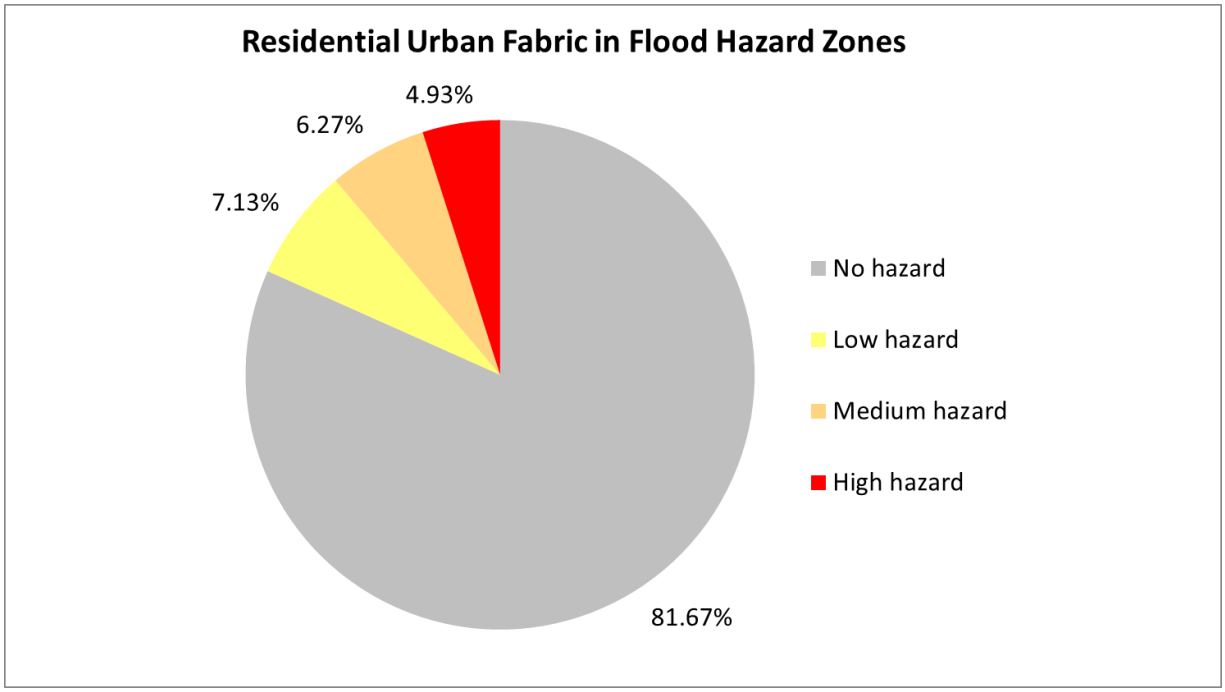

Figure 40: Proportion of Residential Urban Fabric in flood hazard zones in Saint Louis core city area

Figure 41: Subset of map of Residential, Industrial, Commercial and Public Urban Fabric combined with Flood Hazard Zoning in Saint Louis' core city area (Background Image: Sentinel 2, recorded on 10/09/2017)

For the larger urban area only 0,5% of the landuse class "Artificial Surface" is situated in Medium and High Flood Hazard Zones. Additional 0,9% of this landuse class is situated in Low Flood Hazard Zones (cf. Figure 42).

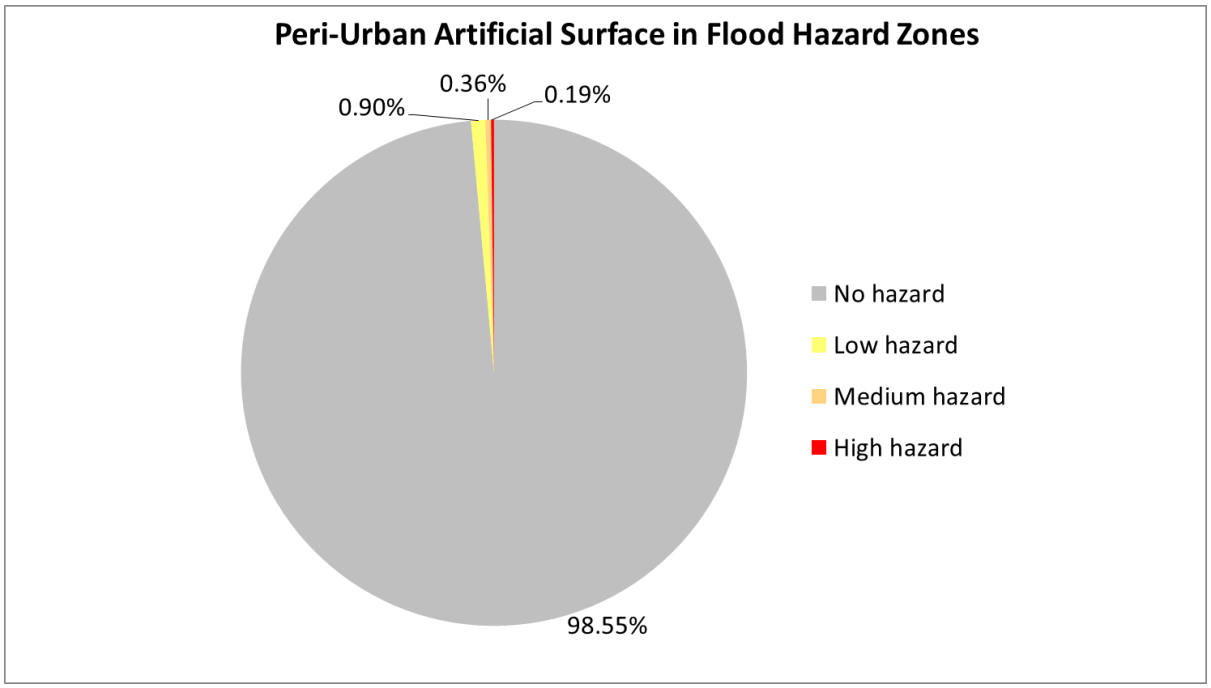

Figure 42: Proportion of Artificial Surfaces in flood hazard zones in Saint Louis larger urban area

Flood Risk

Generally, flood risk zones are well known - but to limited degree respected and enforced. In Saint-Louis, following many years of drought, the local population occupied parts of the river bed normally under water; consequently, many districts may be flooded in the event of a major rise in water level. High flooding risk can be observed on the Island of Sor, especially in the neighbourhoods of Pikine, Diaminar, Ndiolofène, Cité Niakh, and Diamaguene (cf. Figure 26).

Flood risk is exacerbated by rapid urbanization, insufficient drainage, and poor sewage infrastructure, which has resulted in the settling of low-lying areas and a reduction in soil infiltration potential. Rising sea levels and increasingly intense storms are the primary causes of coastal erosion and flood risks (GFDRR 2014).

Two local areas where in-depth analysis was done by Vedeld et al. (2016) were Diaminar and Goxxumbacc (cf. Figure 26), both selected as particularly flood risk exposed and vulnerable communities. They had a known history of engagement in flood risk management at the level of the community and the district (sub-wards). Diaminar neighbourhood is an informal and mostly unplanned settlement situated on a low-lying area (located on the Island of Sor) that is exposed to annual river floods and rainwater stagnation due to inadequate drainage and limited sewerage and storm drain systems. The local houses and buildings are also affected by salinization from seawater intrusion. The second case, Goxxumbacc, is a larger, mostly informal settlement located on the spit Langue de Barbarie on the seashore of the Atlantic Ocean. The area is mostly exposed to coastal flooding, while flash floods also constitute a problem, but not as severe as in Diaminar.

It is important to be aware that the applied methodology of flood risk classification involves some degree of human interpretation. Therefore, flood risk levels must be considered as relative metrics rather than absolute ones.

For the following calculations the permanent water cover as defined by the EO4SD LULC classification by NEO again is not considered.

As the expansion of flood risk zones is equal to that of hazard zones this results in a similar picture with regard to the total extent of the risk zones (cf. Figure 36 and Figure 37). Because of the higher exposition of urban land use the high and very high risk categories (accumulated) occur disproportionately high in the core city area (approx. 1,9% vs. 0,03% in the larger urban region, cf. Figure 43 and Figure 44). Areas classified as medium- and low-risk zones can be observed more frequent in the larger urban region (45,4% vs. 32,9% in the core city area, cf. Figure 43 and Figure 44). This is mainly a result of the high hazard classification for large areas to the north of Saint Louis which are flooded regularly during the rainy season.

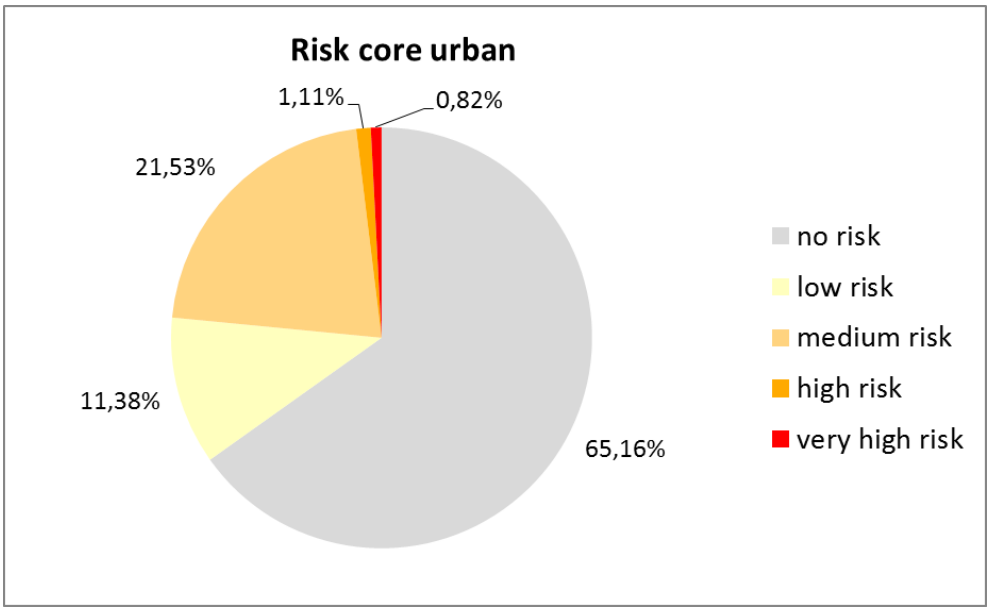

Figure 43: Percentages of flood risk zones in Saint Louis core city area

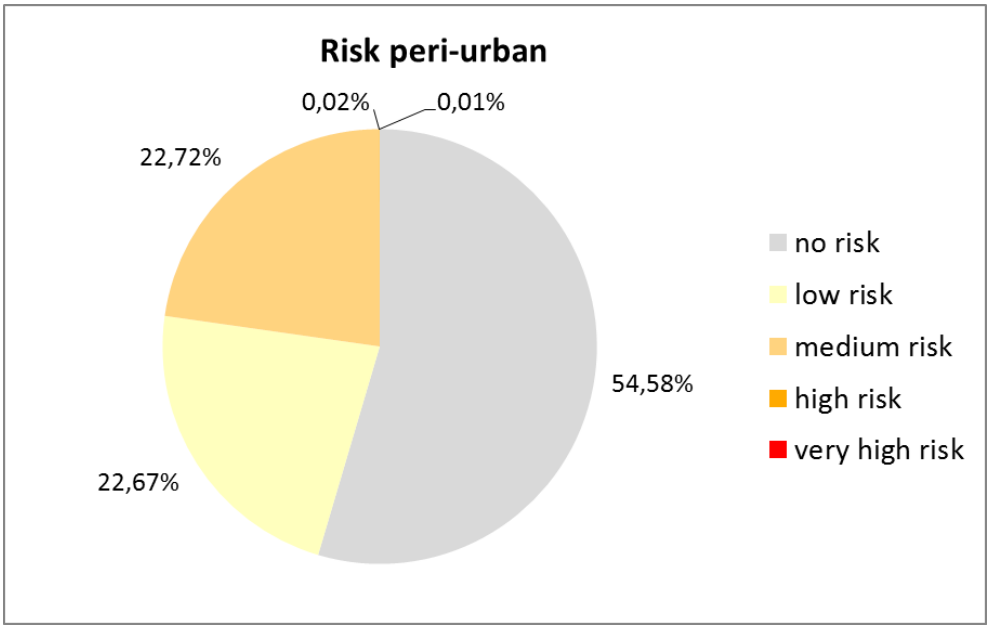

Figure 44: Percentages of flood risk zones in Saint Louis larger urban region

Residential Urban Fabric with high damage potential was analyzed more in detail and combined with the Flood Risk Map both in the core city area as well as in the total area (urban and peri-urban):

A subset of the Flood Risk map combined with Residential, Industrial, Commercial and Public Urban Fabric in Saint Louis' core city area is given in Figure 45. The focus of high-risk zones in Land use classes with high damage potential can well be observed to the East and Northeast of the the Island of Sor.

The statistics for Residential Urban Fabric only in Saint Louis core city area is shown in Figure 46: based on these statistics, almost 11%% of Saint Louis' Residential Urban Fabric is situated in high to very high risk zones, another 7,18% in medium risk zones.

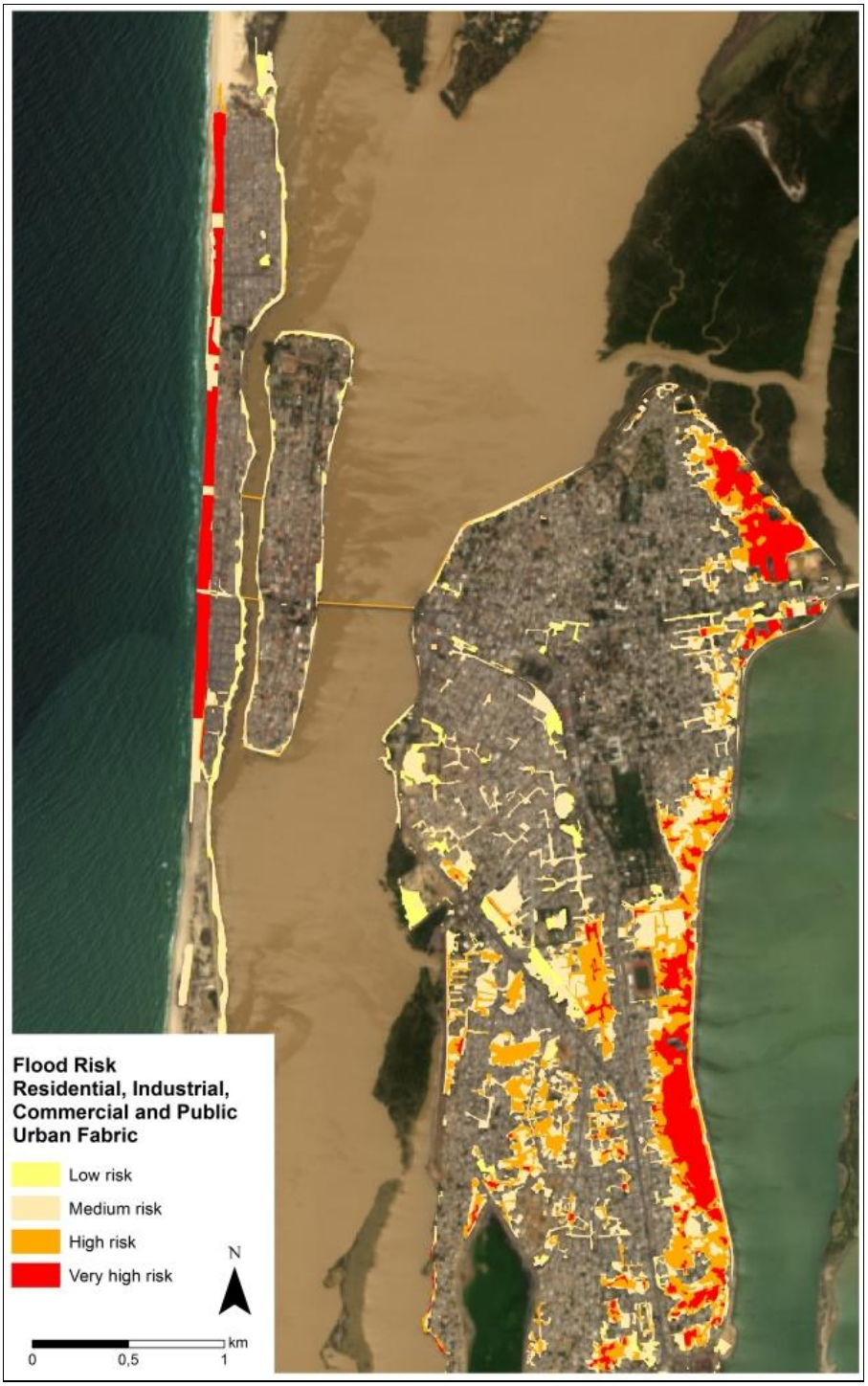

Figure 45: Subset of map of Residential, Industrial, Commercial and Public Urban Fabric combined with Flood Risk Zoning in Saint Louis' core city area (Background Image: Sentinel 2, recorded on 10/09/2017)

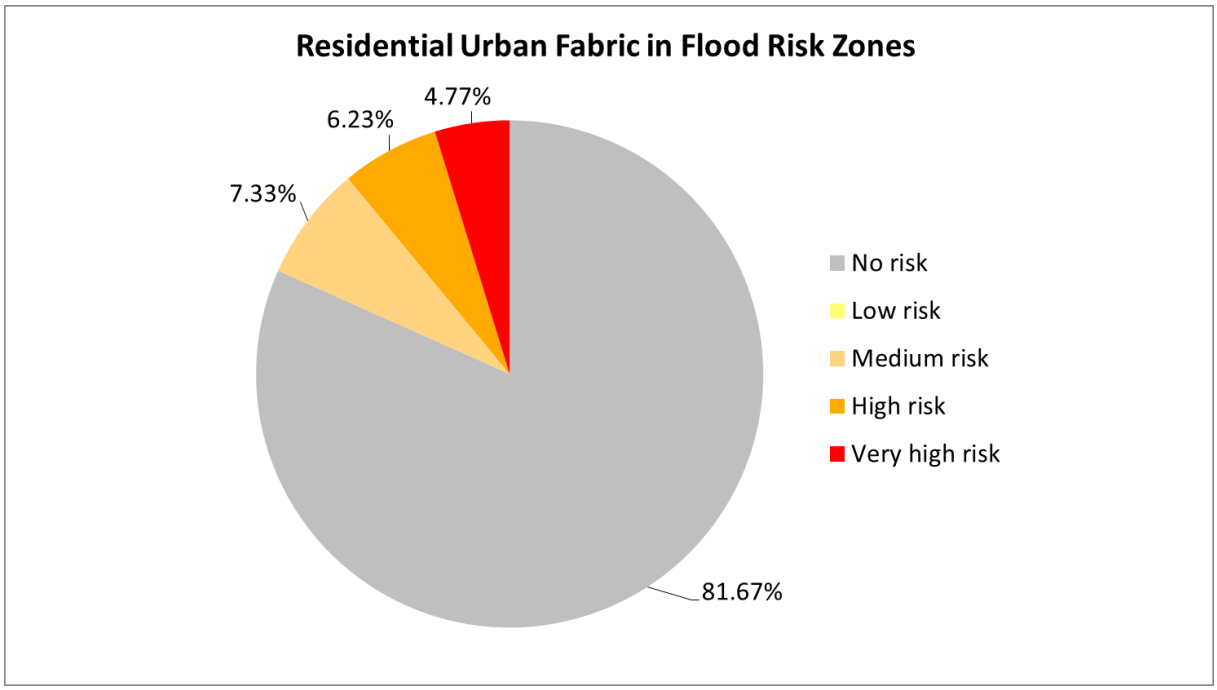

Figure 46: Proportion of Residential Urban Fabric in flood hazard zones in Saint Louis core city area

For the peri-urban area, only 0,55% of the land use class "Artificial Surface" is situated in high and very high flood risk zones. Additional 0,9% of this land use class is situated in medium flood risk zones.

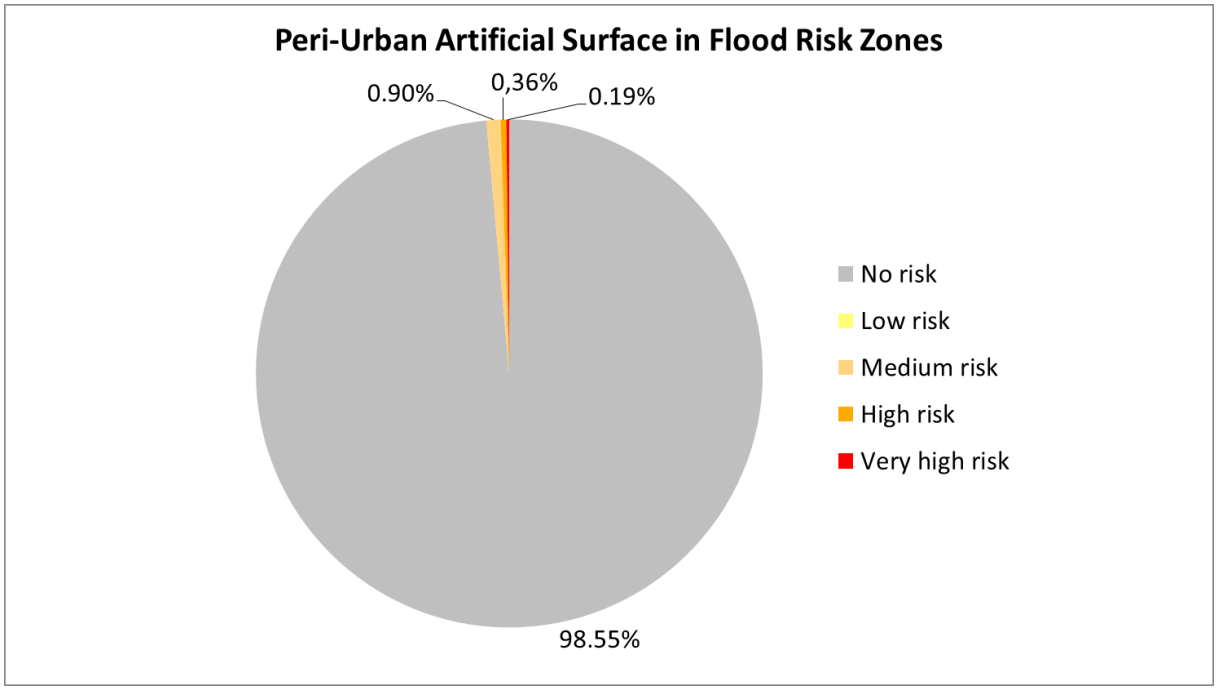

Figure 47: Proportion of Artificial Surfaces in flood risk zones in Saint Louis peri-urban area

6 References

Czaplewski, R. L. (2003). Chapter 5: Accuracy assessment of maps of forest condition: statistical design and methodological considerations, pp. 115–140. In Michael A. Wulder, & Steven E. Franklin (Eds.), Remote sensing of forest environments: concepts and case studies. Boston: Kluwer Academic Publishers (515 pp.).

European Union (2011). Mapping Guide for a European Urban Atlas, Version 11.0

Goodchild, M., Chih-Chang, L. and Leung, Y. (1994): Visualizing fuzzy maps, pp. 158-67. In Heamshaw, H.H. and Unwin, D.J. (Eds.), Visualization in geographical information systems. Chichester: Wiley.

Olofsson, P., Foody, G. M., Stehman, S. V., & Woodcock, C. E. (2013). Making better use of accuracy data in land change studies: Estimating accuracy and area and quantifying uncertainty using stratified estimation. Remote Sensing of Environment, 129, 122–131. doi:10.1016/j.rse.2012.10.031

Selkowitz, D. J., & Stehman, S. V. (2011). Thematic accuracy of the National Land Cover Database (NLCD) 2001 land cover for Alaska. Remote Sensing of Environment, 115(6), 1401–1407. doi:10.1016/j.rse.2011.01.020.

Internet

Road classification, European Commission, 2017, https://ec.europa.eu/transport/road_safety/specialist-/knowledge/road/designing_for_road_function/road_classification_en, last accessed 2017.08.17

Flood-related products

Coly, A., D'Almeida, A., Diakhaté M.M., Lo, M., Sy, B.A., Ndour, N.M., Gueye, S., Sall, F., & Sy, A.A. (2011): Report on climate related hazard in the city of Saint-Louis. Internal CLUVA report (D5.2), University of Gaston Berger.

Coly A, Sall F, & Weets G (2012): Changements climatiques et vulnérabilité des villes africaines – Saint Louis du Sénégal. Rapport de Synthese, CLUVA (D5.8), UGB.

Dasgupta, S., Asif, Z., Subhendu, R., Mainul, H., Sarwar, J. & Ainun, N. (2015): Urban Flooding of Greater Dhaka in a Changing Climate: Building Local Resilience to Disaster Risk. Directions in Development. Washington, DC: World Bank. doi:10.1596/978-1-4648-0710-7. License: Creative Commons Attribution CC BY 3.0 IGO

Diagne, K. (2007): Governance and natural disasters: addressing flooding in Saint Louis, Senegal.- Environment & Urbanization, International Institute for Environment and Development (IIED). Vol 19(2): 552–562. DOI: 10.1177/0956247807082836 www.sagepublications.com.

Durand, P., Anselme, B., & Thomas, Y.-F. (2010): L'impact de l'ouverture de la brèche dans la langue de Barbarie à Saint-Louis du Sénégal en 2003 : un changement de nature de l'aléa inondation ?.- https://journals.openedition.org/cybergeo/23017, *Retrieved 2019-04-15*

Feyisa, G. L., Meilby, H., Fensholt, R. et Proud, S. R. (2014): Automated Water Extraction Index : A new technique for surface water mapping using Landsat imagery. Remote Sensing of Environment, 140, 23–35. https://doi.org/10.1016/j.rse.2013.08.029.

GFDRR (2014): Senegal: Urban Floods Recovery and Reconstruction Since 2009.- Country Case Study Series. Guide for Disaster Recovery Frameworks.

Kane, C. (2010): Vulnérabilité du système socio-environnemental en domaine sahélien: l'exemple de l'estuaire du fleuve Sénégal. De la perception à la gestion des risques naturels. Thèse de doctorat de 3ème cycle, Université de Strasbourg.

Kane, C., Kane, A., & Humbert J. (2014): Management of a tropical river: Impacts on the resilience of the Senegal river estuary. The land/ocean interactions in the coastal zone of West and Central Africa, Springer International Publishing Switzerland, pp.41-48, Estuaries of the world, 10.1007/978-3-3619-06388-1_4. halshs-01070061.

Nicholson, S. (2005): On the question of the "recovery" of the rains in the West African Sahel.- Journal of Arid Environments, vol. 63, no. 3, pp. 615–641.

Roca, T., Schwarz, B., Tellman, B., Sullivan, J., Kuhn, C., Mahtta, R., Pandey, N., Hammett, L., & Pestre, G. (2017): Vulnérabilité sociophysique aux inondations au Sénégal. Une analyse exploratoire sur la base de nouvelles données et de Google Earth Engine.- Notes Techniques No. 25, Agence Française de Développement: http://librairie.afd.fr.

Seck, A. (2010): Urban Development, Climate Change and Flood Risk management – a case study of Saint Louis, Senegal. M.Sc. Thesis MWI.2010.032, UNESCO-IHE, April 2010.

Steijn, R.C. (2011): Some considerations on Water and Climate Change Impacts – St. Louis, Senegal.- Shelter Report No. C04021.002622R1r2, ARCADIS, Emmeloord, The Netherlands.

Vedeld T., Coly A., Mare`me, N., & Hellevik, N.S. (2016): Climate adaptation at what scale? Multi-level governance, resilience, and coproduction in Saint Louis, Senegal.- Nat Hazards (2016) 82:173 – 199, Springer, DOI 10.1007/s11069-015-1875-7.

"Senegal city is 'most threatened'". BBC News. 2008-06-13. *Retrieved 2019-05-25.*

http://projects.worldbank.org/P166538?lang=en. The World Bank - Projects and Operations. *Retrieved 2019-05-25.*

"http://africa.archive.wetlands.org/News/tabid/2929/ID/3844/Special-Report-Senegal--Environment-disaster--Doune-Baba-Dieye-in-the-Gandiole-swept-from-the-map.aspx". Wetlands International. *Retrieved 2019-04-20.*

"http://floodlist.com/africa/senegal-city-races-to-move-families-as-sea-swallows-homes". Floodlist. *Retrieved 2019-04-20.*

"france-help-senegals-saint-louis-battle-coastal-erosion".RFI News, 2018-02-04-. *Retrieved 2019-05-25.*

This page is intentionally left blank.

Annex 1 – AOI Calculation based on the DG Regio approach

This page is intentionally left blank.

AOI Calculation Methodology based on the DG Regio Approach

So far, no internationally accepted definition for the term "Urban Area" and the related Peri-Urban area exists. Different initiatives are currently trying to address a standardised approach for defining the term "Urban Area". During discussions with the GPSC Co-ordinator it was considered important to use an uniform definition for the GPSC cities in order for the cities to exchange information and share products/experiences and conduct potential comparative studies.

In this context, it was decided to use an international approach for the demarcation of the Areas of Interest (AOI) for mapping the GPSC cities in terms of Core Urban area and Peri-Urban area. Thus, the approach is based on the European Union's Directorate-General for Regional and Urban Policy (DG REGIO) method and the definitions are described in the Regional Working Paper 2014 from the European Commission on "A harmonised definition of cities and rural areas: the new degree of urbanisation" (European Commission, 2014). Following the naming of the DG Regio approach, the Urban Core is named as "High Density Core" and the Peri-Urban area is termed "Urban Cluster". Within the DG REGIO approach, the High Density Core is defined as contiguous grid cells of 1 km^2 with a density of at least 1 500 inhabitants per km^2 and a minimum population of 50 000. The Urban Cluster is defined as clusters of contiguous grid cells of 1 km^2 with a density of at least 300 inhabitants per km^2 and a minimum population of 5 000.

The DG REGIO methodology used in the EO4SD-Urban project was slightly adjusted to Non-European countries. For the first two GPSC cities (namely Bhopal and Vijayawada) produced within the project the Global Human Settlement Population (GHSP) grid with a spatial resolution of 1 km were used for the classification into "High Density Core" and "Urban Cluster". The raster dataset is available for the years 1975, 1990, 2000, 2015. This dataset depicts the distribution and density of population, expressed as the number of people per cell. The data can be downloaded under following link http://data.jrc.ec.europa.eu/dataset/jrc-ghsl-ghs_pop_gpw4_globe_r2015a.

In 2019, a higher resolution population layer (spatial resolution of 10 m) produced by the German Aerospace Centre (DLR) became available. The AOIs for the remaining GPSC cities (namely Melaka, Abidjan, Dakar and Campeche) were produced based on the DLR population layer.

In the following, a more detailed description of the calculation methodology for the High-Density Core and the Urban Cluster follows. The calculation is exemplary described on the AOI generation for the city of Melaka.

To start with, Figure 48 shows the city of Melaka and the surrounding area. Figure 49 shows the population distribution grid over Melaka produced by the European Commission. Figure 50 shows the DLR population grid with 10 meter spatial resolution for Melaka while Figure 51 illustrates the aggregated DLR population grid with 1 km spatial resolution.

Figure 48: Satellite image showing Melaka and the surrounding area.

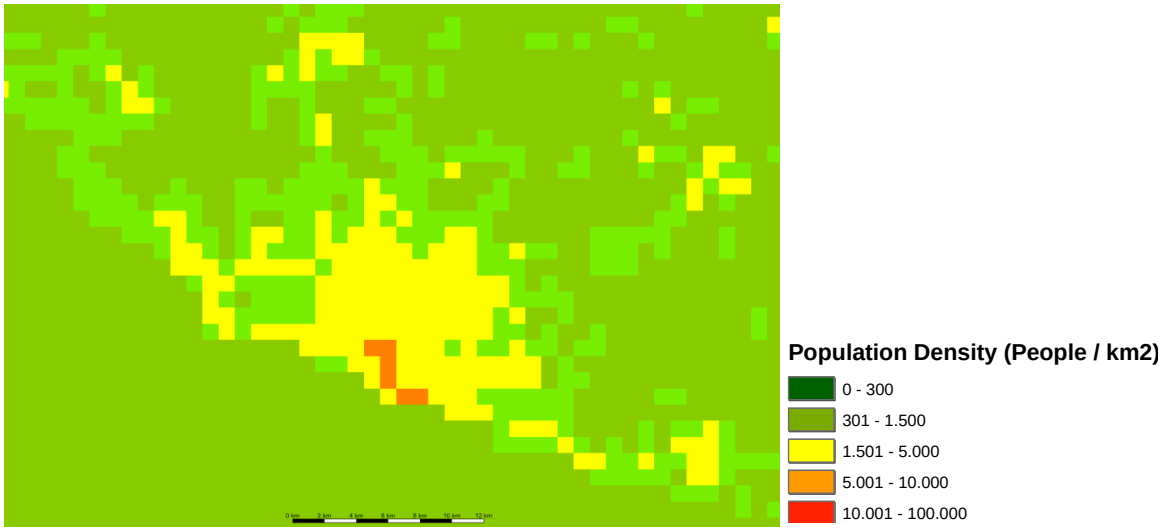

Figure 49: Global Human Settlement Population Layer (spatial resolution of 1 km).

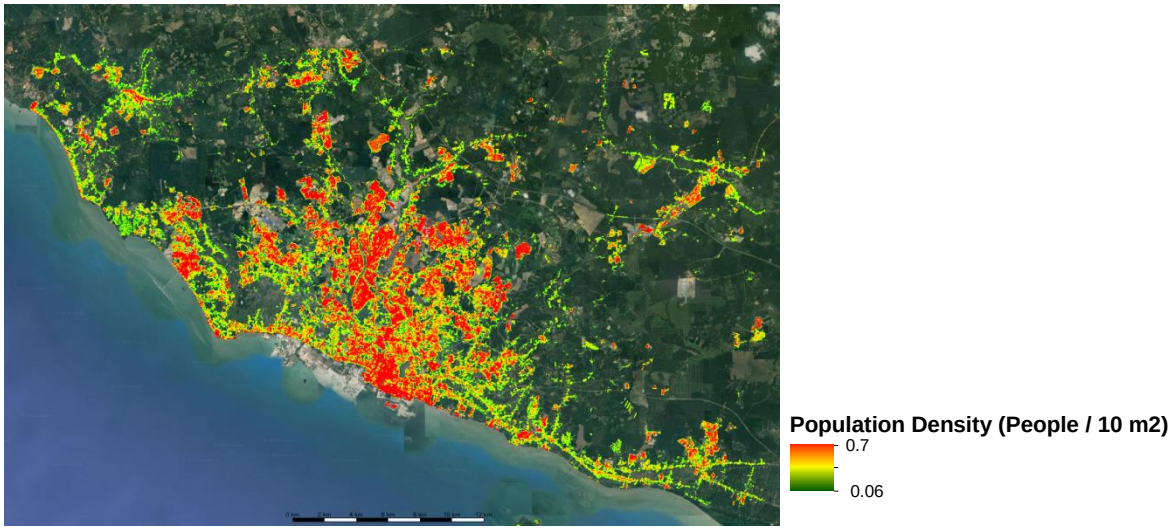

Figure 50: DLR population layer (spatial resolution of 10 m).

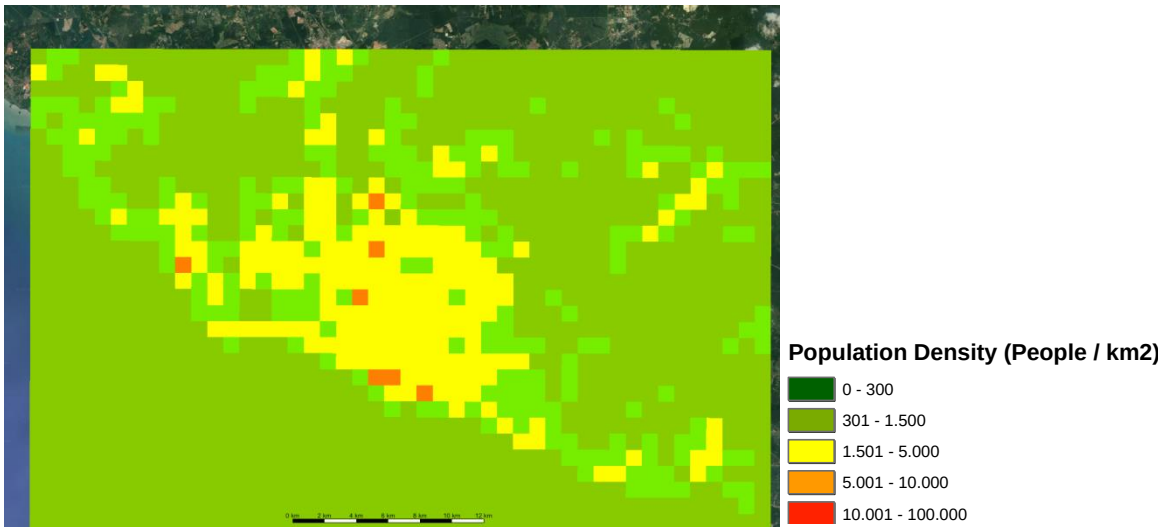

Figure 51: Aggregated DLR population layer (spatial resolution of 1 km).

The High Density Core AOI for a city is created by merging the contiguous grid cells of 1 km^2 with a density of at least 1500 inhabitants per km^2 and a minimum population of 50 000. In the definition of the High Density Core the contiguity is only allowed via a vertical or horizontal connection. In a next step, gaps are filled. Due to the coarse resolution of the population grid cells additional grid cells were in a last step added for under estimated settlement areas. The same was done for over estimations, here grid cells were removed.

Figure 52 shows the High Density Core AOI (red line) overlaid on the DLR population layer (left) and on a RGB satellite image (right).

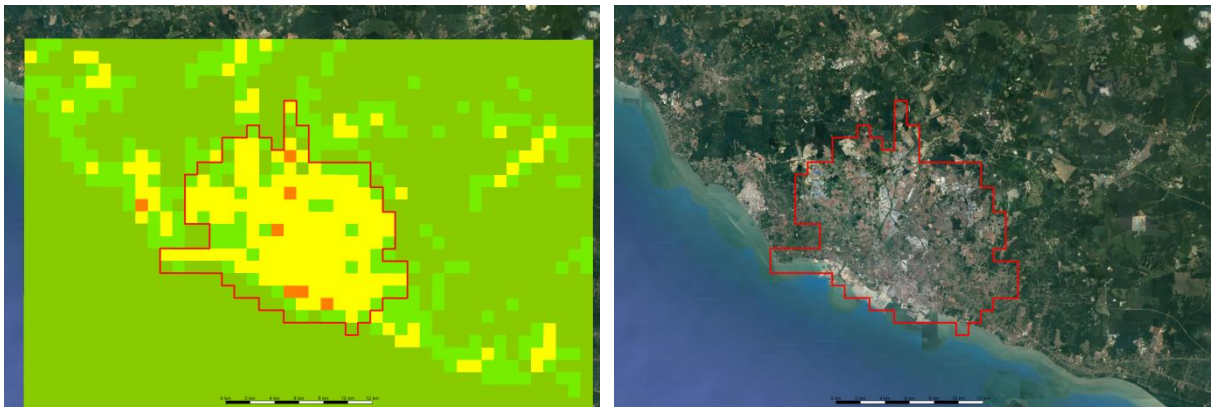

Figure 52: High Density Core area of Melaka calculated based on the aggregated DLR population layer. The image on the left shows the AOI overlaid on the DLR population layer. On the right, the AOI is overlaid on a RGB satellite image.

The Urban Cluster is created very similar to the High Density Core. Continuous grid cells of 1 km^2 with a density of at least 300 inhabitants per km^2 and a minimum population of 500 are merged together to form the Urban Cluster. The contiguity within the Urban Cluster can also be diagonal. After gaps are filled, areas, which were over or under estimated by the population grid were removed or added to the AOI. Figure 53 shows the Urban Cluster AOI (magenta line) overlaid on the DLR population layer (left) and on a RGB satellite image (right).

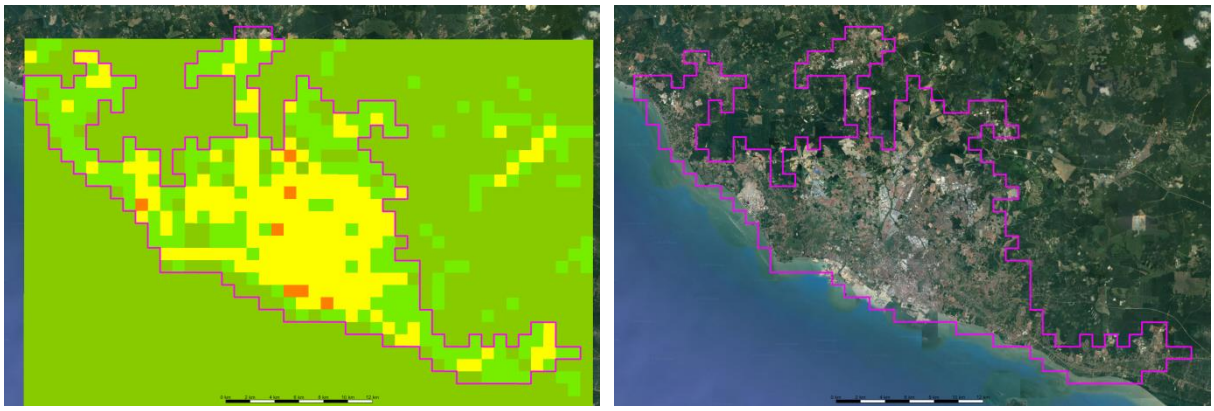

Figure 53: Urban Cluster area of Melaka calculated based on the aggregated DLR population layer.

In some cases, the city counterparts requested that the AOIs for the High Density Core and the Urban Cluster follow the municipal or administrative boundary of the city. In this case, the municipal/administrative boundary was used but enlarged in areas where the AOI created according to the adjusted DG Regio approach was bigger.

This page is intentionally left blank!

Annex 2 – Processing methods for EO4SD-Urban products

This page is intentionally left blank!

Summary of Processing Methods

Urban and Peri-Urban Land Use/Land Cover and Change

The input includes Very High Spatial Resolution (VHR) imagery from different sensors acquired at different time. The data is pre-processed to ensure a high level of geometric and radiometric quality (ortho-rectification, radiometric calibration, pan-sharpening).

The complexity when dealing with VHR images comes from the internal variability of the information for a single land-use. For instance, an urban area is represented by a high number of heterogeneous pixel values hampering the use of automated pixel-based classification techniques.

For these VHR images, it is possible to identify textures (or pattern) inside an entity such as an agricultural parcel or an urban lot. In other words, whereas pixel-based techniques focus on the local information of each single pixel (including intensity / DN value), texture analysis provides global information in a group of neighbouring pixels (including distribution of a group intensity / DN values but also spatial arrangement of these values). Texture and spectral information are combined with a segmentation algorithm in an Object Based Image Analysis (OBIA) approach to reach a high degree of automation for most of the peri-urban rural classes. However, within urban land, land use information is often difficult to obtain from the imagery alone and ancillary/in situ data needs to be used. The heterogeneity and format of these data mean that another information extraction method based on Computer Aided Photo-Interpretation techniques (CAPI) need to be used to fully characterise the LULC classes in urban areas. Therefore, a mix of automated (OBIA) and CAPI are used to optimise the cost/quality ratio for the production of the LULC/LUCC product. The output format is typically in vector form which makes it easier for integration in a GIS and for subsequent analysis.

Level 4 of the nomenclature can be obtained based on additional information. These can be generated by more detailed CAPI (e.g. identification of waste sites) or by an automated approach based on derived/additional products. An example is illustration by categorising the density of the urban fabric which is related to population density and can then subsequently used for disaggregating population data.

Information on urban fabric density can be obtained through several manners with increasing level of complexity. The Imperviousness Degree (IMD) or Soil Sealing (SL) layer (see separate product) can be produced relatively easily based on the urban extent derived from the LULC product and a linear model between imperviousness areas and vegetation vigour that can be obtained from Sentinel 2 or equivalent NDVI time series. This additional layer can be used to identify continuous and discontinuous urban fabric classes. Five urban fabric classes can be extracted based on a fully automated procedure:

- Continuous Dense Urban Fabric (Sealing Layer-S.L. > 80%)
- Discontinuous Dense Urban Fabric (S.L. 50% - 80%)
- Discontinuous Medium Density Urban Fabric (S.L. 30% - 50%)
- Discontinuous Low Density Urban Fabric (S.L. 10% - 30%)
- Discontinuous Very Low Density Urban Fabric (S.L. < 10%)

Manual enhancement is the final post-processing step of the production framework. It will aim to validate the detected classes and adjust classes' polygon geometry if necessary to ensure that the correct MMU is applied. Finally, a thorough completeness and logical consistency check is applied to ensure the topological integrity and coherence of the product.

Change detection: Four important aspects have to be considered to monitor land use/land cover change effectively with remote sensing images: (1) detecting that changes have occurred, (2) identifying the nature of the change, (3) characterising the areal extent of the change and (4) assessing the spatial pattern of the change.

The change detection layer can be derived based on an image-to-image approach provided the same sensor is used. An original and efficient image processing chain is promoted to compare two dates' images and provide multi-labelled changes. The approach mainly relies on texture analysis, which has the benefits to deal easily with heterogeneous data and VHR images. The applied change mapping approach is based on spectral information of both dates' images and more accurate than a map-to-map comparison.

Summary of Processing Methods

World Settlement Extent

The rationale of the adopted methodology is that given a series of radar/optical satellite images for the investigated AOI, the temporal dynamics of human settlements are sensibly different than those of all other land-cover classes.

While addressing settlement-extent mapping for the period 2014-2015 multitemporal S1 IW GRDH and Landsat-8 data acquired at 10 and 30m spatial resolution were taken into account. Concerning radar data, each S1 scene is pre-processed by means of the SNAP software available from ESA; specifically, this task includes: orbit correction, thermal noise removal, radiometric calibration, Range-Doppler terrain correction and conversion to dB values. Scenes acquired with ascending and descending pass are processed separately due to the strong influence of the viewing angle in the backscattering of built-up areas. As a means for characterizing the behaviour over time, the backscattering temporal maximum, minimum, mean, standard deviation and mean slope are derived for each pixel. Texture information is also extracted to ease the identification of lower-density residential areas. As regards optical data, only Landsat-8 scenes with cloud cover lower than 60% are taken into consideration (indeed, further rising this threshold often results in accounting for images with non-negligible misregistration error). Data are calibrated and atmospherically corrected using the LEDAPS tool available from USGS and the CFMASK software is applied for removing pixels affected by cloud-cover and cloud-shadow. Next, a series of 6 spectral indices suitable for an effective delineation of settlements (identified through extensive experimental analysis) are extracted; these include – among others – the Normalized Difference Built-Up Index (NDBI), the Modified Normalized Difference Water Index (MNDWI) and the Normalized Difference Vegetation Index (NDVI). For all of them, the same set of 5 key temporal statistics used in the case of S1 data are generated for each pixel in the AOI. Moreover, to improve the detection of suburban areas, for each of the 6 temporal mean indices also here texture information is computed. For matching the spatial resolution of Sentinel data, the whole stack of Landsat-based features is finally resampled to 10m spatial resolution.

To identify reliable training points for the settlement and non-settlement class, a strategy has been designed which jointly exploits the temporal statistics computed for both S1 and Landsat data, along with additional ancillary information. In the case of optical data, in general the most of settlement pixels can be effectively outlined by properly jointly thresholding the corresponding NDBI, NDVI, and MNDWI temporal mean; likewise, this holds also for non-settlement pixels. Regarding radar data, it generally occurs that the temporal mean backscattering of most settlement samples is sensibly higher than that of all other non-settlement classes. Nevertheless, in complex topography regions: i) radar data show high backscattering comparable to that of urban areas; and ii) bare rocks are present, which often exhibit a behaviour similar to that of settlements in the Landsat-based temporal statistics. Accordingly, to exclude these from the analysis, all pixels are masked whose slope - computed based on SRTM 30m DEM for latitudes between -60° and +60° and the ASTER DEM elsewhere - is higher than 10 degrees.

Support Vector Machines (SVM) are used in the classification process. However, as the criteria defined above for outlining training samples might results in a high number of candidate points, for AOIs up to a size of ~10000 km² the most effective choice proved extracting 1000 samples for both the settlement and non-settlement class. Nonetheless, since results might vary depending on the specific selected training points, as a means for further improving the final performances and obtain more robust classification maps, 20 different training sets are randomly generated and given as input to an ensemble of as many SVM classifiers; then, a majority voting is applied. Afterwards, the stacks of Landsat-8-based and S1-based temporal features are classified separately as this proved more effective than performing a single classification on their merger. In both cases, a grid search with a 5-fold cross validation approach is employed to identify for each training set the optimal values for the learning. Here, those resulting in the highest cross-validation overall accuracy are then selected and used for classifying the corresponding study region.

A final post-classification phase is dedicated to properly combining the Landsat- and S1-based classification maps and automatically identifying and deleting potential false alarms. To this purpose, an advanced post-editing object-based approach has been specifically designed.

The above-described methodology has been further adapted for outlining the settlement extent in the past solely based on Landsat-5/7 imagery available since 1984; indeed, no long-term SAR data archive at comparable spatial resolution is freely accessible for the same timeframe (e.g., ESA ERS-1/2 data are available from 1991 without systematic world coverage and often proved too complicated to pre-process). In particular, for the given target period and AOI, all available Landsat imagery with cloud cover lower than 60% is pre-processed in the same fashion as described in the previous paragraphs and the same set of temporal statistics and texture features are extracted. Based on the hypothesis that settlement growth occurred over time (meaning that a pixel cannot be marked as settlement at an earlier time if it has been defined as non-settlement at a later time), all pixels categorized as non-settlement in the 2014-2015 extent map are excluded from the analysis. Then, training samples are derived by thresholding the temporal mean NDBI, MNDWI and NDVI; specifically, a dedicated strategy has been implemented for automatically determining the thresholds for the 3 indices by comparing their cumulative distribution function (CDF) for the target period with that exhibited for the period 2014-2015. Also in this case, an ensemble of 20 SVMs is used, each one trained on a different subset of 2000 samples (i.e., 1000 for the settlement and 1000 for the non-settlement class) and majority voting is then employed for generating the final map. It is worth noting that, when deriving the past settlement extent for multiple times, both the masking and threshold adaptation are performed on the basis of the results derived for the next target period.

Summary of Processing Methods

Percentage Impervious Surface

Imperviousness product is intended to represent the impervious surfaces because of urban development, layers of completely or partly impermeable artificial material (asphalt, concrete, etc.) and infrastructure construction. Therefore, the Imperviousness Degree (IMD) or Soil Sealing (SL) information can be produced relatively easily based on the Urban Extent derived from the baseline LULC information product and the linear model between impervious areas and vegetation presence that can be determined and characterized from Landsat or Sentinel-2 NDVI time series.

More precisely, the raster product is generated at 10m - 30m spatial resolution by properly exploiting Landsat-4/5/7/8 or Sentinel-2 multitemporal imagery acquired over the study area within a given time interval of interest in which no relevant changes are expected to occur (typically a time period of 1-2 years allows to get very accurate results). Each acquired EO data is pre-processed (ortho-rectification, radiometric calibration, pansharpening, cloud-masking). Then, the Normalized Difference Vegetation Index (NDVI) is extracted for each image within the urban mask (corresponding to Urban Extent product). NDVI is inversely correlated with the amount of impervious areas, i.e. the higher the NDVI is, the higher the expected presence of vegetation, hence the lower the corresponding imperviousness degree. The core idea is to compute per each pixel its temporal maximum which depicts the status at the peak of the phenological cycle. It is worth noting that for different pixels in the study area, different number of scenes might be available.

However, in the hypothesis of sufficient minimum number of acquisitions unavailable for computing consistent statistics, this does not represent an issue. Indeed, in this framework, it is also possible to get spatially consistent datasets useful for the desired analyses, even when investigating large territories. Areas associated with different levels of impervious surfaces are then extracted by visual interpretation from data sources with higher spatial resolution (e.g. VHR imagery, Google Earth imagery). OSM layers or information derived from in-situ campaigns are other auxiliary data sources which can also be used for this purpose. At the end, reference data are extracted in various parts of the study region and then rasterized and aggregated at the spatial resolution of input EO data.

A support vector regression SVR module is then used for properly correlating the resulting training information with the temporal maximum NDVI to finally derive the Percentage of Impervious Surface (PIS) or Imperviousness Degree (IMD) for the entire AOI. Specifically, 8bit integer values from the raster product range from 0 (no impervious surface in the given pixel) to 100 (completely impervious surface in the given pixel).

Summary of Processing Methods

Flood Risk

Historic flood extent mapping

The flood extent is derived from historical optical satellite imagery of 30 meter resolution (Landsat 5 and Landsat 8) and 10 meter resolution (Sentinel 2).

The relevant datasets were corrected atmospherically applying the Dark Object Subtraction (DOS) approach. Landsat 8 imagery was pan-sharpened to 15 m resolution.

For defining the water extent the water cover was classified by applying the Automated Water Extraction Index AWEIsh (Feyisa et al. 2014) which makes use of the reflectance values of Blue, Green, Near Infrared and Shortwave Infrared spectral bands of the Landsat 5, Landsat 8, and Sentinel-2 sensors. The AWEIsh is an index formulated to effectively eliminate non-water pixels, including dark built surfaces in areas with urban background. The equation is intended to effectively eliminate shadow pixels and improve water extraction accuracy in areas with shadow and/or other dark surfaces.

Two sets of flood masks are produced from the S1 stack. The first is based on simple backscattering thresholds applied to individual VH polarization images. This results in 39 individual water masks, which can be analysed in terms of their frequency of being water.

The second approach uses the multitemporal stack statistics to separate flooded areas from periodically flooded areas and permanent water based on thresholds derived from reference data. Areas with a low mean backscatter and a low coefficient of variation are mostly permanent water. Flooded areas show a higher coefficient of variation and a low minimum backscatter, but periodically flooded areas tend to show a higher mean backscatter than areas with short-period flooding.

The delimitation of permanent water cover (representing a high water-level during the rainy season) is based on the EO4SD LULC classification.

Finally, mapping of flood extents by visual interpretation of VHR imagery as available in Google Earth was done.

Flood hazard mapping

The flood hazard map was generated based on the occurrence of flood events during the past 10 years. The map aims to give an idea about the flood presence in terms of both frequency and extent in the city, and illustrates which part is in generally flooded more often than other areas.

Water extents representing seasonal floods of the Senegal River as well as rainwater stagnation after heavy rains are based on

- data from Landsat 5, Landsat 8 (provided by the US Geological Survey), and Sentinel-2 (provided by the European Space Agency)
- and on visual interpretation of VHR data as available in Google Earth

The flood hazard classification was done according to the approach selected by NEO on Cambodia cities during EO4SD Phase 1: a "number of occurrences" was calculated by combining flood extents as derived from HR imagery and from visual interpretation of VHR imagery. This data was classified according to the following specifications for the hazard definition:

- area flooded once between 2009 and 2018: low hazard
- area flooded twice or three times: medium hazard
- area flooded more than three times: high hazard

It has to be underlined that both approaches for the flood extent identification differ significantly and that the analysis of VHR data does not cover the peri-urban area. Furthermore, in some cases, the areas identified as flooded in HR and VHR data respectively refer to the same event.

The estimation of the area threatened by tidal waves and coast erosion in Langue de Barbarie is based on available reports and press releases as well as on the extrapolation of the mapped difference (done by visual interpretation) of the coastline between 2003 and 2019.

Flood risk mapping

Risk is defined as a combination of probability and consequences. A detailed and uniform land-use map is an important prerequisite to perform flood risk calculations, since it determines what is damaged in case of flooding.

Two different datasets regarding the urban landuse were made available for this analysis:

- LULC product generated by NEO through EO4SD-Urban based on VHR data (WorldView-4 acquired on 29/11/2018) covering the core urban area
- LULC product generated by NEO through EO4SD-Urban based on HR data (Sentinel 2 acquired on 09/12/2018) covering the larger urban area

The exposition is classified following an approach developed by NEO (based on: Dasgupta et al. 2015) integrating economic costs, social damage, physical damage and flood duration. Four land use damage levels are defined based on this estimation.

Both land-use classification results were recoded to pre-defined categories and merged after categorization.

The flood risk product is a combination of hazard with Land Use / Land Cover (LULC) information. The Flood Risk matrix is generated based on the classification of exposition and flood hazard. The flood risk level is classified in four qualitative classes based on the combination of flood hazard and land use damage.

This page is intentionally left blank!

Annex 3 – Filled Quality Control sheets

Quality Control Sheets for the following products are provided in the form of independent documents:

- Urban and Peri-Urban Land Use / Land Cover
- Flood History and Risk
    - Flood Extent
    - Flood Hazard
    - Flood Risk